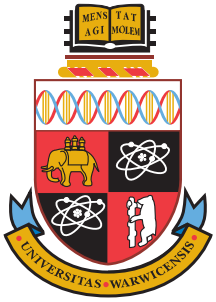

Regulation of nutrient uptake, substrate conversion, and bio-production in micro-organisms

by

Olga Alexandrovna Nev

Thesis

Submitted to the University of Warwick

for partial fulfilment of the requirements of the degree of

Doctor of Philosophy

Supervisor: Dr Hugo A. van den Berg

MOAC Doctoral Training Centre

May 2017

THE UNIVERSITY OF WARWICK

Contents

List of Figures

List of Tables

Abbreviations

ATP	Adenosine-5′-triphosphate
CAC	Citric acid cycle
CoA	Co-enzyme A
DNA	Deoxyribonucleic acid
Fts	Filamentous temperature sensitive
NAD^+	Oxidized form of nicotinamide adenine dinucleotide
NADH	Reduced form of nicotinamide adenine dinucleotide
$NADP^+$	Oxidized form of nicotinamide adenine dinucleotide phosphate
NADPH	Reduced form of nicotinamide adenine dinucleotide phosphate
ODE	Ordinary differential equation
PE	Phosphorylation equivalents
PMF	Proton-motive force
PWS	Piecewise smooth
RE	Reducing equivalents
Redox	Reduction-oxidation
RNA	Ribonucleic acid
SDE	Stochastic differential equation
VIS	Variable-Internal-Stores

Acknowledgements

I am deeply grateful to my supervisor Dr Hugo van den Berg. I am indebted to him for his intellectual support, scientific professionalism, as well as his patience and belief in my potential. His invaluable advise and help with content, style, illustrations, and English made it possible for me to complete this thesis. I will always admire him as a great scientist, an inspiring mentor, a talented human being, and a sincere person.

I am warmly thankful to my husband, who comforted and inspired me in moments of despair, and who never doubted in my capacities. His support always motivated me to keep moving.

I am obliged to my brother for his contribution to Chapter 4 as a software developer. His cooperation and support helped me to complete the thesis earlier.

I also wish to express my thanks to my parents and friends for their encouragement and belief in me.

I am grateful to the European Union for the financial support of the research on which this thesis is based, which was administrated under the auspices of the CAS-IDP training network led by Professor Alison Rodger which provided an academic content and administrative support.

Declaration

This thesis by published work is submitted to the University of Warwick in support of my application for the degree of Doctor of Philosophy. It has been composed by myself and has not been submitted in any previous application for any degree.

The work presented was carried out by the author, with the following exceptions: the theory was developed and interpreted in discussions with the supervisor; the *Mathematica* code for simulations carried out in Chapter 4 was translated into the *Java* coding language by software developer Oleg A. Nev, but the simulations were subsequently ran by myself; artwork pertaining to micro-organisms was kindly provided by the supervisor. Furthermore, Chapters 2– 4 were published as papers and as such benefited from the comments and suggestions provided by anonymous referees.

Chapter 2 was published as:

Nev O. A. and van den Berg H. A. (2017) Variable-Internal-Stores models of microbial growth and metabolism with dynamic allocation of cellular resources. *J. Math. Biol.*, 74 (1), 409–445.

Chapter 3 was published as:

Nev O. A. and van den Berg H. A. (2017) Differential inclusions with sliding modes to represent microbial metabolism and growth under conditions of starvation. *Dyn. Systems*, doi: 10.1080/14689367.2017.1298726.

Chapter 4 was published as:

Nev O. A., Nev O. A. and van den Berg H. A. (2017) Optimal management of nutrient reserves in micro-organisms under time-varying environmental conditions. *J. Theor. Biol.*, 429, 124–141.

Abstract

This thesis presents the development and analysis of a macro-chemical kinetics model of microbial metabolism and growth, belonging to the class of Variable-Internal-Stores (VIS) models. Such models can account for changes in the internal state of a micro-organism in response to variations in environmental conditions. In addition to VIS, the model developed in the present thesis describes the adaptive allocation of molecular building blocks among various types of catalytic machinery by means of so-called 'regulatory rules' which can be reconstructed from observational data, as shown in Chapter 4. In Chapter 2 I show that this novel VIS-with-reallocation model has a unique, stable equilibrium point and reduces to classical models of microbial growth and metabolism. In Chapter 3 this mathematical model is treated as a piecewise smooth system, which allows me to investigate the behaviour of the model under conditions of starvation, and, in particular, to describe this behaviour in terms of Fillipov sliding modes. In Chapter 4, I study the response of the model to time-varying environmental conditions of the 'feast-or-famine' type of nutrient limitation, where I address the question of maximally adaptive regulation of reserve densities and show that optimal reserve management is governed by the frequency of environmental fluctuations on time scale comparable to that of the organism's physiology.

Chapter 1

Introduction

This thesis describes the development of a macro-chemical kinetics model of metabolism and growth in micro-organisms that allows the integration of observations on metabolic regulation and nutrient disposition with data regarding the ambient conditions to which the organisms are subjected. The model focuses on the rates of exchange of matter and energy between micro-organisms and their environment, with a view to applications in both fundamental ecology and biotechnology, for instance in assessing the contribution made by microbiota to mass and energy fluxes in ecosystem. This introductory chapter will motivate the development of such models. Section 1.1 describes the basic biology of both prokaryotic and eukaryotic micro-organisms. Section 1.2 discusses standard culture systems. Section 1.3 reviews modelling strategies, ranging from the most minimal models to biochemically detailed models and explains where the modelling philosophy adopted in the present thesis lies within this range.

1.1 General microbiology

This section describes the basic principles of the biology of both prokaryotic and eukaryotic cells that underpin the model developed in this thesis.

1.1.1 Prokaryotes

This section focuses on prokaryotic micro-organisms and their structural and physiological traits, classifying intracellular components according to the macro-chemical concept proposed in this thesis.

Structural components and nutrient uptake apparatus

This section discusses components of prokaryotic cells that in the macro-chemical classification system proposed in this thesis belong to the so-called *structural component* group, which includes the cell en-

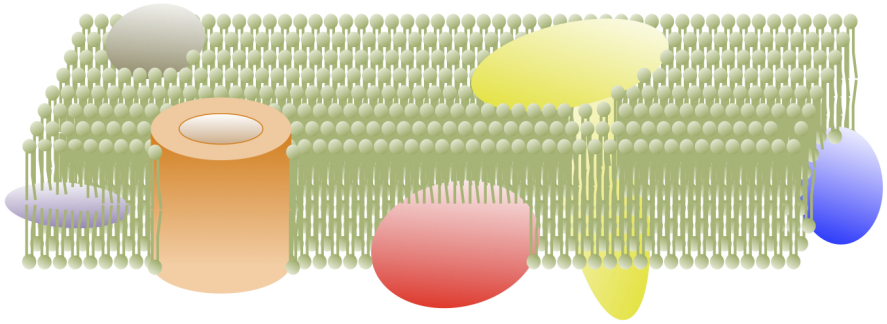

Figure 1.1: Structure of a phospholipid bilayer. Lipid molecules form a bilayer in such way that hydrophobic 'tails' are isolated from the surrounding aqueous environment, while the hydrophilic 'heads' interact with this environment. The membrane contains numerous proteins which may span the membrane, or be attached or anchored to the membrane, depending on their type and function.

velope and the genetic material, as well as intermediates of core metabolic pathways. In addition, we discuss transporters and binding proteins involved in the assimilation of nutrients from the environment; in the conceptual scheme of the present thesis, such proteins are grouped together as *uptake machinery*.

Cell envelope Prokarytotes are unicellular micro-organisms that are characterised by the absence of a true nucleus. They are among the most primitive and ancient known forms of life [48]. The cytoplasm of prokaryotic cells is enclosed by a bilipid membrane, the schematic structure of which is shown in Fig. 1.1. The cytoplasmic membrane is a phospholipid bilayer in which various proteins are embedded. Within this bilayer, the fatty acid tails of the constituent lipid molecules point inward, toward each other, thereby forming a hydrophobic region [98]. Membrane proteins perform various biological activities, such as cell-to-cell interaction, signalling, or transporting substances across the membrane. Certain membrane proteins called integral membrane proteins are partly or fully embedded in the membrane or span it [97]. There are also peripheral proteins which are not embedded in the cytoplasmic membrane, but firmly associated with its surface (Fig. 1.1).

Depending on the reaction of the cell to the Gram stain, bacterial species are classified as either Gram-positive or Gram-negative [58]. In Gram-positive cells a rigid polysaccharide layer called peptidoglycan forms 90% of the cell wall, whereas in Gram-negative bacteria the peptidoglycan layer is very thin, and there is a second bilipid membrane called the outer membrane, which consists of phospholipids, proteins, and polysaccharides [109]. The area between outer and cytoplasmic membranes is filled by a special layer with a high protein concentration, which is called the periplasm [55]. The main structural differences of the cell wall between Gram-positive and Gram-negative bacteria are shown in Fig. 1.2.

Besides being a permeability barrier that separates the inside from the outside of a cell, the cell wall

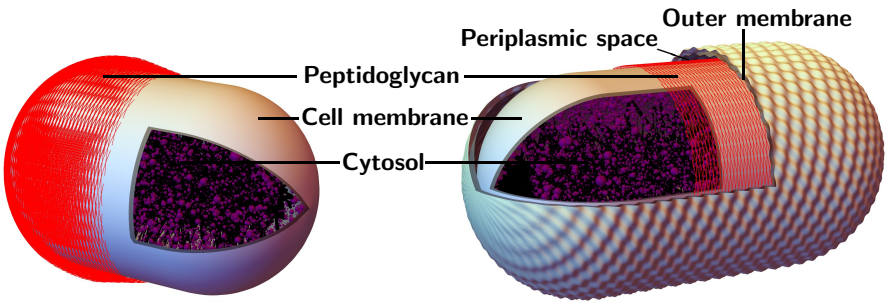

Figure 1.2: Comparison of the cell wall in Gram-positive and Gram-negative bacteria. Both Gram-positive (left) and Gram-negative (right) bacteria have a cell membrane enclosing the cytosol, with a peptidoglycan (murein) layer covering the external surface of the cell membrane. Whereas this peptidoglycan is thick in Gram-positive bacteria, it is quite thin in Gram-negative bacteria. However, in the latter, the cell envelope is completed by an additional outer membrane, which forms a periplasmic space between the outer and inner membranes.

provides the cell with a form of energy storage called proton-motive force (PMF), which drives transport and motility functions of the cell [98].

Nutrient transport Whereas some hydrophobic molecules can pass through the membrane by diffusion, others require a dedicated pathway to be translocated across the membrane [78]. The latter is mediated by means of transport proteins that function individually or in groups depending on the transport mode they realise. Membrane-spanning transporters can transfer molecules across the membrane by themselves (uniport), or along with another substance, which may experience a net transport in the same direction as the target molecule (symport) or in the opposite direction (antiport) [98]. In uniport, transport may take the form of facilitated diffusion, or be driven by the favourable energetics derived from group translocation or ATP hydrolysis. Symport and antiport derive this energy from the gradient of the cotransported species (e.g. if this is H^+, the PMF is driving the process). A group translocation system consists of different types of proteins, some of which chemically modify the transported substances during their uptake across the membrane (e.g. by means of phosphorylation) [11]. A-B-C systems were first found in Gram-negative bacteria [22, 69]. They involve substrate-binding proteins in the periplasm, membrane-integral proteins in both outer and inner membranes, and ATP-hydrolysing proteins in the transportation process; this transport system is driven by the hydrolysis of adenosine-5′-triphosphate (ATP). Since Gram-positive bacteria lack a periplasm, their binding proteins in A-B-C systems are typically lipoproteins bound to the membrane by a lipid group [69] or they are fused to the transmembrane domain of the transporter [23]. The transport modes are represented schematically in Fig. 1.3.

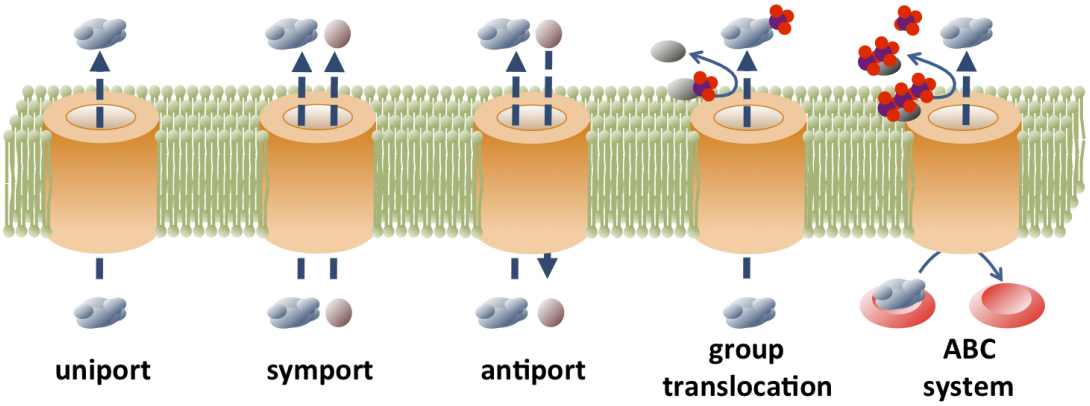

Figure 1.3: Modes of transport.

Genetic material Genetic information required for growth, development, metabolism, and reproduction is stored in the form of the deoxyribonucleic acid (DNA). The latter is composed of a sugar-phosphate backbone, with a nitrogen-rich organic base attached to each sugar moiety (Fig. 1.4). There are 4 bases (adenine, thymine, cytosine, and guanine), which serve as the 'alphabet' used to encode information. For instance, to encode one of the 22 amino acids that occur in microbial proteins, a three-base 'word' (codon, triplet) is used (there are $4^3 = 64$ such 'words'). To encode the entire protein, the requisite number of codons is concatenated into a functional unit called the cistron. One or several cistrons under the control of a single upstream activating region (promoter, operator) make up an operon. Having several proteins under common control often makes functional sense, for instance if they are enzymes pertaining to a particular biochemical pathway. Promoter and cistron(s) together constitute a gene. Several hundreds to many thousands of genes make up the genome of a given micro-organism [9].

Bacterial cells typically have a single circular chromosome [143], which is folded into a structure termed the nucleoid [144]. In addition to the large DNA molecule, bacteria may contain small loops of DNA called plasmids, which can be transferred between bacterial cells [55].

Synthetic machinery

This section describes the molecular machinery of a cell that is devoted to the synthesis of catalytic machinery via the processes of transcription and translation. This type of machinery will be referred to as *synthetic machinery* in this thesis.

Gene expression Besides DNA, nucleic acids are present in the cell in the form of ribonucleic acid (RNA), which is less stable than DNA, and is employed by the cell as messenger, transporter, and syn-

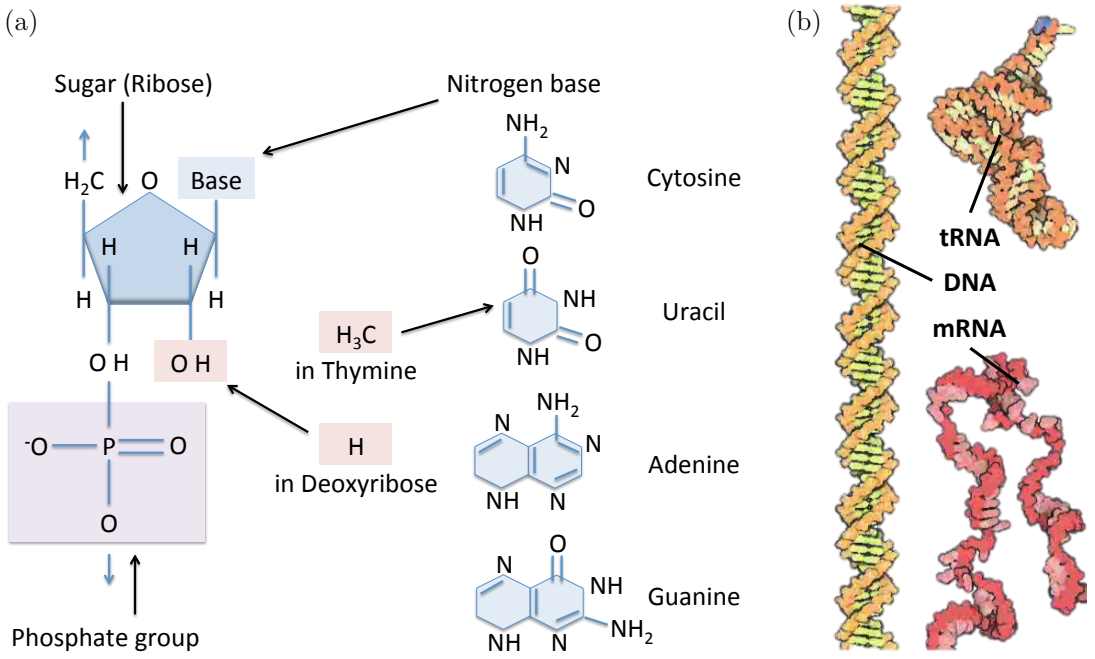

Figure 1.4: Nucleic acids: RNA and DNA. (a) Structure of RNA. In DNA, the sugar deoxyribose is present instead of ribose, and the nitrogen base thymine replaces uracil. **(b)** Double-stranded helix molecule of DNA together with the molecules of messenger and transport RNAs (taken from [55]).

thetic apparatus [55]. Figure 1.4 illustrates key differences between DNA and RNA. DNA has the sugar deoxyribose in its backbone, whereas RNA has the sugar ribose. Furthermore, the nucleotide thymine in DNA is replaced by uracil in RNA. Three major types of RNA molecules are messenger RNA (mRNA), transfer RNA (tRNA), and ribosomal RNA (rRNA).

Both DNA and RNA are involved in the process of gene expression, which consists of transcription and translation. During the transcription process, genetic information is transferred from DNA to RNA by means of the enzyme RNA polymerase, which recognizes a specific start site on the DNA and whose interactions with the DNA are governed by an upstream region called the promoter. At the translation stage, mRNA transfers the genetic information from the genome to the ribosome. The ribosome is a complex molecular machine, composed of rRNA molecules and proteins, which plays a central role in the synthesis of proteins. The ribosome 'reads' the ribonucleotide sequence in mRNA as a sequence of codons, each of which encodes the corresponding amino acid. The tRNA transfers the amino acid corresponding to each codon by binding of the complementary tRNA anticodon to the mRNA codon. The ribosome then moves to the next mRNA codon to continue the process, thus creating a polypeptide chain, which consists of amino acid residues linked by peptide bonds. The amino acid carried by the tRNA is transferred to this growing polypeptide chain, thus leaving an uncharged tRNA molecule which

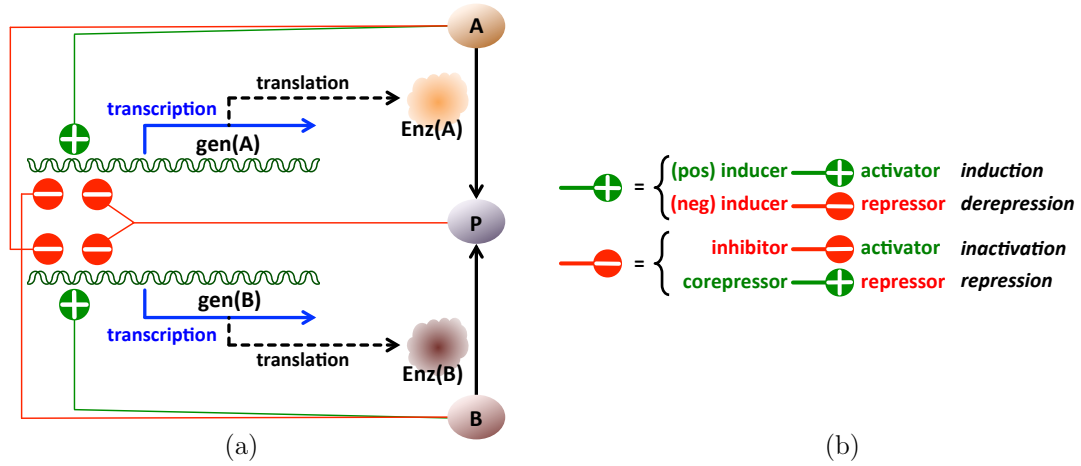

Figure 1.5: Regulatory mechanisms in bacteria. (a) Diagram illustrating modes of control in prokaryotic gene regulation. Two alternative substrates (***A*** and ***B***) are both converted to a common product (***P***), via reactions catalysed by specific enzymes (***enz(A)*** and ***enz(B)***) which are encoded by genes (***gen(A)*** and ***gen(B)***). In negative feedback control, the expression of both these genes is inhibited by product ***P***. In positive feedforward control, the expression of the gene corresponding to the enzyme converting a given substrate is stimulated by that same substrate, whereas in negative feedforward control, the expression of the gene corresponding to the enzyme converting a given substrate is inhibited by the alternate substrate. These various modes can co-exist together, mediated via several regions upstream from the promoter, where activating and repressing proteins can interact with the DNA and thus modify the rate of assembly of the RNA polymerase at the promotor. **(b)** Modes of regulation of gene expression. Stimulation of the expression of a given gene can be mediated by activation, in which an activator protein interacts with the upstream regulating region of the gene; this involves interaction with an inducer. Stimulation may also be effected via derepression, in which a repressor (an inhibitory transcription factor) is rendered less effective by an inducer. Inhibition of gene expression can likewise be achieved in two ways, either via inactivation of the activator protein via interaction with an inhibitor, or via activation of the repressor by binding to a corepressor. Inducers, inhibitors, and corepressors are frequently metabolities (substrates or products) but can also be components of an intracellular signalling cascade.

is released from the ribosome. The process stops when the so-called stop codon is reached, after which the polypeptide chain is released by the ribosome and is folded into an active protein [98].

Regulatory mechanisms In order to thrive, micro-organisms have to be able to respond rapidly to changes in the environment. One of the ways in which they can do this is adjusting gene expression. Cells regulate their uptake machinery both qualitatively and quantitatively in order to conserve energy and resources. This regulation is performed by the cell either via activity control or via amount control, or via a combination of these two modes. Activity can be adjusted only after the completion of protein synthesis, whereas the amount is regulated at a level of either transcription or translation [42].

Regulation at the level of transcription requires proteins that can bind to DNA; these are called regulatory proteins. This type of regulation is divided into positive and negative control types [98] which are shown in Fig. 1.5. In negative control, transcription is blocked. If a certain substance is present in sufficient amounts, then the enzyme that catalyses its production does not need to be synthesised. Negative control can be exerted in two different ways: repression and inactivation. In repression, the so-called core-

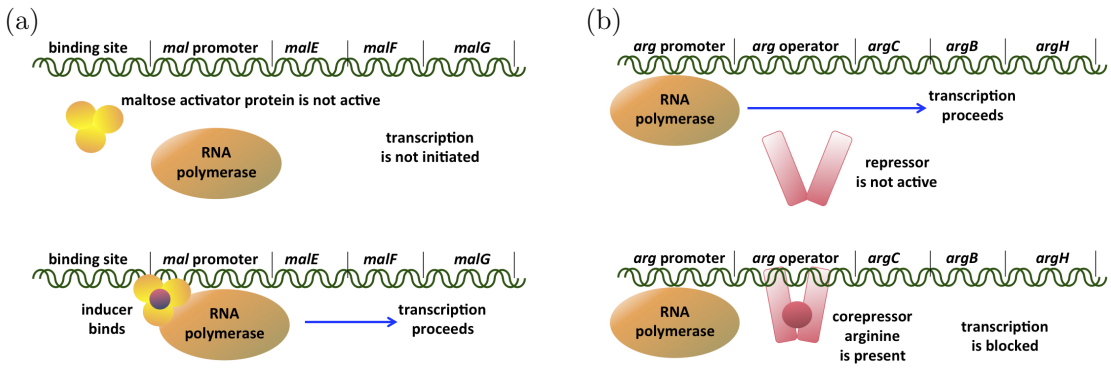

Figure 1.6: Examples of regulatory mechanisms in bacteria. **(a)** Transcription of the maltose transport system gene is initiated via the induction regulatory mechanism, in which the inducer binds the maltose activatory protein, which binds the RNA polymerase and thus makes it starting transcription. **(b)** Transcription of the arginine biosynthetic pathway gene is blocked via the repression regulatory mechanism, in which the corepressor binds the arginine repressor, thus makes it active and lets it stopping transcription.

pressor binds to the corresponding regulatory protein called the repressor, which subsequently changes its conformation and blocks transcription. The example of repression of transcription of the arginine biosynthetic pathway gene is shown in Fig. 1.6 (b). In inactivation, an inhibitor binds to a regulatory protein called the activator, and thus inhibits its activation and, subsequently, transcription. In positive control, an enzyme is produced only if the substance, whose synthesis is catalysed by this enzyme, is present. This type of regulation can be operated either via induction or via derepression. The former is carried out by a specific protein called the activator that activates the binding of RNA polymerase to DNA, as follows: the so-called inducer binds to the activator protein which interacts with the DNA at an activator-binding site and allows RNA polymerase to begin transcription [27, 92]. The example of induction of transcription of the maltose transport system gene is shown in Fig. 1.6 (a). In derepression, the inducer binds to the repressor and thus stops the repression of transcription.

There are additional modes of regulation which come into play under conditions of extreme stress. Nutrient shortage in the environment induces an increase in a number of uncharged tRNAs in a cell, and as the number of uncharged tRNA relative to the number of charged tRNA grows, the ribosome wastes a greater portion of its time interacting with uncharged tRNA, which thus leads to a stall of the ribosome along with a production of small nucleotides called alarmones. The alarmones initiate the so-called stringent response that is characterised by a cessation of rRNA and tRNA synthesis and ribosome production as well as by a decrease in protein and DNA synthesis and amino acid production [24, 109].

Another stress response is the so-called heat shock response, which bacteria display in response to high temperatures. The cell starts synthesising proteins called heat shock proteins that are dedicated to

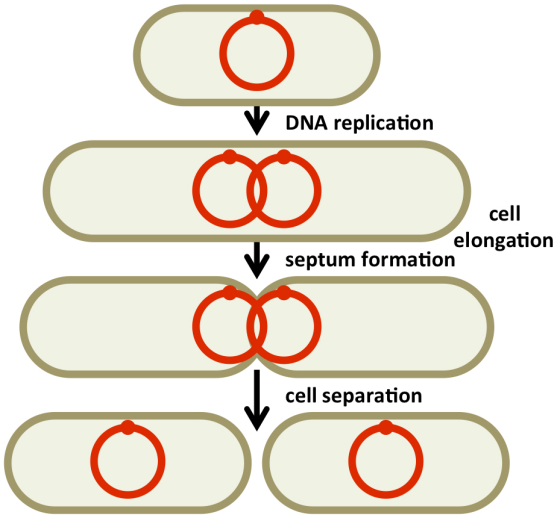

Figure 1.7: Schematic representation of a cell division process. First, DNA is replicated and the cell is elongated. Then new materials are generated and new DNAs are divided. Finally, two daughter cells are formed.

helping the cell to recover from heat stress [167]. The same regulatory mechanism is used to withstand critical conditions caused by chemicals or radiation.

Growth machinery

In this section we review processes related to cellular growth, which are mediated by the *growth machinery* that synthesises the cell envelope and mediates genome duplication and cell division. In addition, the growth machinery shares the molecular apparatus with the synthetic machinery to generate novel structural components.

Cell division The process during which an increase in the number of cells is observed can be defined as microbial growth [98]. This process involves a large complex of different chemical reactions occurring in a cell, such as energy transformation reactions, monomer synthesis reactions, and polymerization reactions, in which monomers are joined together to form macromolecules. A schematic representation of this process is given in Fig. 1.7.

During cell division, the cell divides in two daughter cells. This process is called a binary fission. At the beginning, the cell elongates to approximately twice its original length and DNA replicates. Within the replication process, both strands of the DNA are used as templates for synthesis of two new strands. When the DNA replication completes, Fts proteins (filamentous temperature sensitive proteins) form the cell division apparatus called the divisome by polymerizing in a ring termed as a Z-ring [28, 39, 146] and placing it at the center of the cell with an assistance of other proteins [29]. New cell wall material and

membrane are subsequently synthesised, and the two chromosomes are pulled apart. Then the ring that was formed by Fts proteins depolymerises, and a special partition called a septum is formed from the ring materials. Finally, the septum divides the cell in two approximately equal parts [28, 39, 146].

Growth rate The time required to produce one generation is called the generation time. This time depends on environmental conditions as well as on genetic traits of cells. If the number of cells doubles during a constant interval of time, growth is said to be exponential.

The relationship between the initial number of cells and their number after a period of exponential growth can be expressed mathematically by the formula $N = N_0 2^n$, where N_0 and N denote, respectively, the initial and final number of cells, and n is the number of new generations that occurred during the considered period of time. The generation time g can be calculated as t/n, where t is duration of growth. If W is the biomass of the population, then $\dot{W} \equiv dW/dt$ is its growth rate and $\dot{W}/W$ is the so-called specific growth rate, which characterises the growth rate relative to the size of the population. Since exponential growth is characterised by a constant specific growth rate, we have $\dot{W}/W = \text{const} = \mu$, whence $W(t) = W(0)e^{\mu t}$. Since $N/N_0 = W/W_0$, we have $2^n = e^{\mu t} = e^{\mu n g}$, whence we find that the doubling time g equals $(\ln 2)/\mu$.

Reserve components

In this section we review the components of a bacterial cell that underlie the storage of nutrients and which are mobilised to supply the central pools of core metabolites. In this thesis these components are usually called *reserves*.

Bacterial cells form the main chemical compounds that are essential for growth from the nutrients that are assimilated from the environment. About 50% d/w of a typical cell consists of carbon, which is a major element in all macromolecules in a cell. Nitrogen comprises about 12% d/w of a bacterial cell, and is a key element in proteins and nucleic acids. Other essential elements, such as phosphorus, sulfur, potassium, magnesium, and calcium are present in smaller amounts [109].

Prokaryotic cells may store nutrients in the form of metabolite pools, reserve compounds, granules, and other elemental inclusions, whose main function is to store energy and structural building blocks [8, 109, 120]. For instance, glycogen serves as a reserve compound for carbon and energy, whereas polyphosphate is a reservoir of inorganic phosphate, and magnetosomes represent storages of iron mineral magnetite. Figure 1.8 shows several examples of reserves in prokaryotic cells.

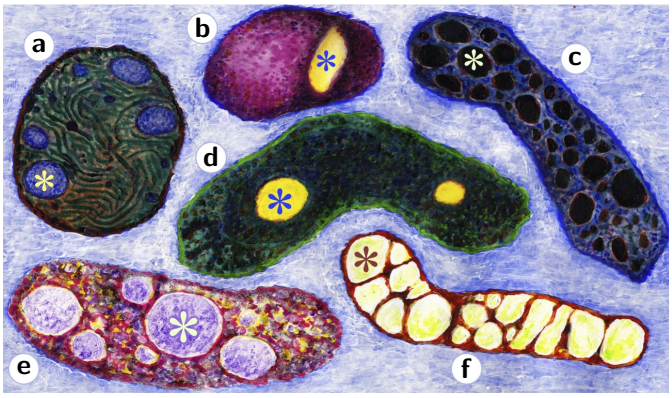

Figure 1.8: A variety of reserve inclusions in prokaryotes. Depicted are inclusions of (a): cyanophycin, *Anabaena variabilis* [168]; (b): sulfur, *Thermoanaerobacter sulfurigignens* [93]; (c): glycogen, *Methylacidiphilum fumariolicum* [80]; (d): polyphosphate, *Campylobacter jejuni* [50]; (e): polyhydroxybutyrate, *Rhodovibrio sodomensis* [98]; (f): triacylglycerol, *Rhodococcus opacus* [3].

Metabolism of prokaryotes

The chemical transformations within a cell that are required to maintain all essential processes for its life are collectively called metabolism [98]. The core pathways of a bacterial metabolism are schematically presented in Fig. 1.9.

To be able to drive cellular processes and to grow, micro-organisms have to process the nutrients assimilated from the environment to provide the cell with energy that is required to drive metabolism and to furnish the building blocks for the macromolecules; cells also have to remove waste products from the cell. Metabolic reactions are typically divided into two categories: catabolic reactions that involve the breaking down of organic substances, and accordingly release energy, and anabolic reactions that help to create cellular components, and therefore consume energy [98].

Energy can be transmitted in cells via reduction-oxidation reactions (or redox reactions) [133]. Such reactions occur in pairs which implies that for any substance called an electron donor to be oxidized, another substance called an electron acceptor must be reduced [141]. Energy released in these reactions is conserved primarily in the form of certain phosphorylated compounds, such as adenosine-$5'$-triphosphate (ATP), which is used to drive energy-requiring functions of the cell [109]. In addition, other energy-rich compounds, such as derivatives of coenzyme A (e.g. acetyl-CoA) can also be produced by the cell [59]. Long-term energy storage in prokaryotes typically involves glycogen, poly-β-hydroxybutyrate, polyphosphate, or elemental sulfur. These reserves can be used in the absence of an external energy source in order to drive growth or maintain cell integrity. On the other hand, if an external energy source is present, reserves are not required. Thus, the rate of reserve turnover is adjusted to demand. By contrast ATP is

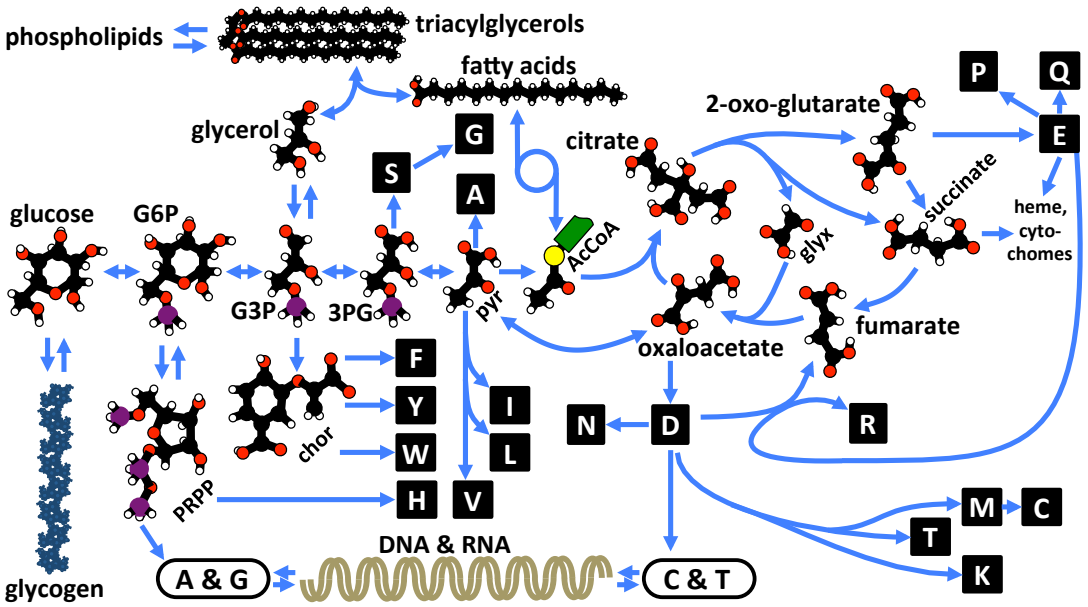

Figure 1.9: Core metabolism of *Escherichia coli*. Atoms are presented as follows: black for C, white for H, red for O, and purple for P. The main pathways are denoted by arrows: single-headed arrows for irreversible paths, and double-headed arrows for reversible paths. Single letter in circles indicate nucleotides. Single letters in squares indicate amino acids. Other denotions are as follows: **G6P** for glucose-6-phosphate, **PRPP** for phosphoribosyl-bisphosphate, **Chor** for chorismate, **G3P** for glyceraldehyde-3-phosphate, **3PG** for 3-phosphoglycerate, **Pyr** for pyruvate, **AcCoA** for acetyl-coenzyme A, and **glyx** for glyoxylate.

constantly turning over, produced via catabolic reactions and consumed via anabolic reactions [98].

Fermentation and respiration are two modes of regeneration of ATP. Both start from the break down of glucose in glycolysis, which consists of the three following steps: the first stage of preparatory reactions that lead to production of two three-carbon sugar phosphates (glyceraldehyde-3-phosphate); the second phase, where energy is released and conserved in the form of ATP and two molecules of pyruvate are formed; and the last step, in which the fermentation products ethanol and CO_2 (or lactate) are formed [21]. The redox reactions that occur during this process take place in the absence of a terminal electron acceptor. If oxygen or another terminal acceptor is present (e.g. an inorganic compound), it is not necessary to synthesise the fermentation products, since glucose can be oxidized completely to CO_2 leading to the increased production of ATP via the PMF. Thus in this case respiration process takes place, whose early two stages are the same as those of glycolysis, but the last stage occurs in the form of the pathway called a citric acid cycle (CAC), in which pyruvate is completely oxidizied to CO_2.

1.1.2 Eukaryotes

Eukaryotic cells are more complex and larger in size (at least 10 times by mass) than prokaryotic cells [98]. The main components of the eukaryotic cell are shown in Fig. 1.10. The main difference between prokary-

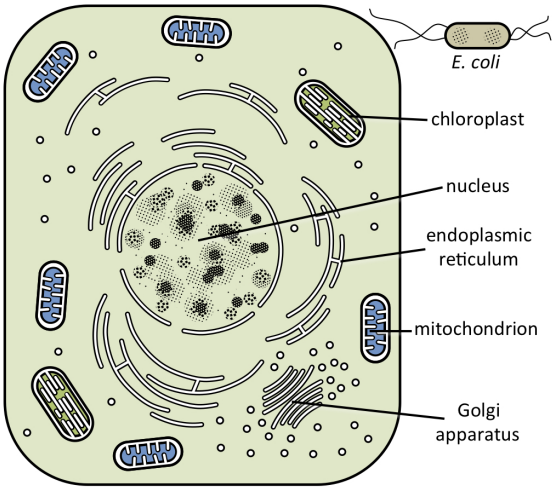

Figure 1.10: Differences between prokaryotic and eukaryotic cells. The *Escherichia coli* cell is much smaller than the typical eukaryotic cell, where membrane-bound organelles, such as chloroplast and mitochondria, are present. The nucleus of eukaryotes contains several chromosomes and is separated from the cytoplasm by an envelope. In addition, prokaryotes lack certain membranous structures, such as the Golgi apparatus, vacuoles, and the endoplasmic reticulum, which are present in eukaryotic cells.

otic and eukaryotic cells is that the latter contain membrane-bound cellular organelles that are not present in prokaryotic cells, most notably the nucleus, the endoplasmic reticulum, and the Golgi apparatus [55]. Moreover, prokaryotes lack a nucleolus, a subcellular structure that is involved in the synthesis of ribosomes [115]. The nuclear region in a typical prokaryotic cell contains a single chromosome that is not enveloped by a nuclear membrane, whereas in a standard eukaryotic cell it accommodates more than one chromosome and is surrounded by a double membrane layer that is contiguous with the endoplasmic reticulum. Another striking difference is the presence of mitochondria and chloroplasts in eukaryotes, organelles that have much in common with prokaryotic cells and be regarded as the descendants of endosymbiontic (cyano)bacteria [55]. Finally, the cell envelope in prokaryotic cells is more complex, both chemically and structurally, than in eukaryotic cells [85].

In this thesis I analyse data obtained in several micro-organisms (Fig. 1.11), such as the prokaryote *Escherichia coli*, which is a Gram-negative bacterium. Chapter 2 presents the data obtained for the eukaryotic micro-organism *Pavlova lutheri* (formerly known as *Monochrysis lutheri*), which is a haptophyte. Chapter 4 discusses regulation of intracellular nutrient storages in two eukaryotic micro-organisms: *Scenedesmus sp.*, which is a chlorophyte, and *Skeletonema costatum*, which is a diatom.

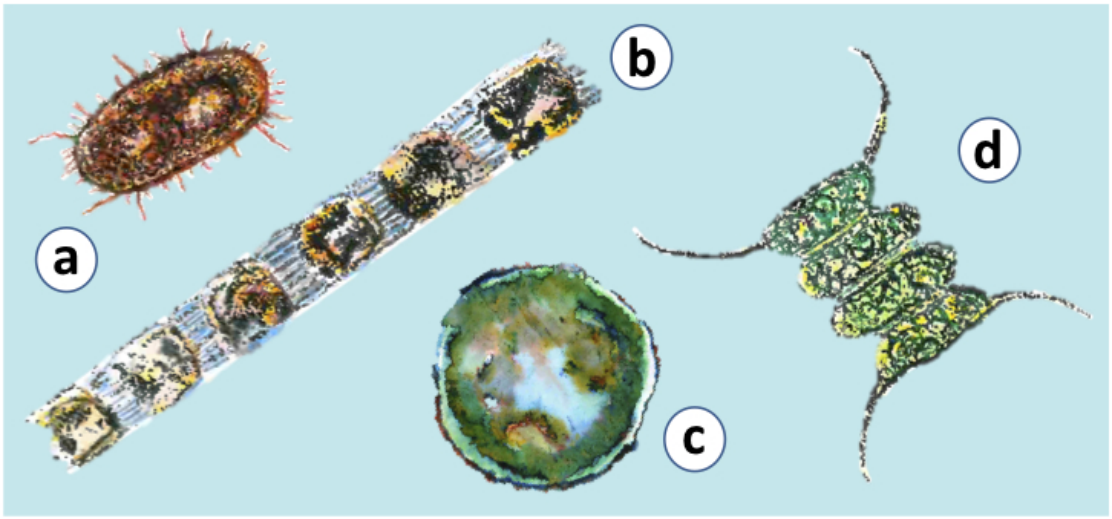

Figure 1.11: Four organisms investigated in this thesis: (a) the Gram-negative bacterium *Escherichia coli* [109], **(b)** the diatom *Skeletonema costatum* [1], **(c)** the haptophyte *Pavlova lutheri* [1], **(d)** the chlorophyte *Scenedesmus sp.* [1]

1.2 Standard culture systems

There are various ways of cultivating micro-organisms in bioreactors. The main methods of cultivation are batch cultivation and chemostat cultivation. There are several variations on these two types; examples include fed-batch cultivation or continuous cultivation with biomass retention [161].

1.2.1 Batch culture system

A batch culture is an enclosed vessel (e.g. tube or flask) whose contents are altered by the metabolic activities of the organisms growing inside the vessel [103]. The entire growth cycle of micro-organisms living in such a culture system can be divided into four stages: the lag phase, the exponential growth phase, the stationary phase, and the death phase [107]. The lag phase is typically observed if at least one of the following cases takes place: the population is inoculated in a fresh new medium; the population is transferred from a nutrient-rich medium to a nutrient-poor one; the population is old or the cells are damaged [98]. The exponential growth phase follows after the lag phase, and ends when the initial supply of nutrients runs out or accumulated waste products inhibit further growth (both factors can work together) [169]. Eventually, the growth rate becomes zero, and the population reaches a stationary phase, during which some cells begin to die and disintegrate; others may continue to divide [86]. Figure 1.12 illustrates these stages. If incubation continues, the population enters a death phase, during which the rate of death overtakes the rate of residual cells divisions and the colony as a whole exhibits an exponential rate of decline.

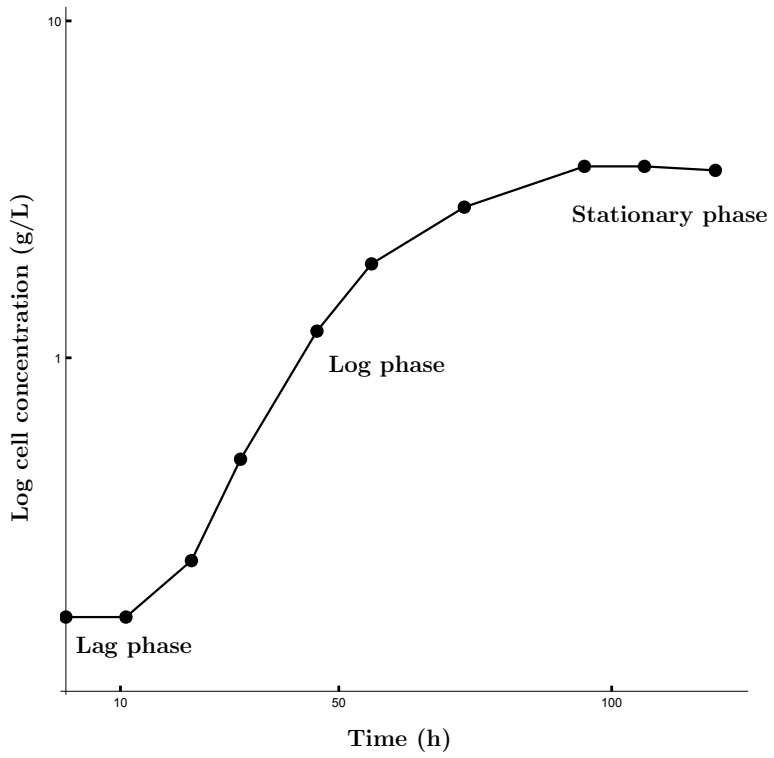

Figure 1.12: Growth cycle for bacterial cells in the batch culture. *Trichoderma reesei* data taken from [96].

The biomass-specific substrate consumption rate per unit of biomass of the population q_s $\left(\frac{\text{mol N}}{\text{mol W h}}\right)$ in the batch culture can be described as a function of the nutrient concentration $[\text{N}]$ $\left(\frac{\text{mol N}}{\text{L}}\right)$ by means of the Michaelis-Menten equation [104]:

$$q_s = q_{\text{s,max}} \frac{[\text{N}]}{K_m + [\text{N}]} \,, \tag{1.1}$$

where $q_{\text{s,max}}$ $\left(\frac{\text{mol N}}{\text{mol W h}}\right)$ represents the maximum substrate consumption rate, and K_m $\left(\frac{\text{mol N}}{\text{L}}\right)$ is the Michaelis-Menten constant, which denotes the concentration of the substrate at the half-maximal consumption rate [153]. Equation (1.1) can be derived by investigating the kinetics of an enzymatic reaction mechanism, i. e. by relating a reaction rate v to the concentration of a substrate $[\text{S}]$. The mathematical model of such reaction proposed by L. Michaelis and M. Menten [104] can be schematically presented as follows:

$$\text{E} + \text{S} \underset{\text{k}_{\text{rev}}}{\overset{\text{k}_{\text{for}}}{\rightleftarrows}} \text{ES} \xrightarrow{k_{\text{cat}}} \text{P} + \text{E} \,, \tag{1.2}$$

where E is an enzyme binding to a substrate S to form an enzyme-substrate complex ES, which delivers a product P as well as releases the original enzyme E. The first step of this reaction is a reversible process (shown by the double arrows in eqn (1.2)), whereas the second step is non-reversible (shown by the single arrow in eqn (1.2)). The parameters k_{for}, k_{rev}, and k_{cat} denote, respectively, the forward, reverse,

and catalytic reaction rate constants. Since $d[\mathrm{ES}]/dt = 0$, we have:

$$k_{\mathrm{for}}[\mathrm{E}][\mathrm{S}] - k_{\mathrm{rev}}[\mathrm{ES}] - k_{\mathrm{cat}}[\mathrm{ES}] = 0 \,,$$

hence

$$[\mathrm{E}] = K_m \frac{[\mathrm{ES}]}{[\mathrm{S}]} \quad \text{with } K_m = \frac{k_{\mathrm{rev}} + k_{\mathrm{cat}}}{k_{\mathrm{for}}} \,.$$

The reaction rate v equals to $d[\mathrm{P}]/dt = k_{\mathrm{cat}}[\mathrm{ES}]$, and thus we obtain:

$$v = \frac{v_{\max}}{1 + K_m/[\mathrm{S}]} \quad \text{with } v_{\max} = k_{\mathrm{cat}}[\mathrm{E}_0] \,,$$

where $[\mathrm{E}_0] = [\mathrm{E}] + [\mathrm{ES}] = [\mathrm{ES}](1 + K_m/[\mathrm{S}])$ is the initial (free) enzyme concentration. Replacing v with q_s and $[\mathrm{S}]$ with $[\mathrm{N}]$, we obtain eqn (1.1).

In a general case, where the cooperativity between different binding sites of the same enzyme is taken into account, eqn (1.1) can be extended to the Hill equation [70]:

$$q_s = q_{\mathrm{s,max}} \frac{[\mathrm{N}]^n}{K_m^n + [\mathrm{N}]^n} \,, \tag{1.3}$$

where n is the Hill coefficient that describes the degree of interaction (cooperativity) between different binding sites of the same enzyme. The Hill coefficient $n = 1$ will be used throughout this thesis for the sake of simplicity. Whereas $n = 1$ has been confirmed for numerous systems (e.g. [41, 123]), the case $n > 1$ may be appropriate for certain uptake systems (e.g. [91]); however, the general principles of the dynamic reallocation theory carry through provided the functional response is monotonically increasing.

The Pirt equation [118] describes the relation between q_s and the specific growth rate $\mu(1/\mathrm{h})$ during the exponential phase:

$$q_s = \mu / Y_{\mathrm{s,max}} + m_s \,, \tag{1.4}$$

where $Y_{\mathrm{s,max}} \left(\frac{\mathrm{mol\ W}}{\mathrm{mol\ N}}\right)$ is the maximum yield of biomass, and $m_s \left(\frac{\mathrm{mol\ N}}{\mathrm{mol\ W\ h}}\right)$ is a maintenance coefficient, which shows the biomass-specific rate of substrate consumption to maintain activities performed by the micro-organism in the absence of growth. Since $\mu = \dot{W}/W$, where W is the biomass of the population and the dot indicates the differentiation in respect to time (cf. Section 1.1.1), we have:

$$\dot{W} = Y_{\mathrm{s,max}}(q_s - m_s)W \,,$$

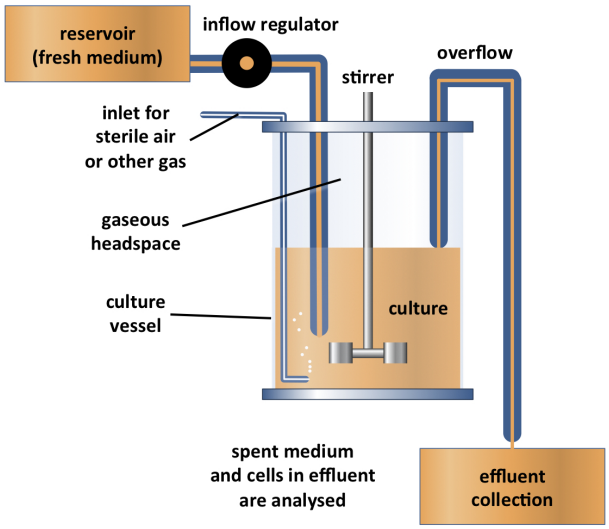

Figure 1.13: The chemostat. The main vessel contains a well-stirred culture medium, which is replenished from the reservoir. The culture vessel maintains a constant volume of culture, since the inflow of a fresh medium from the reservoir equals the outflow of a spent medium (overflow) from the vessel.

and together with eqn (1.1) this yields:

$$\dot{W} = Y_{\mathrm{s,max}} \left(q_{\mathrm{s,max}} \frac{[\mathrm{N}]}{K_m + [\mathrm{N}]} - m_s \right) W \,. \tag{1.5}$$

The following conservation law applies if intracellular reserves do not vary:

$$[\mathrm{N}]_0 = [\mathrm{N}] + W/(Y_{\mathrm{s,max}} V) + m_s/V \int_0^\tau W(\tau) d\tau \,, \tag{1.6}$$

where $[\mathrm{N}]_0 \left(\frac{\mathrm{mol\ N}}{\mathrm{L}}\right)$ expresses the initial nutrient concentration and $V(\mathrm{L})$ is the volume of the medium in which the culture is grown. This allows us to obtain a system of differential equations for W and $[\mathrm{N}]$.

1.2.2 Chemostat culture system

For many studies it is advantageous if cultures can be maintained in constant environmental conditions for long periods, which is not possible with closed cultures of the batch type, since the culture is always undergoing dynamical change in the latter type of culture. However, such steady-state conditions can be achieved in a continuous-flow culture, or chemostat (Fig. 1.13). The cultivation in the chemostat is characterised by a continuous supply of fresh medium and withdrawal of an equal volume of cultivation broth, which allows the cultivation volume to remain constant [37]. After a certain time the system reaches a state in which the chemostat volume, the cell number, and the nutrient status remain constant; the system is then said to be in steady state.

In the chemostat, both growth rate and population density can be controlled independently and si-

multaneously. To provide such control, the experimenter can manipulate two key parameters: the first parameter is dilution rate $D = F/V\,(1/\mathrm{h})$, where $V\,(\mathrm{L})$ is the volume of the main vessel, and $F\,(\mathrm{L/h})$ is the flux at which fresh medium is pumped in, and spent medium is removed from, the chemostat; and the second parameter is the concentration of limiting nutrients $[\mathrm{N}]_R\,(\mathrm{mol\ N/L})$ in the reservoir. Varying the dilution rate, different growth rates can be achieved.

The balance equation for biomass concentration $[W]\,(\mathrm{mol\ W/L})$ in the chemostat of volume V is as follows:

$$\frac{d(V[W])}{dt} = \mu V[W] - F[W]\,, \tag{1.7}$$

where μ is a biomass-specific growth rate [153]. Since the vessel volume V remains constant in time, we have:

$$\frac{d[W]}{dt} = \mu[W] - \frac{F}{V}[W]\,. \tag{1.8}$$

The balance equation for nutrient concentration $[\mathrm{N}]$ in the main vessel is as follows:

$$\frac{d[\mathrm{N}]}{dt} = \frac{F}{V}\left([\mathrm{N}]_R - [\mathrm{N}]\right) - \widetilde{\sigma}_W \mu[W]\,, \tag{1.9}$$

where $[\mathrm{N}]_R$ is the nutrient concentration in the reservoir, and $\widetilde{\sigma}_W\,(\mathrm{mol\ N/mol\ W})$ is a stoichiometric coefficient [153]. At steady state, the concentration of biomass $[W]$ and the concentration of nutrient in the culture vessel $[\mathrm{N}]$ do not change in time, so that $d[W]/dt = 0$, and $d[\mathrm{N}]/dt = 0$. Hence we obtain the following steady-state chemostat equations:

$$\mu = D\,; \qquad [\mathrm{N}] = [\mathrm{N}]_R - \widetilde{\sigma}_W[W]\,, \tag{1.10}$$

where $D = F/V$– dilution rate. The first equation shows that by setting the dilution rate D of the chemostat to a certain value, we are able to cultivate micro-organisms at specific growth rate equal to D, which makes the chemostat an important laboratory tool to study the physiology of microbes under well-defined conditions (constant growth rate, constant environmental conditions) or to examine how the growth rate affects, for instance, the rate of product formation. Figure 1.14 shows how bacterial concentration $[W]$, bacterial yield Y, doubling time g, and nutrient concentration $[\mathrm{N}]$ depend on the dilution rate at the steady state in the chemostat [130]. Calculations based on the steady-state chemostat eqns (1.10) together with the Monod equation $\mu([\mathrm{N}]) = \widehat{\mu}\,(1 + K_S/[\mathrm{N}])^{-1}$ [107] (which was originally proposed as a purely empirical equation, where $\widehat{\mu}\,(1/\mathrm{h})$ is an asymptotic lowest upper bound to the growth rate, and $K_S\,(\mathrm{mol\ N/L})$

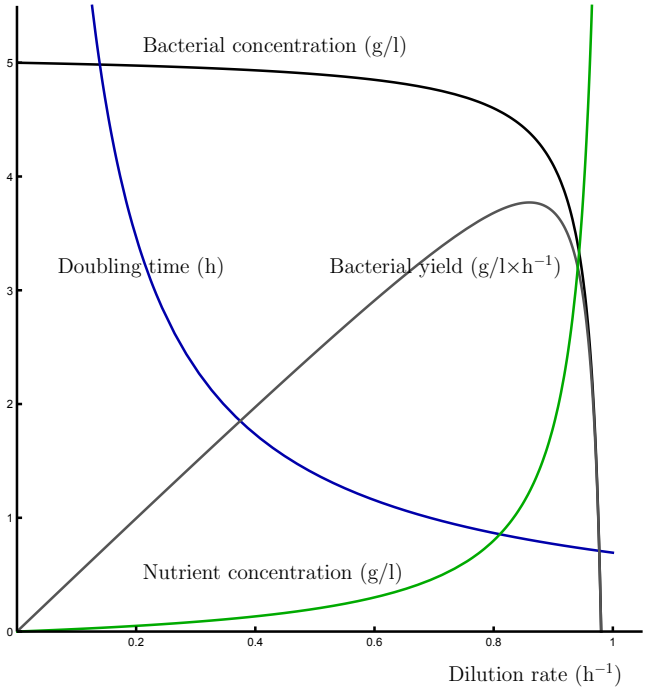

Figure 1.14: Steady-state relationships in the chemostat. Relationship between bacterial concentration, bacterial yield, doubling time, and nutrient concentration in the steady state depending on different dilution rates in the chemostat described by eqns (1.11) with parameters $\widehat{\mu} = 1$ h^{-1}, $K_S = 0.2$ g/l, $\widetilde{\sigma}_W = 1$, $[N]_R = 10$ g/l.

is the nutrient concentration at which $\mu = 0.5\widehat{\mu}$) yield the following expressions which describe these relationships:

$$\begin{aligned} [W] &= \left([\mathrm{N}]_R - \frac{DK_S}{\widehat{\mu} - D} \right) \widetilde{\sigma}_W^{-1} \, ; \\ g &= (\ln 2)/D \, ; \\ Y &= D \left([\mathrm{N}]_R - \frac{DK_S}{\widehat{\mu} - D} \right) \widetilde{\sigma}_W^{-1} \, ; \\ [\mathrm{N}] &= \frac{DK_S}{\widehat{\mu} - D} \, . \end{aligned} \tag{1.11}$$

Chemostat systems allow us to maintain a culture growing at a chosen constant relative growth rate for a long period of time, as well as to repeat experiments under the same conditions, which facilitates the study of competitiveness of different organisms under the same environmental conditions. Competition between various species or strains of a single species can be exploited to eliminate all but one, and thus the chemostat can be used as a tool to isolate specific types of bacteria, which can subsequently be studied in more detail [98]. Moreover, under certain specific conditions, such as nutrient shortage, long-term chemostat cultivation leads to adaptation of the cells to these conditions, which suggests that the chemostat can also be used in evolutionary engineering.

1.3 Mathematical models of microbial growth

Models of bacterial growth can be in general written as

$$\dot{W} = \mu(\mathbf{x}, \mathbf{u})W \ , \tag{1.12}$$

where $W \in \mathbb{R}^+$ is a suitable measure of biomass, $\mathbf{x} \in \mathbb{R}^p$ represents the internal state, $\mathbf{u} \in \mathbb{R}^q$ represents external conditions that affect growth and metabolism, μ is a function $\mathbb{R}^{p+q} \mapsto \mathbb{R}^+$, called the *model*, and the dot indicates differentiation with respect to time [24]. Here, W, $\mathbf{x}$, and $\mathbf{u}$ are all allowed in general to be functions of time t. Classic models tend to be characterised by $p = 0$ or $p = 1$ (i. e. they have little or no structuring in terms of the internal state), whereas detailed 'system biology' or 'in silico' models can have very large p, on the order of hundreds or thousands [38].

1.3.1 Classic macroscopic models

Models are specified by the choice of the function $\mu : \mathbb{R}^{p+q} \mapsto \mathbb{R}^+$. For instance, the Monod model is as follows:

$$\mu([\mathrm{N}]) = \widehat{\mu}\,(1 + K_S/[\mathrm{N}])^{-1} \ , \tag{1.13}$$

where [N] is the ambient concentration of the limiting nutrient and $\widehat{\mu}$ and K_S are positive parameters [107]. As Monod pointed out [107], the parameter K_S should not be confused with the parameter K_m in eqn (1.1). In terms of our general description, eqn (1.12), $p = 0$ and $q = 1$: there are no state variables other than W and there is a single environmental variable, [N], on which the specific growth rate μ depends. If we allow [N] to vary in time, we have $W(t) = W_0 \exp\left\{\int_0^t \mu\left([\mathrm{N}](\tau)\right) d\tau\right\}$. One way to extend this model to $q > 1$, but still with $p = 0$, is to posit a multiplicative form $\mu(u_1, u_2, \dots) = \widehat{\mu} f_1(u_1) f_2(u_2) \cdots$ [26, 56], where the $u_1, u_2, \dots$ are relevant environmental factors (such as levels of light, nutrients, and redox substrates) and the $f_1, f_2, \dots$ are appropriate functions $\mathbb{R}^+ \mapsto [0, 1]$ that express how these factors affect growth.

Another approach is used by Pirt [74, 118], who proposed eqn (1.4) to describe the relationship between the the specific growth rate μ and consumption rate q_s of the substrate used as an energy source.

A related concept known as an 'endogenous metabolism' was introduced by Herbert [67] to study the dependence between the growth yield and the growth rate:

$$\dot{W} = (\mu - a)W \ , \tag{1.14}$$

where the term aW is the expenditure of the organism for the 'endogenous metabolism', which is essentially equal to the maintenance energy. This idea was further developed by Marr et al. [100] in the following equation, proposed as an empirical description for continuous culture (chemostat) data:

$$\frac{1}{W} = \frac{a}{W_{\max}} \frac{1}{D} + \frac{1}{W_{\max}} , \tag{1.15}$$

where D is the dilution rate of the chemostat and $W_{\max}$ corresponds to the maximum possible biomass concentration.

In the opposite situation, when growth is assumed to depend on the internal state of the micro-organism only, so that $p = 1$ and $q = 0$, we obtain another modelling subclass, whose most-studied member is perhaps the Droop equation [36]:

$$\mu(Q) = \widehat{\mu}(1 - Q_0/Q) . \tag{1.16}$$

Here, Q characterises the internal state of the cell, namely, the internal nutrient 'pool' called the cell quota, which comprises the particle species of interest in any of its biomolecular speciations (e.g. free molecules, part of polymers, machinery etc.). By definition, the cell quota is the intracellular density of the chemical element of interest (amount per cell), which can roughly be thought of as an average concentration [35]. The parameter Q_0 is the so-called 'subsistence quota', which can be interpreted as the minimum cell quota required by the cell to maintain its structural integrity. Growth at a non-zero rate requires $Q > Q_0$. A similar equation was proposed by Caperon [16] in the following form:

$$\mu(q) = \widehat{\mu} q (q + A)^{-1} , \tag{1.17}$$

where q expresses the reserve nutrient content of the cell, and A is the so-called growth kinetic constant, which Caperon identified with Q_0 [15]. In terms of the Droop model, $q = Q - Q_0$.

Although these macroscopic models are attractive due to their mathematical tractability, more detailed information regarding the physiological properties or state of the micro-organism might be required for an accurate account of macromolecular kinetics for the limiting situations, such as the existence of various limiting nutrients in the environment or the presence of starvation periods, when external supplies are insufficient to cover maintenance (endogenous metabolism) requirements.

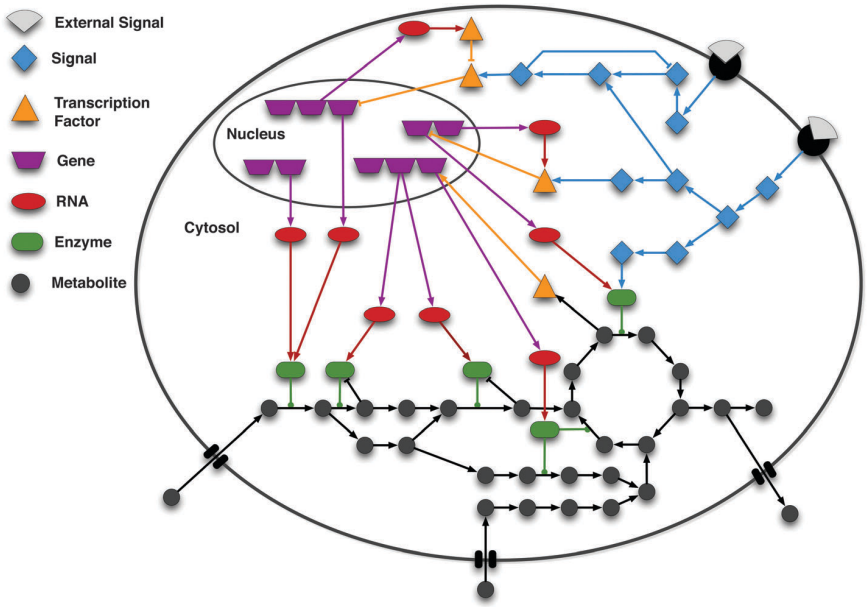

Figure 1.15: Schematic representation of signalling, gene regulation and metabolic network inside of the cell (taken from [53]). Edges of the graph represent the interactions between the molecules. In particular, activating interactions are shown by arrow shaped edges; inhibitory interactions by blunt edges; and enzyme reaction catalyses are edges with a circle on the top end.

1.3.2 Microscopic models

Regarding models with $p > 1$, one might decide to account explicitly for the position and movement of every molecule inside the cell ($p \sim 10^8$) or at least for the concentrations of all molecular species. Microscopic models in most of the cases are focused on specific subsystems of the cell describing either metabolism, gene expression, or signal transduction [53]. These models typically define cellular processes as interactions between a large number of biological molecules that can be described as networks by means of graphs with nodes connected via edges [83] as schematically shown in Fig. 1.15. Depending on the specific properties of the given biological network under consideration, different formalisms can be employed to simulate its dynamic behaviour.

In the case of signalling and regulatory networks, formalisms range from Boolean approaches used for large-scale network representation [51, 54, 79, 84, 108, 162], to ODEs whose use appears to be restricted to small and/or medium-sized networks [71, 81]. Signalling and regulatory networks describe signal flows, whereas metabolic networks support mass and energy flows, which makes logical or Boolean methods perhaps less suitable to simulate metabolism [53]. Metabolic networks are typically represented by means of a constraint-based approach [44]. Authors of this modelling class employ various techniques including flux balance analysis, metabolic flux analysis, pathway analysis by elementary modes, or extreme pathways [129]. For example, the method of extreme pathways has been applied to study the

regulation of metabolism in human red blood cells [121], whereas flux balance analysis has been used to investigate the yield-optimal behaviour of *Escherichia coli* in dependence of oxygen availability [160]. Other techniques have been employed, for instance, to model the electron transport chain of mitochondria [5] or to describe the kinetics of the electron transport chain of purple non-sulfur bacteria [82].

The construction and analysis of models that are capable of describing the cell as a whole system is challenging. One good example is the model of central metabolism of *Escherichia coli*, where the state variables are metabolite concentrations, gene expression levels, transcription factor activities, metabolic fluxes, and biomass concentration [38].

Although the micro-chemical approach seems to be straightforward, the models of this class typically have high-dimensional state spaces (i.e., a large number of dynamic degrees of freedom: the latter was represented in Section 1.3.1 by p) and substantial parametrization problems, and therefore may become unattractive due to their complexity.

1.3.3 Variable-Internal-Stores-with-reallocation model

The cases $p = 0$ and $p \sim 10^8$ represent the opposite ends of a range, on which the modeller has to choose an optimal compromise in accordance with the available information and the purpose of the modelling exercise. Given that the dynamics of other intracellular compounds besides structural biomass is often physiologically relevant, this thesis will focus on models where $p \neq 0$. Our modelling strategy is to try to formulate models that (i) are sufficiently versatile to accommodate detailed information, particularly 'big data' such as transcriptomics, proteomics, and metabolomics, (ii) are consistent with basic principles such as conservation laws, (iii) remain relatively tractable, and, in particular, reduce to the simple classic models as special cases. Variable-Internal-Stores (VIS) models [35, 61, 165] fulfil these desiderata. The point of departure is to consider the dependence of the growth not only on nutrient influx from the environment, but also on reserve levels inside of the cell (cf. Section 1.1.1). Taking into account internal stores allows for an accurate description of the rates of resource consumption and bioproduction yields [24]. A basic example of the VIS model with a single internal variable store is the Droop cell quota model [35] discussed in Section 1.3.1.

In addition to internal stores (reserves), this thesis will consider variations in the distribution of molecular building blocks among various types of molecular machinery [10, 152]. This allocation of building blocks is an important dynamic variable [95], since both prokaryotes and eukaryotes adjust expression

of genes in response to changes in external conditions as well as in the status of internal availability of substrate [109], as discussed in Section 1.1.1, and changes in the gene expression profile are reflected in corresponding changes in the relative rates at which molecular building blocks are incorporated in molecular machinery [90].

The VIS-with-reallocation model achieves mathematical closure in the form of regulatory rules that drive this re-allocation. In this thesis, I show how these regulatory rules (r-functions) can be reconstructed by combining stoichiometric constraints with experimental observations of the behaviour of micro-organisms in response to changes in environmental conditions.

With such a model in hand, I investigate the question of adaptive microbial behaviour depending on ambient conditions, in particular, under nutrient shortage and time-varying environmental conditions.

1.4 Introduction to publications

This section previews subsequent chapters of this thesis that have been derived from peer-reviewed papers. Certain basic equations and figures in these chapters are repeated to render the individual chapters self-contained. Such equations and figures will be cited locally in each chapter.

Variable-Internal-Stores models of microbial growth and metabolism with dynamic allocation of cellular resources

Variable-Internal-Stores models of microbial metabolism and growth have proven to be invaluable in accounting for changes in cellular composition as microbial cells adapt to varying conditions of nutrient availability. Here, such a model is extended with explicit allocation of molecular building blocks among various types of catalytic machinery. Such an extension allows a reconstruction of the regulatory rules employed by the cell as it adapts its physiology to changing environmental conditions. Moreover, the extension proposed here creates a link between classic models of microbial growth and analyses based on detailed transcriptomics and proteomics data sets. We ascertain the compatibility between the extended Variable-Internal-Stores model and the classic models, demonstrate its behaviour by means of simulations, and provide a detailed treatment of the uniqueness and the stability of its equilibrium point as a function of the availabilities of the various nutrients.

Full citation: Nev O. A. and van den Berg H. A. (2017) Variable-Internal-Stores models of microbial growth and metabolism with dynamic allocation of cellular resources. *J. Math. Biol.*, 74 (1), 409–445.

Microbial metabolism and growth under conditions of starvation modelled as the sliding mode of a differential inclusion

We consider a model of bacterial growth with variable internal stores, extended with adaptive resource allocation and investigate the behaviour of this model under conditions of starvation, i.e. severe nutrient shortage, treating the behaviour under the starvation regime in terms of a differential inclusion and derive Filippov solutions. This Filippov sliding mode representation appears to be a simple but sound qualitative description of metabolic 'shut down' in response to starvation. We discuss a natural connection between biologically motivated modelling approaches to metabolic 'shut down' and numerical regularisation techniques to approximate Filippov solutions.

Full citation: Nev O. A. and van den Berg H. A. (2017) Differential inclusions with sliding modes to represent microbial metabolism and growth under conditions of starvation. *Dyn. Systems*. In press, doi: 10.1080/14689367.2017.1298726.

Optimal management of nutrient reserves in micro-organisms under time-varying environmental conditions

Intracellular reserves are a conspicuous feature of many bacteria; such internal stores are often present in the form of inclusions in which polymeric storage compounds are accumulated. Such reserves tend to increase in times of plenty and be used up in times of scarcity. Mathematical models that describe the dynamical nature of reserve build-up and use are known as 'cell quota,' 'dynamic energy/nutrient budget,' or Variable-Internal-Stores models. Here we present a stoichiometrically consistent macro-chemical model that accounts for variable stores as well as adaptive allocation of building blocks to various types of catalytic machinery. The model posits feedback loops linking expression of assimilatory machinery to reserve density. The precise form of the 'regulatory law' at the heart of such a loop expresses how the cell manages internal stores. We demonstrate how this 'regulatory law' can be recovered from experimental data using several empirical data sets. We find that stores should be expected to be negiglibly small in stable growth-sustaining environments but prominent in environments characterised by marked fluctuations on time scales commensurate with the inherent dynamic time scale of the organismal system.

Full citation: Nev O. A., Nev O. A. and van den Berg H. A. (2017) Optimal management of nutrient reserves in micro-organisms under time-varying environmental conditions. *J. Theor. Biol.*, 429, 124–141.

Chapter 2

Variable-Internal-Stores models of microbial growth and metabolism with dynamic allocation of cellular resources

2.1 Introduction

Models of bacterial growth can be written as $\dot{W} = \mu(\mathbf{x},\mathbf{u})W$, where $W \in \mathbb{R}^+$ is a suitable measure of biomass, $\mathbf{x} \in \mathbb{R}^p$ represents the internal state, $\mathbf{u} \in \mathbb{R}^q$ represents external conditions that impinge on $\dot{W}$, and the dot indicates differentiation with respect to time [24]. A basic model in this class specifies $\mu([\mathrm{N}]) = \widehat{\mu}\,(1+K_S/[\mathrm{N}])^{-1}$, where [N] is the ambient concentration of the limiting nutrient and $\widehat{\mu}$ and K_S are positive parameters [107]. Here, $p = 0$ and $q = 1$: there are no state variables other than W and there is a single environmental variable on which the specific growth rate μ depends. We allow [N] to vary in time so that $W(t) = W_0 \exp\left\{\int_0^t \mu\,([\mathrm{N}](\tau))\,d\tau\right\}$. One way to extend this model to $q > 1$, but still with $p = 0$, is to posit a multiplicative form $\mu(u_1,u_2,\dots) = \widehat{\mu} f_1(u_1) f_2(u_2)\cdots$ [26, 56], where the $u_1,u_2,\dots$ are salient environmental factors (such as levels of light, nutrients, redox substrates) and the $f_1,f_2,\dots$ are appropriate functions $\mathbb{R}^+ \mapsto [0,1]$ that express how these factors affect growth.

Regarding models with $p > 0$, one might decide to account explicitly for the position and movement of every molecule inside the cell ($p \sim 10^8$) or at least for the concentrations of all molecular species ($p \sim 10^3$–10^5, depending on how species are defined [38]). The cases $p = 0$ and $p \sim 10^8$ represent opposite ends of a spectrum; which of the two is more suitable depends on the available information as well as the purpose at hand; we are often interested in the rates at which other compounds besides the biomass are

being produced, and this typically requires physiological structuring beyond $p = 0$. Our point of departure is a class of models that lies at a mid-way point on this spectrum, with p somewhere between 1 and a few dozen, known as Variable-Internal-Stores (VIS) models [35, 61, 165]. Taking into account internal stores, which in prokaryotes occur as metabolite pools, reserve compounds, and elemental inclusions [8, 109, 120], allows an accurate description of the rates of resource consumption and bioproduction yields [24].

In addition to VIS, we consider variations in the distribution of molecular building blocks among various types of molecular machinery [10, 152]. It is *a priori* likely that this allocation of building blocks is an important dynamic variable [95]; expression of genes is modulated, in prokaryotes as in eukaryotes, in response to changes in external conditions as well as in the status of internal availability of substrate [109], and changes in the gene expression profile are reflected in corresponding changes in the relative rates at which molecular building blocks are incorporated into molecular machinery [90]. Furthermore, in prokaryotes, the ability to adjust resource re-allocation among catalytic machinery has been shown to be an evolutionarily relevant trait, at least for certain kinds of ecological life history [156]. Finally, VIS-with-reallocation models should enable the reconstruction of regulatory rules that drive this re-allocation by combining stoichiometric constraints with observations of transient behaviour following changes in environmental conditions. For instance, in a continuous-culture system, such perturbations can be imposed by the experimenter and the response measured in terms of cellular composition, cellular density, as well as consumption and production of relevant chemical species (e.g. [26]).

The present paper describes the basic structure of VIS-with-reallocation models, taking care to distinguish fundamental stoichiometric principles such as mass conservation from the constitutive relations that express these regulatory rules. We discuss the compatibility of this new class of models with well-established empirical laws in microbial growth and metabolism, as well as the observability of these constitutive relations. Moreover, we prove the uniqueness and stability of the equilibrium point under a reasonable assumption on the general appearance of the constitutive relations.

2.2 Variable-Internal-Stores with dynamic allocation theory

The model consists of stoichiometric equations, which are based on standard chemical conservation principles, presented in Section 2.2.1, and constitutive relations, which express specific assumptions regarding the regulatory control pathways; one simple choice is discussed in Section 2.2.2. A schematic representation of the model (for $n = 2$) is given in Fig. 2.1. Notation is summarised in Table 2.1, and key simplifying

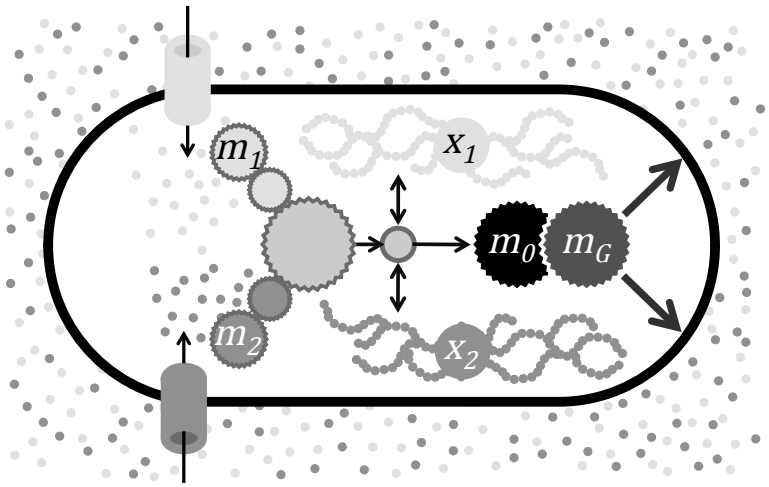

Figure 2.1: Schematic representation of the model described by the system (2.8) for the case $n = 2$. Two types of nutrients are assimilated by dedicated pathways (m_1 and m_2) that feed into core metabolism from which building blocks are sluiced to machinery synthesis (m_0) and growth (m_G). Core metabolism also exchanges molecular building blocks with reserves (x_1 and x_2).

assumptions are summarised in Table 2.2.

Table 2.1: Notation employed in the equations describing the model

Symbol	Biological interpretation	Units
State unscaled variables		
$M_i \quad i \in \{0,1,\ldots,n,G\}$	C-molar amount of i-type molecular machinery	Moles of carbon
$X_j \quad j \in \{1,\ldots,n\}$	Molar amount of the primary element X_j in a reserve j	Moles of the primary element in a reserve
W	C-molar amount of the structural component	Moles of carbon
$\widetilde{\mu}$	Specific growth rate	Per unit of time
State scaled variables		
$m_i \quad i \in \{0,1,\ldots,n,G\}$	Density of i-type molecular machinery	Dimensionless
$x_j \quad j \in \{1,\ldots,n\}$	Density of a reserve j	Dimensionless
μ	Specific growth rate	Dimensionless
Unscaled stoichiometric coefficients		
$\widetilde{\phi}_i \quad i \in \{0,1,\ldots,n,G\}$	The rate of production of the machinery of type i	Units of M_i per unit of M_0 per unit of time
$\widetilde{\psi}_{ji} \quad i,j \in \{1,\ldots,n\}$	The gain of reserve j per unit machinery of type i	Units of X_j per unit of M_i per unit of time
$\widetilde{\sigma}_{jW} \quad j \in \{1,\ldots,n\}$	The loss of reserve j for growth	Units of X_j per unit of W
$\widetilde{\sigma}_{ji} \quad i \in \{0,1,\ldots,n,G\}$ $j \in \{1,\ldots,n\}$	The loss of reserve j for synthesis of the machinery of type i	Units of X_j per unit of M_i
$\widetilde{\psi}_W$	The rate of production of the structural component	Units of W per unit of M_G per unit of time

Table 2.1: Notation employed in the equations describing the model

Symbol	Biological interpretation	Units
Scaled stoichiometric coefficients		
ψ_{ji} $i,j \in \{1,\ldots,n\}$	The gain of reserve j per unit machinery of type i	Dimensionless
σ_{ji} $i \in \{0,1,\ldots,n,G\}$ $j \in \{1,\ldots,n\}$	The loss of reserve j for synthesis of the machinery of type i	Dimensionless
ψ_W	The rate of production of the structural component	Dimensionless
Constitutive relationships		
α_i $i \in \{0,1,\ldots,n,G\}$	Portion of the zero-machinery devoted to the synthesis of machinery of type i	Dimensionless
$\widetilde{r}_i$ $i \in \{0,1,\ldots,n,G\}$	Concentration of translationally active mRNA for the machinery of type i	Units of concentration
r_i $i \in \{0,1,\ldots,n,G\}$	Scaled variable for the $\widetilde{r}_i$	Dimensionless
K	Slope of the increasing part of the piecewise function r_G	Dimensionless
ε	Defines the interval on the abscissa for the increasing part of the piecewise function r_G	Dimensionless
Miscellany		
n	Number of chemical species of nutrient	
$\hat{\hat{\phi}}_i$ $i \in \{1,\ldots,n\}$	Maximum rate of the flux through the assimilatory machinery of type i	Units of nutrient per unit of M_i per unit of time
f_i $i \in \{1,\ldots,n\}$	Defines the ambient conditions for the nutrient i	Dimensionless
$\mathbf{R}$	Chemical composition of the reserves as an $n \times n$ matrix	
$\mathbf{N}$	Chemical composition of the nutrients as an $n \times n$ matrix	
γ_{ji} $i,j \in \{1,\ldots,n\}$	(j,i)th element of $\mathbf{R}^{-1} \cdot \mathbf{N}$	Dimensionless
$\hat{m}$	Scaling parameter for M_0/W	Units of M_0 per unit of W

Table 2.2: Assumptions used in the analysis of the model

Assumption	Biological interpretation
$\sigma_{ji} = \sigma_j$ for all i $i,j \in \{1,\ldots,n\}$	Amounts of reserves expended on the synthesis of different types of machineries are the same
$\psi_{ji} = 0$ whenever $j \neq i$ $i,j \in \{1,\ldots,n\}$	The elemental ratios of the reserves are identical to the elemental ratios of the nutrients
$\widetilde{r}_0$ is constant	Constitutive expression (housekeeping mRNA)

2.2.1 Stoichiometric equations

Basic definitions and dynamics

The bacterial cell is conceptually divided into several components, comprising molecular machinery, reserve compounds, and a structural component. The latter includes the cell envelope, genetic material, and core metabolites, small molecules that occur as intermediates of catabolic and anabolic pathways that are maintained at appropriate cellular concentrations by mechanisms not represented explicitly in the model. The C-molar amount of the structural component will be denoted as W.

Molecular machinery is divided into $n+2$ components, where n is the number of chemical species of nutrient for which we wish to account (this choice is informed by available data as well as the envisaged application of the theory). Components 1 through n represent the apparatus dedicated to the assimilation of the corresponding nutrients (transporters, binding proteins), in addition to the catalytic machinery that transforms these nutrients into core metabolites. Component 0 is the machinery required to synthesise machinery. Component $n+1$, which will be given the subscript G, represents machinery devoted to growth, that is, the synthesis of the cell envelope and duplication of the genome. The C-molar amounts of these $n+2$ types of machinery will be denoted as M_i.

Reserve components correspond to storage of nutrients which is mobilised by the cell to replenish the central pools of core metabolites. We allow for n distinct types of such variable internal stores. Certain reserves can be quantified in terms of C-moles, such as organic polymers such as poly-β-hydroxybutyrate, saccharides, as well as storage proteins, whereas others, such as sulphur globules and polyphosphate inclusions that contain no carbon [120], are expressed in terms of molar amounts of the primary element X_j. These X_j-molar amounts (where X_j is possibly but not necessarily C) will be denoted as X_j.

Although machinery is a heterogeneous assembly of proteins, nucleic acids, and co-factors [109], it is nonetheless reasonable to assume that its chemical composition exhibits negligible fluctuations about the average typical of each kind of machinery. The dynamics of each component can then simply be written as follows:

$$\dot{M}_i = \alpha_i M_0 \widetilde{\phi}_i \,, \tag{2.1}$$

where $i \in \{0,1,\ldots,n,G\}$, α_i is an allocation coefficient indicating which portion of the zero-machinery is devoted to the synthesis of machinery of type i, and $\widetilde{\phi}_i$ is a stoichiometric coefficient. Parameters are indicated with a tilde to signify that they are dimensional; this allows the use of the same symbols when

the model is rendered dimensionless. Being a fraction, α_i is non-negative and subject to the constraint

$$\sum_{i\in\{0,1,\ldots,n,G\}} \alpha_i = 1\ . \tag{2.2}$$

A unit of zero-machinery spends a fraction α_i of its time producing i-type machinery. Thus, when $\alpha_i = 1$, every unit of time, $\widetilde{\phi}_i$ units of machinery of type i are being produced per unit of zero-machinery. The reserve components change according to the balance of uptake and expenditures [24]:

$$\dot{X}_j = \sum_{i=1}^{n} \widetilde{\psi}_{ji} M_i - \widetilde{\sigma}_{jW}\dot{W} - M_0 \sum_{i\in\{0,1,\ldots,n,G\}} \widetilde{\sigma}_{ji}\alpha_i\widetilde{\phi}_i\ , \tag{2.3}$$

where $\widetilde{\psi}_{ji}$ is the gain of reserve j per unit machinery of type i, $\widetilde{\sigma}_{ji}$ is a stoichiometric coefficient for the synthesis of machinery of type i, and $\widetilde{\sigma}_{jW}$ is a stoichiometric coefficient for growth. The last coefficient can be further analysed into an assimilatory component, i.e. reserve j is used as building block, and a dissimilatory component, i.e. j is used as energy source; in general, reserve j might be used in both ways and $\widetilde{\sigma}_{jW}$ represents the net effect. Growth proceeds in proportion to the quantity of machinery that is dedicated to it:

$$\dot{W} = \widetilde{\psi}_W M_G\ , \tag{2.4}$$

where $\widetilde{\psi}_W$ is a stoichiometric coefficient. The specific growth rate equals $W^{-1}\dot{W}$.

Let $\widehat{\widetilde{\phi}}_i f_i M_i$ denote the flux of nutrient molecules through assimilatory machinery of type i, where $\widehat{\widetilde{\phi}}_i$ is a maximum rate and $f_i \in [0,1]$ depends on ambient conditions and possibly also on modulation by cellular factors [30, 64]. Suppose that $E^{(1)}, E^{(2)}, \ldots$ are the elements of interest. These could be any subset of the biogenic elements (C, H, O, N, S, P,...) but in fact, any functional group or carbon skeleton that is not transformed by the metabolism of the organism of interest can be treated as an 'element.' For the sake of simplicity, we take the number of elements of interest to be equal to the number of reserves n. Nutrient i has chemical formula (in its molecular form) $E^{(1)}_{\nu_{1i}}, E^{(2)}_{\nu_{2i}} E^{(3)}_{\nu_{3i}} \ldots E^{(n)}_{\nu_{ni}}$, where the subscript ν_{ki} is the number of element k in a molecule of nutrient i. The chemical composition of the nutrients can be collected in an $n \times n$ matrix $\mathbf{N}$ whose ith column is $[\nu_{1i}, \nu_{2i}, \nu_{3i}, \ldots, \nu_{ni}]^T$. Similarly, the chemical composition of the reserves can be represented in an $n \times n$ matrix $\mathbf{R}$ whose jth column is the formula of reserve j. Inasmuch as reserve compounds are chemically distinct for different nutrients, we can assume that the inverse $\mathbf{R}^{-1}$

exists. Then we have

$$\begin{pmatrix} \sum_{i=1}^{n} \widetilde{\psi}_{1i} M_i \\ \vdots \\ \sum_{i=1}^{n} \widetilde{\psi}_{ni} M_i \end{pmatrix} = \mathbf{R}^{-1}\mathbf{N} \begin{pmatrix} \widehat{\widetilde{\phi}}_1 f_1 M_1 \\ \vdots \\ \widehat{\widetilde{\phi}}_n f_n M_n \end{pmatrix} ,$$

hence

$$\sum_{i=1}^{n} \widetilde{\psi}_{ji} M_i = \sum_{i=1}^{n} \gamma_{ji} \widehat{\widetilde{\phi}}_i f_i M_i ,$$

where γ_{ji} denotes the (j,i)th element of $\mathbf{R}^{-1} \cdot \mathbf{N}$. We then have an explicit expression for the stoichiometric coefficient $\widetilde{\psi}_{ji}$:

$$\widetilde{\psi}_{ji} = \gamma_{ji} \widehat{\widetilde{\phi}}_i f_i . \tag{2.5}$$

Scaling

Choosing suitable parameters as natural units, we may render the equations dimensionless, which can facilitate the analysis of a mathematical model [153]. Adopting $\widetilde{\phi}_0^{-1}$ as unit of time, we define scaled variables as follows:

$$m_i = \frac{M_i \widetilde{\phi}_0}{W \widehat{m} \widetilde{\phi}_i} ; \qquad x_j = \frac{X_j}{W \widetilde{\sigma}_{jW}} . \tag{2.6}$$

Here $\widehat{m}$ is a scaling parameter for M_0/W; its significance will be discussed in Section 2.2.2. Scaled stoichiometric parameters are defined as follows:

$$\psi_{ji} = \frac{\widetilde{\psi}_{ji} \widetilde{\phi}_i \widehat{m}}{\widetilde{\sigma}_{jW} \widetilde{\phi}_0^2} ; \qquad \psi_W = \frac{\widetilde{\psi}_W \widetilde{\phi}_G \widehat{m}}{\widetilde{\phi}_0^2} ; \qquad \sigma_{ji} = \frac{\widetilde{\sigma}_{ji} \widetilde{\phi}_i \widehat{m}}{\widetilde{\sigma}_{jW} \widetilde{\phi}_0} . \tag{2.7}$$

On this scaling, the specific growth rate $(W\widetilde{\phi}_0)^{-1}\dot{W}$ is equal to $\psi_W m_G$; it is convenient to give this quantity its own symbol μ. The biochemical similarity of different types of machinery implies that the relative amounts of reserves expended on their synthesis will be similar as well. This motivates the assumption that for every reserve j, we have $\sigma_{ji} = \sigma_j$ for all machineries i. The scaled state variables $\{m_0, \ldots, m_G, x_1, \ldots, x_n\}$ represent densities: these are intensive variables, as opposed to the original variables $\{M_0, \ldots, M_G, X_1, \ldots, X_n\}$, which are extensive (i.e., $\propto W$). After scaling, we have the following dynamics:

$$\begin{cases} \dot{m}_i &= \alpha_i m_0 - \mu m_i & \text{for } i \in \{0, 1, \ldots, n, G\} \\ \dot{x}_j &= \sum_{i=1}^{n} \psi_{ji} m_i - \mu (1 + x_j) - m_0 \sigma_j & \text{for } j \in \{1, \ldots, n\}. \end{cases} \tag{2.8}$$

For the sake of simplicity, we shall assume henceforth that $\psi_{ji} = 0$ whenever $j \neq i$. This is reasonable when the elemental ratios of the reserves are identical, or nearly identical, to the elemental ratios in the nutrients, since in that case $\mathbf{R} \propto \mathbf{N}$ and hence $\mathbf{R}^{-1} \cdot \mathbf{N}$ will be diagonal. Choosing the elements of interest

judiciously can also ensure that the matrix $\mathbf{\Psi}$ is diagonal. For instance, for *E. coli* growing on glucose and ammonia, only the off-diagonal elements corresponding to hydrogen and oxygen are non-zero; focussing on only carbon and nitrogen, we obtain a 2×2 diagonal matrix.

2.2.2 Constitutive relationships

To complete the specification of the model, we require expressions for the allocation coefficients α_0, $\ldots$, α_G. One option is to treat these as forcing functions that drive the model. These functions can be observed directly, due to recent advances in ribosome profiling [73, 95] and enzyme re-profiling [90]. Alternatively, the allocation coefficients can be treated as control inputs, to be calculated on the basis of a suitable, evolutionarily relevant optimality criterion [156]. Another option to 'close' the equations is to posit outright the dynamics for the reserve densities x_i, for instance setting $\dot{x}_i = \nu_i (f_i - x_i)$, where ν_i is a positive constant [88] and f_i as in eqn (2.5). This approach, which defines the allocation implicitly, while having the advantage of simple dynamics, would seem to require cellular-level stoichiometric parameters to be in fortuitous agreement with the kinetic parameters of the molecules of the regulatory system [150]. Here, we treat the allocation coefficients as a function of the internal state variables and/or environmental parameters [117]. In particular, we assume that $m_0, \ldots, m_G, x_1, \ldots, x_n$ are mapped to $\alpha_0, \ldots, \alpha_G$ by a suitable $\mathbb{R}^{2(n+1)} \mapsto \mathbb{R}^{n+2}$ function. Recalling that α_i is the fraction of ribosome time devoted to the production of machinery of type i, we propose the following:

$$\alpha_i = \frac{\widetilde{r}_i}{\widetilde{r}_0 + \widetilde{r}_1 + \cdots + \widetilde{r}_n + \widetilde{r}_G} \,, \tag{2.9}$$

where the $\widetilde{r}_i$ represent, roughly speaking, the concentrations of translationally active mRNA for the corresponding types of machinery (corrected for relevant molecular properties, such as affinity for the ribosome and mobility within the cytosol, as mRNA species of various lengths and tertiary structures will differ with respect to this properties, in particular, might affect the arrival rate of the various mRNA species at the ribosome, which potentially translates into a skewing of the relative amounts of 'ribosome time' devoted to each of them, which we tacitly assume can be done via suitable weighting coefficients; synthesis rates in *E. coli* are predominantly under translational, rather than transcriptional control [95]). For the sake of simplicity, $\widetilde{r}_0$ is assumed to be constant, corresponding to constitutive expression. We scale the other $\widetilde{r}_i$ by this constant:

$$r_i = \widetilde{r}_i / \widetilde{r}_0 \,. \tag{2.10}$$

For $j = 1,\ldots,n$, r_j is assumed to be a decreasing function of x_j (we shall take this as a generic sigmoid for the sake of convenience); as the reserve density increases, less of the machinery that feeds it is synthesised. The central mechanism in the present theory resides in a feedback loop connecting reserve densities and allocation of building blocks to machinery; the control logic here is related to that of I-control in control engineering, cf. [74]. The building blocks are fed from core metabolism into the synthesis routes; the allotment is achieved effectively by an allocation of ribosome time (cf. the Scott-Hwa-model [134, 135, 136]). The r_j can be thought of as corresponding to levels of mRNA for the various types of molecular machinery, although issues such as differences in stability of the mRNA molecule, affinity for ribosomes may distort a direct 1-to-1 correspondence (which can be compensated to some extent by assuming that appropriate correction factors have been assimilated into the scaling).

We assume further that r_G is an increasing function of m_0. For the sake of simplicity, we represent it as a piecewise affine function:

$$r_G[m_0] = \begin{cases} 0 & \text{if } m_0 \leq 1-\varepsilon \\ r_{G,\max}/2 + K(m_0-1) & \text{if } 1-\varepsilon < m_0 \leq 1+\varepsilon \\ r_{G,\max} & \text{if } m_0 > 1+\varepsilon\,, \end{cases} \tag{2.11}$$

where K is the slope, and $\varepsilon = r_{G,\max}/(2K)$. The mid-point of this function is set at $m_0 = 1$ (we here exercise our freedom to choose a natural unit for the scaling factor $\widehat{m}$ which we identify as the physiological optimum for type-zero machinery; $m_0 = 1$ follows from this choice). Equation (2.11) expresses the hypothesis that the safeguarding of core catalytic machinery takes precedence over growth [10]. This relationship is suggested by, and consistent with, Herbert's [68] classic observations on the relationship between RNA content and growth rate (the component m_0 corresponding to rRNA). The slope of the relationship observed by Herbert [68] is inversely proportional to K, that is, the larger the value of K, the smaller the variation of RNA content with growth rate. Figure 2.2 illustrates the relationship between relative growth rate and RNA content for the micro-organism *Aerobacter aerogenes* grown in a continuous culture with glycerol as a limiting factor, as observed by Herbert [68]. This relationship appears to be linear and thus can be represented as follows:

$$\widetilde{\mu} = \widetilde{K} \times \mathrm{RNA} + b\,,$$

where $\widetilde{\mu}$ is relative unscaled growth rate, $\widetilde{K}$ and b are, correspondingly, slope and offset parameters. After scaling (as detailed in Section 2.2.1) and applying the definition of the specific growth rate, we

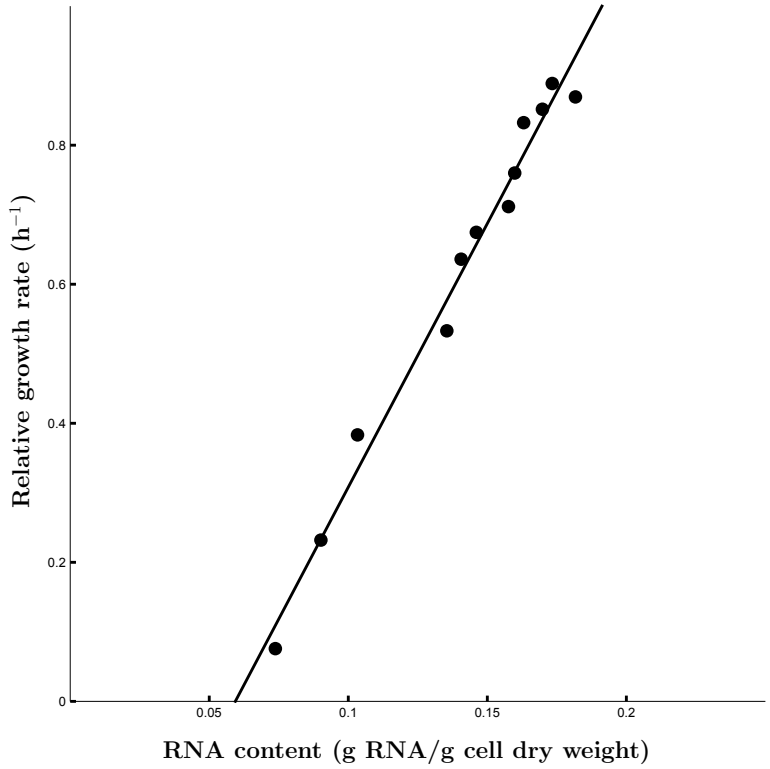

Figure 2.2: Relationship between relative growth rate and RNA content for the micro-organism *Aerobacter aerogenes* grown in a continuous culture with glycerol as a limiting factor, together with the optimal fit of eqn $\widetilde{\mu} = \widetilde{K} \times \mathrm{RNA} + b$ with parameters $\widetilde{K} = 7.58$ h g DW g RNA^{-1}, $b = -0.45$ h^{-1}. Original data taken from [68].

have $\widetilde{\mu} = \psi_W r_G \widetilde{\phi}_0$, giving

$$r_G = \frac{\widetilde{K}}{\psi_W \widetilde{\phi}_0} \times \mathrm{RNA} + \frac{b}{\psi_W \widetilde{\phi}_0} \, .$$

According to Section 4.5.1, we have:

$$\mathrm{RNA} = M_0/\beta_0 \, ,$$

whence together with the scaling for M_0 (cf. Section 2.2.1) we obtain:

$$r_G = \frac{\widetilde{K} W \hat{m}}{\psi_W \widetilde{\phi}_0 \beta_0} m_0 + \frac{b}{\psi_W \widetilde{\phi}_0} \, .$$

Given the values for stoichiometric coefficients provided (as detailed in Section 4.5) and using the estimate for the slope parameter $\widetilde{K}$ obtained from fitting the Herbert data to the linear model (fit shown in Fig. 2.2), we can calculate the slope K from eqn (2.11) by means of the following equation:

$$K = \frac{\widetilde{K} W \hat{m}}{\psi_W \widetilde{\phi}_0 \beta_0} = 8.41 \, .$$

2.3 Consistency with classic models; observability

In this section we investigate the case $n = 1$ in more detail, with an emphasis on the continuity of the present approach with the classic empirical laws proposed by Monod [107] and Droop [35]. In addition, we discuss how the function r_1 can be observed by transforming available observational data in a suitable way. This is important since the *r*-functions are the only non-standard (and possibly controversial) constituents of the model, as its remaining assumptions are closely linked to the law of conservation of mass.

2.3.1 Equilibrium conditions for $n = 1$

System (2.8) takes on the following form for $n = 1$:

$$\begin{gathered} \dot{m}_0 = \alpha_0 m_0 - \mu m_0 \,; \quad \dot{m}_1 = \alpha_1 m_0 - \mu m_1 \,; \\ \dot{m}_G = \alpha_G m_0 - \mu m_G \,; \quad \dot{x}_1 = \psi_1 m_1 - \mu\,(1+x_1) - \sigma_1 m_0 \,, \end{gathered} \tag{2.12}$$

with allocation fractions

$$\alpha_0 = \frac{1}{1+r_1+r_G} \,; \quad \alpha_1 = \frac{r_1}{1+r_1+r_G} \,; \quad \alpha_G = \frac{r_G}{1+r_1+r_G} \,.$$

At equilibrium, the rates of change in system (2.12) equal zero, which can be reduced, via the considerations presented in Section 2.5.1 for general n, to the following pair of equilibrium conditions:

$$\mu = \psi_W r_G m_0 = (1+r_G+r_1)^{-1} \tag{2.13}$$

$$\psi_1 r_1 = \psi_W r_G (1+x_1) + \sigma_1 \,. \tag{2.14}$$

Provided that $r_{G,\max}$ is sufficiently large (which is biologically plausible) the state variable m_0 can be assumed to lie in the interval $(1-\varepsilon, 1+\varepsilon)$. We then have the bounds $\psi_1^{\{+\varepsilon\}} < \psi_1 < \psi_1^{\{-\varepsilon\}}$ and $\mu^{\{-\varepsilon\}} < \mu < \mu^{\{+\varepsilon\}}$, where

$$\psi_1^{\{\pm\varepsilon\}} = \frac{\sigma_1}{r_1(x_1)} + \frac{\psi_W\,(1+x_1)}{2r_1(x_1)} \left(\sqrt{\frac{4}{\psi_W(1\pm\varepsilon)} + (1+r_1(x_1))^2} - (1+r_1(x_1)) \right) \tag{2.15}$$

$$\mu^{\{\pm\varepsilon\}} = \frac{1}{2} \left(\sqrt{\psi_W(1\pm\varepsilon)\left(4 + \psi_W(1\pm\varepsilon)\,(1+r_1(x_1))^2\right)} - \psi_W(1\pm\varepsilon)\,(1+r_1(x_1)) \right) \tag{2.16}$$

and we have written $r_1(x_1)$ to emphasise that r_1 is a function of x_1. In the limit $\varepsilon \to 0$, these bounds converge and eqns (2.15) and (2.16) furnish simple expressions for the steady-state relationships between

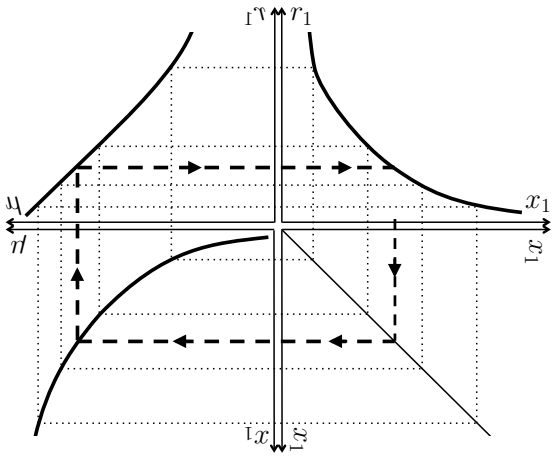

Figure 2.3: Graphical reconstruction of the function $r_1(\cdot)$. If there are known steady-state relationships between reserve density x_1 and specific growth rate μ (bottom left, printed upside down), and between r_1 and μ (top left, mirror reversed), the function r_1 can be plotted in dependence of x_1 (top right) by chasing set values of x_1 around the diagram, as shown by the dashed arrows.

ψ_1, μ, and x_1; this limit obtains when K is sufficiently large.

2.3.2 Observability of the function $r_1(\cdot)$

Two constitutive functions remain to be specified: the dependence of ψ_1 on the ambient concentration of the nutrient, and the function $r_1(\cdot)$. For the former, the Michaelis-Menten hyperbola is a standard choice [153]:

$$\psi_1 = \widehat{\psi}_1 \left(1 + K_{\psi,1}/[\mathrm{N}_1]\right)^{-1} , \tag{2.17}$$

where $\widehat{\psi}_1$ and $K_{\psi,1}$ are positive parameters and $[\mathrm{N}_1]$ is the ambient nutrient concentration.

The function $r_1(\cdot)$ can be recovered from observational data as shown in Fig. 2.3, via the parametric dependence of x_1 and r_1 on μ at steady state. Under strict homeostasis of type-zero machinery (a condition which we will denote as $m_0 \doteq 1$) we have

$$x_1 = \psi_1 \left(\mu^{-2} - \mu^{-1} - {\psi_W}^{-1}\right) - (1 + \sigma_1/\mu) \tag{2.18}$$

$$r_1 = \mu^{-1} - 1 - \mu/\psi_W , \tag{2.19}$$

which means that the construction of Fig. 2.3 can be carried out if the steady-state relationship between ψ_1 and μ is available. Equation (2.17) can be used to recover this curve if μ is known as a function of $[\mathrm{N}_1]$. The latter relationship is the *Monod curve*, an example of which is shown in Fig. 2.4, which

shows data obtained by Monod [107] along with the hyperbola which he proposed as an empirical law:

$$\widetilde{\mu} = \widehat{\mu}(1 + K_{\mu,1}/[\mathrm{N}_1])^{-1} \,, \tag{2.20}$$

where $\widehat{\mu}$ and $K_{\mu,1}$ are positive parameters and $\widetilde{\mu}$ is the measured specific growth rate in an appropriate SI unit (by scaling, $\widetilde{\mu} = \mu\widetilde{\phi}_0$). The resemblance to eqn (2.17) is obvious, although $K_{\psi,1} \neq K_{\mu,1}$ [14]; Monod [107] pointed out that $K_{\mu,1}$ can be one or several orders of magnitude smaller than $K_{\psi,1}$.

Alternatively, the x_1-μ curve may be derived from an empirical law. Reserve density can in some cases be observed directly, when the reserve takes the form of discrete inclusions. However, in other cases, the reserve is composed of molecules that are identical to those occurring as part of the machinery components—for instance, RNA can serve as both functional machinery and reserve, in which case the partitioning between these components is formal but not physical (the individual molecules are not distinguishable as belonging to one or the other). However, it is always possible to observe the total amount per cell, known as the *cell quota*, which can be related to the components via a linear stoichiometric combination:

$$Q_1 = \kappa_W + \kappa_{m,0}m_0 + \kappa_{m,1}m_1 + \kappa_{m,G}m_G + \kappa_{x,1}x_1 \,, \tag{2.21}$$

where the $\kappa_\star$ account for the amount of nutrient that is incorporated per unit of the corresponding component $\star$. An empirical law relating Q_1 and μ is known as a *Droop curve*, after Droop [35] who proposed the following empirical relationship:

$$\widetilde{\mu} = \widehat{\mu}\,(1 - Q_{10}/Q_1) \,, \tag{2.22}$$

where $\widehat{\mu}$ and Q_{10} are positive parameters (see Fig. 2.4). In the special case $m_0 \doteq 1$, eqns (2.21) and (2.22) yield:

$$x_1 = \frac{Q_{10}/\kappa_{x,1}}{1 - \mu\widetilde{\phi}_0/\widehat{\mu}} - \frac{\kappa_{m,1}}{\kappa_{x,1}\mu} + \mu\frac{\kappa_{m,1} - \kappa_{m,G}}{\kappa_{x,1}\psi_W} - \frac{\kappa_W + \kappa_{m,0} - \kappa_{m,1}}{\kappa_{x,1}} \,, \tag{2.23}$$

which furnishes the curve needed for the first transformation in Fig. 2.3 (bottom left panel), the second transformation being given by eqn (2.19), as before.

2.3.3 Strict reserve homeostasis and the transient Monod model

A case of special interest is that of *strict homeostasis of the reserve* x_1. Let

$$r_1 = \widehat{r}_1\,(1 + \exp\{\vartheta_1\,(x_1 - \xi_1)\})^{-1} \,, \tag{2.24}$$

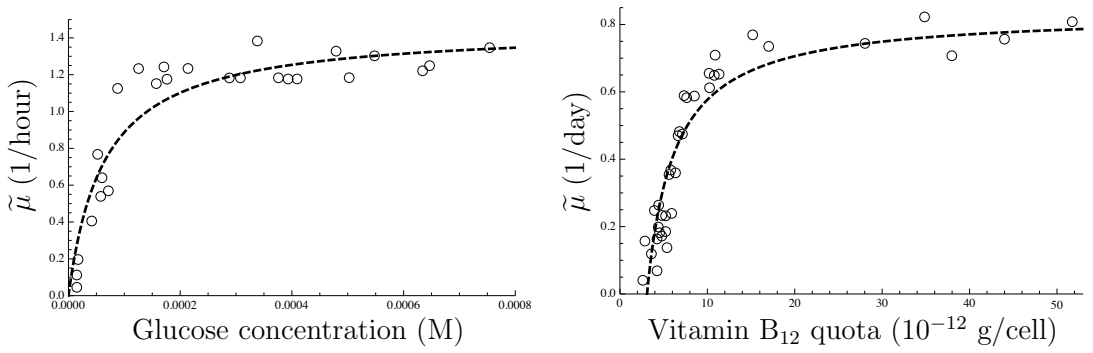

Figure 2.4: Empirical laws. Left: steady-state relationship between ambient nutrient concentration and specific growth rate. *Escherichia coli* data from Monod [107], together with the optimal non-linear least-squares fit of his model, eqn (2.20): $K_{\mu,1} = 6.39 \times 10^{-5}$ M; $\widehat{\mu} = 1.45$ hour^{-1}. Right: steady-state relationship between cell quota and specific growth rate. *Monochrysis lutheri* data from Droop [35], together with the optimal non-linear least-squares fit of his model, eqn (2.22): $Q_{10} = 3.09 \times 10^{-12}$ g/cell; $\widehat{\mu} = 0.835$ day^{-1}.

where $\widehat{r}_1$, ϑ_1 and ξ_1 are positive parameters (any generic sigmoid function will do for the purpose at hand). Consider the limit $\vartheta_1 \to \infty$; the function becomes infinitely steep in the neighbourhood of $x_1 = \xi_1$, so that x_1 remains close to ξ_1 over most of the physiological range (except perhaps at low growth rates). We shall denote this special case as $x_1 \doteq \xi_1$. Combining this with eqn (2.17) and $m_0 \doteq 1$, we obtain the following relationship between $[\mathrm{N}_1]$ and $\widetilde{\mu}$:

$$\frac{\widehat{\psi}_1/(1+\xi_1)}{1+K_{\psi,1}/[\mathrm{N}_1]} = \frac{\sigma_1/(1+\xi_1)+\widetilde{\mu}/\widetilde{\phi}_0}{\widetilde{\phi}_0/\widetilde{\mu}-1-\widetilde{\mu}/(\widetilde{\phi}_0\psi_W)} \,. \tag{2.25}$$

This relationship has five free parameters, which is too many to be determined by least-squares fitting from Monod's data in Fig. 2.4 alone, but good agreement with the data can be attained (in suitable limits for the parameters, the solution for $\widetilde{\mu}$ of eqn (2.25) reduces to Monod's hyperbola).

The ordinary differential equation

$$\dot{W} = W\widehat{\mu}\left(1+K_{\mu,1}/[\mathrm{N}_1]\right)^{-1} \tag{2.26}$$

is often referred to as the Monod model (e.g., [24, 26, 159]), where $[\mathrm{N}_1]$ is treated as an autonomous function of time or coupled to W via a suitable ecological model (for instance, if the culture is growing under batch conditions, $[\mathrm{N}_1]$ will decrease as W increases). Eqn (2.26) is more accurately called the *transient Monod model* to indicate that application to transient conditions ventures beyond the steady-state originally considered by Monod. The transient Monod model has just one component (W is its only state variable); when it occurs as part of an ecological model, stoichiometric consistency requires that $x_1 \doteq \xi_1$, so the assumption of strict reserve homeostasis must be imputed to such studies even when the

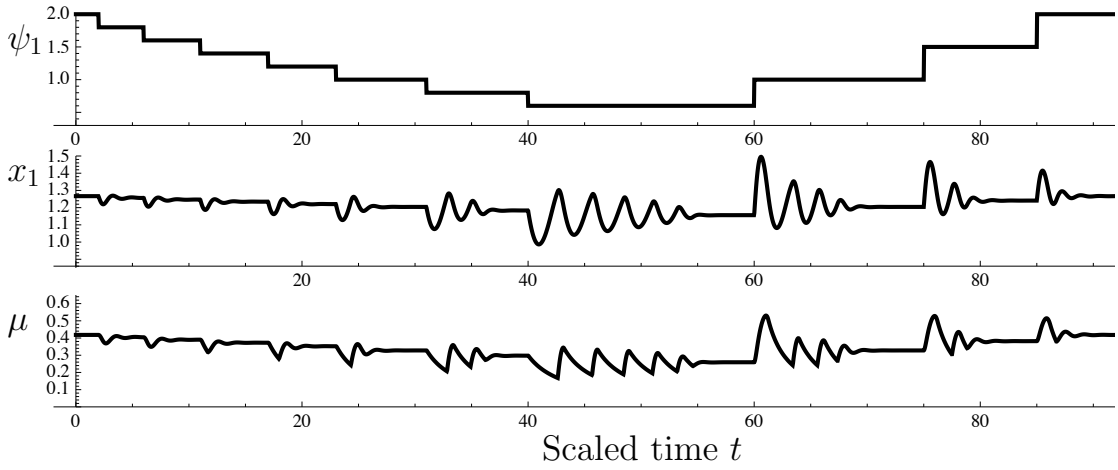

Figure 2.5: Numerical solution of system (2.12). The function r_G was as in eqn (2.11) with $K = 10^4$ and $r_{G,\max} = 5$; $r_1 = 15/(1+\exp\{10(x_1-1)\})$; $\psi_W = 1$; and $\sigma_1 = 1$. Top: imposed time course of ψ_1. Middle: time course of scaled reserve density x_1. Bottom: time course of the specific growth rate μ.

authors do not explicitly commit to this.

The behaviour of the present model under transient conditions differs from the transient Monod model, even under the assumption that the function $r_1(x_1)$ has a steep slope ($\vartheta_1 \to \infty$). Following a change in environmental conditions, for instance a step change in $[N_1]$, x_1 deviates from ξ_1 which triggers a re-allocation of building blocks to the various types of machinery. As $[N_1]$ is held constant at its new value, the m-type state variables relax at a time scale $\sim \mu^{-1}$; while x_1 relaxes back to ξ_1.

However, the transient Monod model and the present model can be treated as equivalent if the changes in $[N_1]$ (and hence ψ_1) occur smoothly and sufficiently slowly. In this 'adiabatic' case, the internal dynamics is sufficiently rapid that its state variables can be coupled quasi-statically to $[N_1]$, or, equivalently, to ψ_1 (cf. Section 2.4.1).

2.4 Simulations

The dynamics, system (2.8), can be studied in qualitative terms by means of numerical solution of the ordinary differential equations. In this section we note several aspects of the model's dynamic behaviour which could be measured, in principle, in the real-life system.

2.4.1 The case $n = 1$

The response of the model to stepwise increases and decreases of ψ_1 is shown in Fig. 2.5. It can be seen that the downward steps in ψ_1, representing a decrease in ambient nutrient availability, lead to downward deflections in the reserve x_1 which governs the dynamic allocation between nutrient uptake machinery and

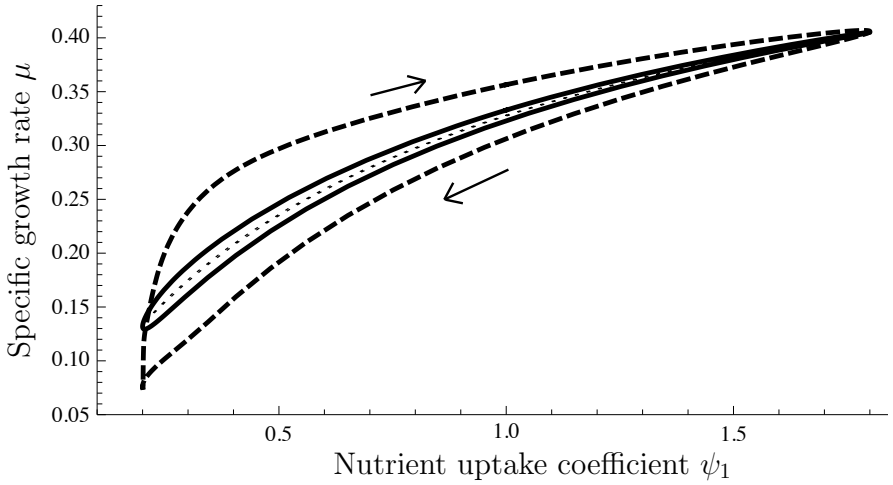

Figure 2.6: Numerical solution of system (2.12); stationary cycle under a sinusoidal variation of ψ_1. The dashed curve obtains for a cycle duration of 60 units of scaled time; the solid curve for a cycle duration of 300 units. Also shown is the 'adiabatic' limit (dotted line) which obtains for an infinitely slow cycle.

proliferative (growth) machinery. The adjustment is rapid and stabilises, although oscillations become more vigorous and long-lasting at lower values of ψ_1; intuitively this can be understood since the actual balance between m_1 and m_G (i.e., the proteome-level profile) relaxes toward the balance dictated by α_1 and α_G with a response time of order μ^{-1}. Thus, even if the change in expression of different kinds of machinery is rapid, the actual m_1/m_G balance reacts more sluggishly at low μ. Upward step changes in ψ_1 induce upward deflections of x_1, which again steer the dynamic re-allocation process. Mathematically, the underdamped oscillations in the behaviour of the reserve x_1 shown in Fig. 2.5 can be explained by the presence of two complex conjugate eigenvalues of the second-order linear ODE which approximates the behaviour of the non-linear system at hand, where the real part of these eigenvalues is the damping rate and the imaginary part corresponds to the oscillation frequency. Such oscillations have been observed in the experimental literature [63].

If a sinusoidal variation in ψ_1 is imposed, the system settles on a stationary cycle. Parametric plots of $\psi_1(t)$ versus $\mu(t)$ over this stationary cycle are shown in Fig. 2.6 for selected values of the period of the cycle. A hysteresis effect is in evidence, which corresponds, loosely speaking, to the proteome-level re-profiling dynamics lagging behind the prevailing value of ψ_1. The hysteresis loop widens as the period of the environmental oscillation shortens. As this duration goes to infinity, the loop tightens up against a curve which corresponds to the 'adiabatic' regime under which the transient Monod model is valid: provided that environmental changes are sufficiently slow, μ can be treated as a function of the environmental conditions.

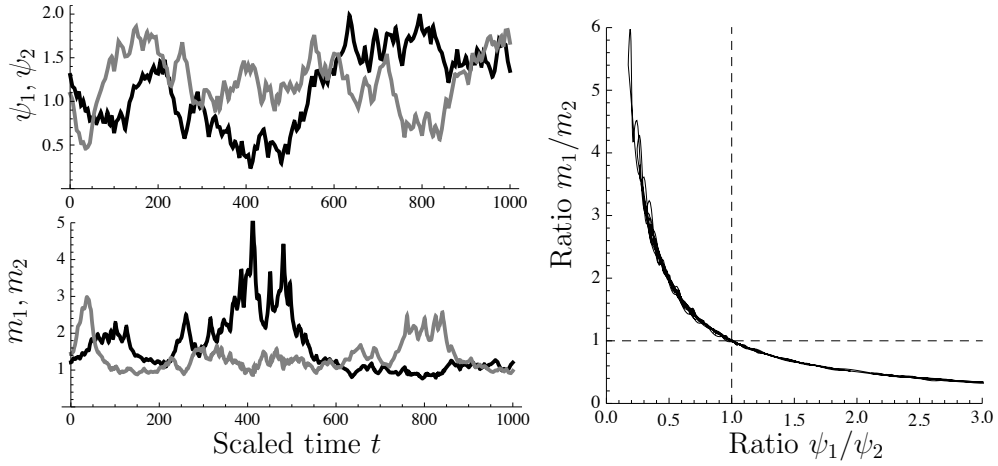

Figure 2.7: Numerical solution of system (2.8) with $n = 2$. The function r_G was as in eqn (2.11) with $K = 10^4$ and $r_{G,\max} = 5$; $r_i = 15/(1+\exp\{10(x_i-1)\})$ and $\sigma_i = 1$ for $i = 1,2$; and $\psi_W = 1$. Left, top: imposed time course of ψ_1 (black line) and ψ_2 (grey line). The random process ψ_i ($i = 1,2$) was simulated by taking a running sum of i.i.d. standard uniform variables with a fixed time step of 2 scaled units of time, translated upward by 0.5 scaled units and capped so that the final signal is constrained to lie between 0.2 and 2. Left, bottom: time course of scaled uptake machinery for nutrient 1 (m_1; black line) and nutrient 2 (m_2; grey line). Right: ψ_1/ψ_2 versus m_1/m_2, showing compensatory shifts in expression of nutrient uptake machinery.

2.4.2 The case $n = 2$

For two or more reserve components, the assumption of monotonically decreasing r_i-functions leads to a re-balancing effect, whereby stoichiometric imbalances between nutrient availabilities are offset, or at least partially offset, by counteracting changes in the allocation fractions to the corresponding types of uptake machinery.

This 'counter-skewing' effect is illustrated in Fig. 2.7, in which the model was simulated for $n = 2$ with uncorrelated white noise in the ψ_1 and ψ_2 time-courses. It can be seen that m_i tends to increase when ψ_i is relatively low, and vice versa. Indeed, when the ratio ψ_1/ψ_2 is plotted against m_1/m_2 over the time course of the simulation run, a perfect hyperbola is obtained.

The model achieves this behaviour by having each reserve feeding back on the expression of the machinery feeding that particular reserve; the balancing in allocation happens at the level of eqn (2.9), which represents the effect of ribosomes distributing themselves pro rata over the mRNA species, as we would expect based on the random encounter processes that underlie molecular kinetics. This shows that it is possible in principle to achieve reserve homeostasis without the need for signals arising from multiple reserves to converge on the upstream activation sequence of any one of the genes for uptake machinery.

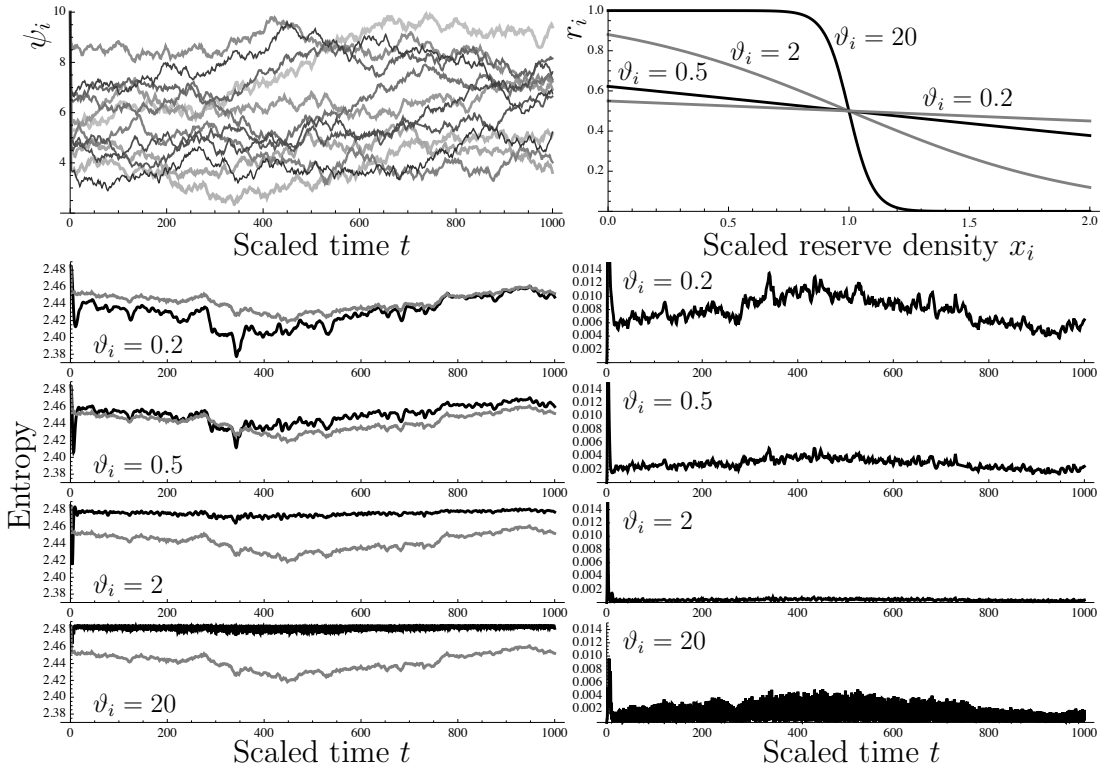

Figure 2.8: Numerical solution of system (2.8) with $n = 12$, with initial condition corresponding to optimal environment, i.e., $\psi_i \equiv \widehat{\psi}_i$ for all i. Left, top: uncorrelated white noise functions for ψ_i ($i = 1, \ldots, 12$) used in all simulations (obtained as explained in the caption to the previous figure). Right, top: sigmoid functions used for r_i in the simulations; all reserves use the same function in any given run, but the steepness parameter ϑ_i was varied as shown. Left, bottom: time course of the reserve entropy (solid line) for various values of ϑ_i; the input entropy of the ψ_i is shown for reference as a grey line. Reserve entropy was defined as $\sum_{i=1}^{n}(x_i/x_T)\ln\{x_T/x_i\}$ with $x_T = \sum_{i=1}^{n} x_i$; ambient entropy was defined as $\sum_{i=1}^{n}(\psi_i/\psi_T)\ln\{\psi_T/\psi_i\}$ with $\psi_T = \sum_{i=1}^{n}\psi_i$. Right, bottom: time course of the relative entropy for various values of ϑ_1; relative entropy was defined as $\sum_{i=1}^{n}(m_T/m_i)\ln\{m_T\psi_T/(m_i\psi_i)\}$ with $m_T = \sum_{i=1}^{n} m_i$.

2.4.3 Multiple reserve components

The qualitative behaviours noted in the foregoing sections are also present at $n \geq 3$. By way of example, the response of a model with $n = 12$ is shown in Fig. 2.8. Again, the ambient medium presents uncorrelated noise. The response to this environmental input is represented for four different steepness values (ϑ_i, see eqn (2.24)) of the r_i-functions. When this value is low, the allocation to the uptake machineries is hardly adjusted. As a result, the entropy of the reserves follows that of the environment; in other words, the fluctuations in the environment are reflected in fluctuations in reserve status (in the simulation shown for $\vartheta_i = 0.2$, the reserve entropy temporarily undershoots the ambient entropy; this is a transient effect due to the initial state of the system).

As ϑ_i increases, the reserve entropy tends more and more toward the maximum value ($\ln 12 \approx 2.485$) at all times, reflecting that strict homeostasis of reserves is achieved. In fact, at the highest value studied ($\vartheta_i = 20$) the reserve entropy signal is rather restless, with rapid downward spikes that arise as a

consequence of the high reactivity of the feedback loop, which tends to induce rapid oscillations.

To visualise the 'counter-skewing' effect, the relative entropy of $\{m_i^{-1}\}_{i=1}^n$ with respect to $\{\psi_i\}_{i=1}^n$ has been plotted as a function of time. This relative entropy decreases with increasing ϑ_i, indicating that the machinery allocation becomes better adapted to the environmental fluctuations. Again, the trace for $\vartheta_i = 20$ appears more agitated than that for $\vartheta_i = 2$, due to the rapid oscillations concomitant with high reactivity.

2.5 Dynamics of the model for general n

We investigate the existence, uniqueness, and stability of equilibria of system (2.8). Setting the rates of change equal to zero yields the equilibrium conditions:

$$\alpha_i m_0 - \mu m_i = 0 \quad \text{for } i \in \{0,1,\ldots,n,G\}, \tag{2.27}$$

$$\psi_j m_j - \mu\,(1+x_j) - m_0\sigma_j = 0 \quad \text{for } j \in \{1,\ldots,n\}. \tag{2.28}$$

We shall assume throughout that $\mathbf{\Psi}$ is a diagonal matrix, and we are primarily interested in the case where K is large (corresponding to strict homeostasis of m_0).

2.5.1 Existence and uniqueness of the equilibrium point

Specifying eqn (2.27) for $i = 0$, we obtain $\mu = \alpha_0$ (since $m_0 > 0$ for a biologically relevant equilibrium). Thus eqn (2.27) can be written as $m_i = (\alpha_i/\alpha_0)m_0$. With eqn (2.9), this becomes $m_i = (r_i/r_0)m_0$ or $m_i = r_i m_0$ since $r_0 \equiv 1$ by scaling. In particular, $m_G = r_G m_0$ and hence $\mu = \psi_W r_G m_0$ (since $\mu = \psi_W m_G$ by definition). With these identities, eqn (2.28) becomes:

$$(\psi_j r_j - \psi_W r_G\,(1+x_j) - \sigma_j)\,m_0 = 0\,,$$

which means that either $m_0 = 0$, which is not biologically relevant, or

$$\psi_W r_G\,(1+x_j) + \sigma_j = \psi_j r_j\,. \tag{2.29}$$

Let us first consider the problem of solving this for x_j given a fixed value of $r_G \in [0, r_{G,\max}]$. The left-hand side of eqn (2.29) is a strictly increasing function of x_j whereas its right-hand side is a strictly decreasing function of x_j (by the assumed properties of the r_j as functions of the x_j). The graphs of these two functions intersect in at most one point. This point will exist if the graph of the left-hand side of

eqn (2.29) lies below that of the right-hand side at $x_j = 0$. For this it suffices that

$$r_{j,\max} \geq (\psi_W r_{G,\max} + \sigma_j)/\psi_j \,, \tag{2.30}$$

where $r_{j,\max}$ denotes the value of r_j at $x_j = 0$. The physiological interpretation suggests that $r_{j,\max} < +\infty$, so that condition (2.30) can only be satisfied if $\psi_j > 0$ for $j = 1,\ldots,n$. Thus, if condition (2.30) is satisfied, eqn (2.29) will have a unique solution $x_j^\star \geq 0$ for all reserves j, for the given value of r_G. This solution $x_j^\star$ can be treated as a function of r_G as defined by eqn (2.29); this function is strictly decreasing. Since the r_j are strictly decreasing in their respective x_j, it follows that $\sum r \equiv \sum_{j\in 0,1,\ldots,n,G} r_j$ is an increasing function of r_G. At equilibrium $\mu = \alpha_0$ and $\alpha_0 = r_0/\sum r = 1/\sum r$, whence $\mu = 1/\sum r$ which is a decreasing function of r_G, or equivalently, a decreasing function of m_0 (since r_G is an increasing function of m_0). In addition, $\mu = \psi_W r_G m_0$, which is an increasing function of m_0. Again we consider the point of intersection between the graphs of these two functions. Repeating a similar argument, we find that $1/\sum r > 0$ and $\psi_W r_G m_0 = 0$ at $m_0 = 1-\varepsilon$, and that therefore it is sufficient if

$$\left(1 + r_{G,\max} + \textstyle\sum_{j=1}^n r_j^\star(r_{G,\max})\right) \psi_W r_{G,\max} \geq (1+\varepsilon)^{-1} \tag{2.31}$$

for a unique intersection point to exist with $1-\varepsilon \leq m_0 \leq 1+\varepsilon$. We concluded earlier that, at equilibrium $m_G = r_G m_0$ and $m_j = r_j m_0$ for $j = 1,\ldots,n$; therefore these are fixed whenever the x_j together with m_0 are fixed. Conditions (2.30) and (2.31) suffice; they could be weakened but even in the form stated, they are not at all stringent from a biological point of view: it is enough that the r_j-functions are sufficiently large for small values of their argument. We henceforth assume that these conditions are met.

2.5.2 Linear stability analysis

We investigate the stability by linearising the system about its equilibrium and verifying the stability of the characteristic polynomial associated with the linearised system. The system matrix of the linearised system is the Jacobian matrix:

$$J(m_0, m_1 \ldots m_n, m_G, x_1 \ldots x_n) = \begin{pmatrix} \frac{\partial f_1}{\partial m_0} & \frac{\partial f_1}{\partial m_1} & \cdots & \frac{\partial f_1}{\partial m_n} & \frac{\partial f_1}{\partial m_G} & \frac{\partial f_1}{\partial x_1} & \cdots & \frac{\partial f_1}{\partial x_n} \\ \frac{\partial f_2}{\partial m_0} & \frac{\partial f_2}{\partial m_1} & \cdots & \frac{\partial f_2}{\partial m_n} & \frac{\partial f_2}{\partial m_G} & \frac{\partial f_2}{\partial x_1} & \cdots & \frac{\partial f_2}{\partial x_n} \\ \vdots & \vdots & \ddots & \vdots & \vdots & \vdots & \ddots & \vdots \\ \frac{\partial f_{2n+2}}{\partial m_0} & \frac{\partial f_{2n+2}}{\partial m_1} & \cdots & \frac{\partial f_{2n+2}}{\partial m_n} & \frac{\partial f_{2n+2}}{\partial m_G} & \frac{\partial f_{2n+2}}{\partial x_1} & \cdots & \frac{\partial f_{2n+2}}{\partial x_n} \end{pmatrix},$$

where $f_1, f_2 \ldots f_{2n+2}$ denote the right-hand sides of system (2.8). Our strategy is to investigate the signs of the coefficients in the limit $K \to \infty$ (the parameter K represents the slope of the increasing part of the

piecewise function r_G in eqn (2.11)). In real-life systems, $K < +\infty$, as attested by the non-zero slope of cellular RNA content ($\sim m_0$) as a function of μ at steady state [68]. In other words, the limit $K \to \infty$ represents an idealised case of strict homeostasis of m_0. While our limiting result establishes that stability is ensured if K is sufficiently large, numerical solutions of the dynamic equations for finite K indicate that, in fact, the system always converges to its equilibrium point, but, as K decreased, with oscillations of increasing amplitude and ring-down time. To establish the result in the limit $K \to \infty$, we exploit a theorem by Strelitz [140] on the stability of monic polynomials.

Signs of the coefficients of the characteristic equation

The characteristic equation is a polynomial of order $2(n+1)$:

$$\lambda^{2n+2} + c_1\lambda^{2n+1} + c_2\lambda^{2n} + \cdots + c_{2n+1}\lambda + c_{2n+2} = 0\,. \tag{2.32}$$

The coefficients c_k can be written as $c_k = (-1)^k S_k$, where S_k is the sum of the principal minors M_k [106]. These M_k are symmetric with respect to the main diagonal of the Jacobian matrix. The coefficients c_k are first-order polynomials in K. For sufficiently large K, it is the term in c_k that is proportional to K that governs the sign; let $\widetilde{c_k}$ denote this term.

It will prove useful to partition the Jacobian matrix as follows:

$$J = \left[\begin{array}{c|c|c|c} J^{\mathrm{I}} & J^{\mathrm{II}} & J^{\mathrm{III}} & J^{\mathrm{IV}} \end{array}\right]\,. \tag{2.33}$$

The submatrices are evaluated at the equilibrium point in the limit $m_0 \to 1$, that is, $\varepsilon \to 0$ (which obtains as $K \to \infty$, cf. eqn (2.11)):

$$J^{\mathrm{I}} = \begin{pmatrix} -\psi_W^2 K r_G^2 \\ \psi_W r_1 r_G - \psi_W^2 r_1 K r_G^2 \\ \vdots \\ \psi_W r_n r_G - \psi_W^2 r_n K r_G^2 \\ \psi_W K r_G + \psi_W r_G^2 - \psi_W^2 K r_G^3 \\ -\sigma_1 \\ \vdots \\ -\sigma_n \end{pmatrix},\; J^{\mathrm{II}} = \begin{pmatrix} 0 & \cdots & 0 \\ -\psi_W r_G & \cdots & 0 \\ \vdots & \vdots & \vdots \\ 0 & \cdots & -\psi_W r_G \\ 0 & \cdots & 0 \\ \psi_1 & \cdots & 0 \\ \vdots & \vdots & \vdots \\ 0 & \cdots & \psi_n \end{pmatrix},\; J^{\mathrm{III}} = \begin{pmatrix} -\psi_W \\ -\psi_W r_1 \\ \vdots \\ -\psi_W r_n \\ -2\psi_W r_G \\ \frac{\sigma_1 - \psi_1 r_1}{r_G} \\ \vdots \\ \frac{\sigma_n - \psi_n r_n}{r_G} \end{pmatrix},$$

$$J^{\mathrm{IV}} = \begin{pmatrix} -\psi_W^2 r_1' r_G^2 & \dots & -\psi_W^2 r_n' r_G^2 \\ \psi_W r_1' r_G - \psi_W^2 r_1 r_1' r_G^2 & \dots & -\psi_W^2 r_1 r_n' r_G^2 \\ \vdots & \vdots & \\ -\psi_W^2 r_1' r_n r_G^2 & \dots & \psi_W r_n' r_G - \psi_W^2 r_n r_n' r_G^2 \\ -\psi_W^2 r_G^3 r_1' & \dots & -\psi_W^2 r_G^3 r_n' \\ -\psi_W r_G & \dots & 0 \\ \vdots & \vdots & \vdots \\ 0 & \dots & -\psi_W r_G \end{pmatrix}.$$

Lemma 1 *Only the minors that contain a diagonal element from J^I contribute terms that are proportional to K; in particular,*

$$\begin{aligned} \widetilde{c}_k &= C_{2n+1}^{k-1} K \psi_W^{k+1} r_G^{k+1} + C_{2n}^{k-2} K \psi_W^k r_G^{k-1} + \\ &+ \sum_{\ell=1}^{n} C_{2n-(2\ell-1)}^{k-(2\ell+1)} K \psi_W^{k+1-\ell} r_G^{k-\ell} (-1)^\ell \sum_{\mathbb{S}\in\mathscr{P}_\ell(\{1,2\dots,n\})} \prod_{m\in\mathbb{S}} r_m' \left(r_G \prod_{m\in\mathbb{S}} \psi_m + \sum_{m\in\mathbb{S}} (\psi_m r_m - \sigma_m) \prod_{j\in\mathbb{S}\setminus m} \psi_j \right) + \\ &+ \sum_{\ell=1}^{n} C_{2n-2\ell}^{k-(2\ell+2)} K \psi_W^{k-\ell} r_G^{k-\ell-1} (-1)^\ell \sum_{\mathbb{S}\in\mathscr{P}_\ell(\{1,2\dots,n\})} \prod_{m\in\mathbb{S}} \psi_m r_m' \,, \end{aligned} \tag{2.34}$$

where $\mathscr{P}_\ell(\{1,2\dots,n\})$ is the set of all subsets of the set $\{1,2\dots,n\}$ with cardinality ℓ.

For example, for $n=2$ and $k=6$ we have:

$$\begin{aligned} \widetilde{c}_6 &= K\psi_W^7 r_G^7 + K\psi_W^6 r_G^5 - \\ &- K\psi_W^6 r_G^5 r_1' \Big(\psi_1 r_G + (\psi_1 r_1 - \sigma_1) \Big) - K\psi_W^6 r_G^5 r_2' \Big(\psi_2 r_G + (\psi_2 r_2 - \sigma_2) \Big) + \\ &+ K\psi_W^5 r_G^4 r_1' r_2' \Big(\psi_1\psi_2 r_G + \psi_1(\psi_2 r_2 - \sigma_2) + \psi_2(\psi_1 r_1 - \sigma_1) \Big) - \\ &- K\psi_W^5 r_G^4 \psi_1 r_1' - K\psi_W^5 r_G^4 \psi_2 r_2' + K\psi_W^4 r_G^3 \psi_1\psi_2 r_1' r_2' \,. \end{aligned} \tag{2.35}$$

Proof. Only the minors that contain a diagonal element from the first column contribute terms proportional to K, because the minors that do not contain elements from J^{I} do not contain any term $\propto K$. There are 2^n-1 non-trivial subsets of the set of size n. To obtain all minors that contribute terms $\propto K$ we have to inspect $2^3-1=7$ types of minor containing a diagonal element taken from J^{I}, as the ways in which such minors can be composed depends on the number of non-trivial subsets of the set of size 3. One of these types only occurs for $k=2$ (minors based on J^{I} and J^{III}) and can be subsumed under type iii. This leaves six types to be distinguished; they are defined as being composed of the following, in addition to the element contributed by the column matrix J^{I}: (i) $k-1$ diagonal elements from J^{II}; (ii) $k-1$ diagonal elements from J^{IV}; (iii) $k-2$ diagonal elements from J^{II} and one from J^{III}; (iv) $k-2$ diagonal elements from J^{IV} and one from J^{III}; (v) diagonal elements from J^{II} and J^{IV} such that their total number is $k-1$; (vi) diagonal elements from J^{II} and J^{IV} such that their total number is $k-2$, in addition to an element

from J^{III}.

We consider these types in terms and collect the terms proportional to K. For the sake of clarity, expressions such as $(-1)^{k-2}$, $(-1)^{k-4}$ etc. will be written as $(-1)^k$ and likewise $(-1)^{k-1}$, $(-1)^{k-3}$ etc. will be written as $(-1)^{k+1}$. The binomial coefficient $\binom{n}{k} = n!(k!(n-k)!)^{-1}$ will be denoted as C_n^k. We will make use of the following:

$$\sum_{i=0}^{k} C_n^i C_n^{k-i} = C_{2n}^k \quad \text{and} \quad C_n^k + C_n^{k-1} = C_{n+1}^k \,. \tag{2.36}$$

Minors of type i have the following form:

$$\begin{vmatrix} -\psi_W^2 K r_G^2 & 0 & \dots & 0 \\ \psi_W r_1 r_G - \psi_W^2 r_1 K r_G^2 & -\psi_W r_G & \dots & 0 \\ \vdots & \vdots & \vdots & \vdots \\ \psi_W r_{k-1} r_G - \psi_W^2 r_{k-1} K r_G^2 & 0 & \dots & -\psi_W r_G \end{vmatrix} = (-1)^k K \psi_W^{k+1} r_G^{k+1} \,.$$

We have C_n^{k-1} such minors, because the first column J^{I} is fixed and we are choosing $k-1$ diagonal elements from a total of n elements in block J^{II}. Thus minors of this type contribute $(-1)^k C_n^{k-1} K \psi_W^{k+1} r_G^{k+1}$ to the right-hand side of eqn (2.34).

Minors of type ii have the following form:

$$\begin{vmatrix} -\psi_W^2 K r_G^2 & -\psi_W^2 r_1' r_G^2 & \dots & -\psi_W^2 r_{k-1}' r_G^2 \\ -\sigma_1 & -\psi_W r_G & \dots & 0 \\ \vdots & \vdots & \vdots & \vdots \\ -\sigma_{k-1} & 0 & \dots & -\psi_W r_G \end{vmatrix} = (-1)^k K \psi_W^{k+1} r_G^{k+1} + \dots$$

where the dots (here and in what follows) correspond to terms that do not contain K. We have C_n^{k-1} such minors, giving a contribution $(-1)^k C_n^{k-1} K \psi_W^{k+1} r_G^{k+1}$ to eqn (2.34).

Minors of type iii have the following form:

$$\begin{vmatrix} -\psi_W^2 K r_G^2 & 0 & \dots & 0 & -\psi_W \\ \psi_W r_1 r_G - \psi_W^2 r_1 K r_G^2 & -\psi_W r_G & \dots & 0 & -\psi_W r_1 \\ \vdots & \vdots & \vdots & \vdots & \vdots \\ \psi_W r_{k-2} r_G - \psi_W^2 r_{k-2} K r_G^2 & 0 & \dots & -\psi_W r_G & -\psi_W r_{k-2} \\ \psi_W K r_G + \psi_W r_G^2 - \psi_W^2 K r_G^3 & 0 & \dots & 0 & -2\psi_W r_G \end{vmatrix} =$$

$$= (-1)^k K \psi_W^{k+1} r_G^{k+1} + (-1)^k K \psi_W^k r_G^{k-1} + \dots \,.$$

We have C_n^{k-2} such minors and the contribution is therefore $(-1)^k C_n^{k-2} \left(K \psi_W^{k+1} r_G^{k+1} + K \psi_W^k r_G^{k-1} \right)$.

Minors of type iv have the following form:

$$\begin{vmatrix} -\psi_W^2 K r_G^2 & -\psi_W & -\psi_W^2 r_1' r_G^2 & \dots & -\psi_W^2 r_i' r_G^2 & \dots & -\psi_W^2 r_{k-2}' r_G^2 \\ \psi_W K r_G + \psi_W r_G^2 - \psi_W^2 K r_G^3 & -2\psi_W r_G & -\psi_W^2 r_1' r_G^3 & \dots & -\psi_W^2 r_i' r_G^3 & \dots & -\psi_W^2 r_{k-2}' r_G^3 \\ -\sigma_1 & (\sigma_1 - \psi_1 r_1)/r_G & -\psi_W r_G & \dots & 0 & \dots & 0 \\ \vdots & \vdots & \vdots & \vdots & \vdots & \vdots & \vdots \\ -\sigma_i & (\sigma_i - \psi_i r_i)/r_G & 0 & \dots & -\psi_W r_G & \dots & 0 \\ \vdots & \vdots & \vdots & \vdots & \vdots & \vdots & \vdots \\ -\sigma_{k-2} & (\sigma_{k-2} - \psi_{k-2} r_{k-2})/r_G & 0 & \dots & 0 & \dots & -\psi_W r_G \end{vmatrix}.$$

These contribute the same term as minors of type iii, i.e. $(-1)^k C_n^{k-2}\left(K\psi_W^{k+1} r_G^{k+1} + K\psi_W^k r_G^{k-1}\right)$. In addition, minors based on the diagonal element of column i in block J^{IV} contribute $(-1)^k r_i'(\sigma_i - r_i\psi_i) K\psi_W^k r_G^{k-1}$. For each i, there are C_{n-1}^{k-3} ways of making up the remaining $k-3$ elements (which are chosen from a total $n-1$ in block J^{IV}). This yields a total contribution of $(-1)^k C_{n-1}^{k-3} \sum_{i\in\mathscr{P}_1(\{1,2\dots,n\})} r_i'(\sigma_i - r_i\psi_i) K\psi_W^k r_G^{k-1}$.

Minors of type v have the following form:

$$\begin{vmatrix} -\psi_W^2 K r_G^2 & 0 & \dots & 0 & -\psi_W^2 r_1' r_G^2 & \dots & -\psi_W^2 r_{k-1-i}' r_G^2 \\ \psi_W r_1 r_G - \psi_W^2 r_1 K r_G^2 & -\psi_W r_G & \dots & 0 & \psi_W r_1' r_G - \psi_W^2 r_1 r_1' r_G^2 & \dots & -\psi_W^2 r_1 r_{k-1-i}' r_G^2 \\ \vdots & \vdots & \vdots & \vdots & \vdots & \vdots & \vdots \\ \psi_W r_i r_G - \psi_W^2 r_i K r_G^2 & 0 & \dots & -\psi_W r_G & -\psi_W^2 r_i r_1' r_G^2 & \dots & \psi_W^2 r_i r_{k-1-i}' r_G^2 \\ -\sigma_1 & \psi_1 & \dots & 0 & -\psi_W r_G & \dots & 0 \\ \vdots & \vdots & \vdots & \vdots & \vdots & \vdots & \vdots \\ -\sigma_{k-1-i} & 0 & \dots & 0 & 0 & \dots & -\psi_W r_G \end{vmatrix}.$$

Each minor contributes a term $(-1)^k K\psi_W^{k+1} r_G^{k+1}$. Since we are choosing $k-1$ diagonal elements from blocks J^{II} and J^{IV}, the multiplicity is $\sum_{i=1}^{k-2} C_n^i C_n^{k-1-i}$, giving a total $(-1)^k \sum_{i=1}^{k-2} C_n^i C_n^{k-1-i} K\psi_W^{k+1} r_G^{k+1}$. Furthermore, each minor containing diagonal elements from column i in J^{II} and column i in J^{IV}, contributes $(-1)^{k+1}\psi_i r_i' K\psi_W^k r_G^k$. There are $\sum_{i=0}^{k-3} C_{n-1}^i C_{n-1}^{k-3-i}$ such minors, since for each i we are choosing $k-3$ diagonal elements from J^{II} and J^{IV} combined. Using $\sum_{i=0}^{k-3} C_{n-1}^i C_{n-1}^{k-3-i} = C_{2n-2}^{k-3}$, we obtain

$$(-1)^{k+1} C_{2n-2}^{k-3} \sum_{i\in\mathscr{P}_1(\{1,2\dots,n\})} \psi_i r_i' K\psi_W^k r_G^k$$

as the total contribution to the right-hand side of eqn (2.34). Next, given a pair (i,j) with $i \neq j$, we consider minors containing diagonal elements from columns i and j in J^{II} and columns i and j in J^{IV}; such a minor contributes $(-1)^k r_i' r_j' \psi_i \psi_j K\psi_W^{k-1} r_G^{k-1}$. The multiplicity is $\sum_{i=0}^{k-5} C_{n-2}^i C_{n-2}^{k-5-i}$, since for a given choice (i,j) there remain $k-5$ elements to be chosen. Summing over all such pairs (i,j) and using

the combinatorics formulae, eqn (2.36), we obtain

$$(-1)^k C_{2n-4}^{k-5} \sum_{(i\,,j)\in\mathscr{P}_2(\{1,2\ldots,n\})} r_i' r_j' \psi_i \psi_j K \psi_W^{k-1} r_G^{k-1} \ .$$

Next, after pairs of columns, we need to consider triples (i,j,k), and so on. The general formula for an ℓ-tuple can be obtained via similar reasoning, and summing over all such tuples we have

$$(-1)^k \sum_{\ell=1}^{n} \left(C_{2n-2\ell}^{k-(2\ell+1)} K \psi_W^{k+1-\ell} r_G^{k+1-\ell} (-1)^\ell \sum_{\mathbb{S}\in\mathscr{P}_\ell(\{1,2\ldots,n\})} \prod_{m\in\mathbb{S}} \psi_m r_m' \right)$$

as the final contribution.

Minors of type vi contain contributions from all blocks of the Jacobian matrix, cf. eqn (2.33). Each minor contributes $(-1)^k \sum_{i=1}^{k-3} C_n^i C_n^{k-2-i} K \psi_W^k \left(\psi_W r_G^{k+1} + r_G^{k-1} \right)$, where the multiplicity arises from the $k-2$ choices from blocks J^{II} and J^{IV} combined. In analogy to type iv, minors of type vi contribute the following term $\propto K$:

$$(-1)^k \sum_{q=1}^{k-3} C_n^q C_{n-1}^{k-3-q} \sum_{i\in\mathscr{P}_1(\{1,2\ldots,n\})} r_i' (\sigma_i - r_i \psi_i) K \psi_W^k r_G^{k-1}$$

and in analogy to type v, minors of type vi contribute the following term $\propto K$:

$$(-1)^k \sum_{\ell=1}^{n} \left(C_{2n-2\ell}^{k-(2\ell+2)} K \psi_W^{k+1-\ell} r_G^{k+1-\ell} (-1)^\ell \sum_{\mathbb{S}\in\mathscr{P}_\ell(\{1,2\ldots,n\})} \prod_{m\in\mathbb{S}} \psi_m r_m' \right) .$$

There are further terms contributed by minors containing diagonal elements from columns i and j in block J^{IV} (where $i \neq j$) in addition to a diagonal element from either columns i or j in block J^{II}; such minors contribute $(-1)^{k+1} r_i' r_j' \left(\psi_i (\psi_j r_j - \sigma_j) + \psi_j (\psi_i r_i - \sigma_i) \right) K \psi_W^{k-1} r_G^{k-2}$. Summing over all pairs (i,j) and using the combinatorics formulae, eqn (2.36), we obtain

$$(-1)^{k+1} C_{2n-3}^{k-5} K \psi_W^{k-1} r_G^{k-2} \sum_{(i\,,j)\in\mathscr{P}_2(\{1,2\ldots,n\})} r_i' r_j' \left(\psi_i (\psi_j r_j - \sigma_j) + \psi_j (\psi_i r_i - \sigma_i) \right) \ .$$

Next we consider triples (i,j,p), with $i \neq j \neq p$, and minors that take diagonal elements from columns i, j, and p from block J^{IV} while block J^{II} contributes diagonal elements from a pair of columns, which is either the pair (i,j), or (i,p), or (j,p). Summing over all triples (i,j,p) and using the combinatorics formulae, eqn (2.36), we obtain

$$(-1)^k C_{2n-5}^{k-7} \sum_{(i\,,j\,,\,p)\in\mathscr{P}_3(\{1,2\ldots,n\})} r_i' r_j' r_p' \Big(\psi_i \psi_p (\psi_j r_j - \sigma_j) + \psi_j \psi_p (\psi_i r_i - \sigma_i) + \psi_i \psi_j (\psi_p r_p - \sigma_p) \Big) K \psi_W^{k-2} r_G^{k-3} \ .$$

Generalising this argument to ℓ-tuples of columns chosen from J^{IV}, we obtain the following:

$$(-1)^k \sum_{\ell=2}^{n} C_{2n-(2\ell-1)}^{k-(2\ell+1)} K \psi_W^{k+1-\ell} r_G^{k-\ell} (-1)^\ell \sum_{\mathbb{S}\in\mathscr{P}_\ell(\{1,2\ldots,n\})} \prod_{m\in\mathbb{S}} r'_m \left(\sum_{m\in\mathbb{S}} (\psi_m r_m - \sigma_m) \prod_{j\in\mathbb{S}\setminus m} \psi_j \right) .$$

A term $(-1)^{k+1}\psi_i r'_i K \psi_W^{k-1} r_G^{k-2}$ is contributed by each minor that takes diagonal elements from column i in J^{II} and from column i in J^{IV}. Taking into account the multiplicity $\sum_{i=0}^{k-4} C_{n-1}^{i} C_{n-1}^{k-4-i}$ and simplifying the sum, we obtain

$$(-1)^{k+1} C_{2n-2}^{k-4} \sum_{i\in\mathscr{P}_1(\{1,2\ldots,n\})} \psi_i r'_i K \psi_W^{k-1} r_G^{k-2} .$$

For a given pair (i,j), with $i \neq j$, minors taking diagonal elements from columns i and j in J^{II} and from columns i and j in J^{IV} contribute $(-1)^k r'_i r'_j \psi_i \psi_j K \psi_W^{k-2} r_G^{k-3}$ each. The multiplicity of such minors is $\sum_{i=0}^{k-6} C_{n-2}^{i} C_{n-2}^{k-6-i}$. Summing over all pairs (i,j) and simplifying, we have

$$(-1)^k C_{2n-4}^{k-6} \sum_{(i\,,j)\in\mathscr{P}_2(\{1,2\ldots,n\})} r'_i r'_j \psi_i \psi_j K \psi_W^{k-2} r_G^{k-3} .$$

Generalising to ℓ-tuples, we obtain

$$(-1)^k \sum_{\ell=1}^{n} C_{2n-2\ell}^{k-(2\ell+2)} K \psi_W^{k-\ell} r_G^{k-\ell-1} (-1)^\ell \sum_{\mathbb{S}\in\mathscr{P}_\ell(\{1,2\ldots,n\})} \prod_{m\in\mathbb{S}} \psi_m r'_m .$$

Equation (2.34) is obtained by collecting terms proportional to K. In particular, terms $\propto K\psi_W^{k+1} r_G^{k+1}$ have the following coefficients:

$$\begin{aligned}
&(-1)^k C_n^{k-1} + (-1)^k C_n^{k-1} + (-1)^k C_n^{k-2} + (-1)^k C_n^{k-2} + (-1)^k \sum_{i=1}^{k-2} C_n^i C_n^{k-1-i} + (-1)^k \sum_{i=1}^{k-3} C_n^i C_n^{k-2-i} = \\
&= (-1)^k \left(\sum_{i=0}^{k-2} C_n^i C_n^{k-1-i} + \sum_{i=0}^{k-3} C_n^i C_n^{k-2-i} + C_n^{k-1} + C_n^{k-2} \right) = \\
&= (-1)^k \left(C_{2n}^{k-1} - C_n^{k-1} + C_{2n}^{k-2} - C_n^{k-2} + C_n^{k-1} + C_n^{k-2} \right) = \\
&= (-1)^k \left(C_{2n}^{k-1} + C_{2n}^{k-2} \right) = (-1)^k C_{2n+1}^{k-1} ;
\end{aligned}$$

terms $\propto K\psi_W^{k} r_G^{k-1}$ have the following coefficients:

$$\begin{aligned}
&(-1)^k C_n^{k-2} + (-1)^k C_n^{k-2} + (-1)^k \sum_{i=1}^{k-3} C_n^i C_n^{k-2-i} = (-1)^k \left(C_n^{k-2} + \sum_{i=0}^{k-3} C_n^i C_n^{k-2-i} \right) = \\
&= (-1)^k \left(C_n^{k-2} + C_{2n}^{k-2} - C_n^{k-2} \right) = (-1)^k C_{2n}^{k-2} ;
\end{aligned}$$

terms $\propto K\psi_W^{k+1-\ell} r_G^{k+1-\ell} (-1)^\ell \sum_{\mathbb{S}\in\mathscr{P}_\ell(\{1,2\ldots,n\})} \prod_{m\in\mathbb{S}} \psi_m r'_m$ have the following coefficients:

$$(-1)^k C_{2n-2\ell}^{k-(2\ell+1)} + (-1)^k C_{2n-2\ell}^{k-(2\ell+2)} = C_{2n-(2\ell-1)}^{k-(2\ell+1)} \quad \text{where } \ell \in \{1\ldots n\};$$

terms $\propto K\psi_W^{k+1-\ell} r_G^{k-\ell}(-1)^\ell \sum_{\mathbb{S}\in\mathscr{P}_\ell(\{1,2\ldots,n\})}\prod_{m\in\mathbb{S}} r'_m \left(\sum_{m\in\mathbb{S}}(\psi_m r_m-\sigma_m)\prod_{j\in\mathbb{S}\setminus m}\psi_j\right)$ have the following coefficients:

$$(-1)^k C_{n-1}^{k-3} + (-1)^k \sum_{q=1}^{k-3} C_n^q C_{n-1}^{k-3-q} = \sum_{q=0}^{k-3} C_n^q C_{n-1}^{k-3-q} = C_{2n-1}^{k-3} \quad \text{for } \ell = 1$$

and $(-1)^k C_{2n-(2\ell-1)}^{k-(2\ell+1)}$ for $\ell \in \{2\ldots n\}$.

Recall that $c_k = (-1)^k S_k$ where S_k is the sum of the principal minors M_k that are symmetric with respect to the main diagonal of J; thus S_k is a polynomial in K. Letting $\widetilde{S}_k$ denote the terms in this polynomial that are proportional to K, we have $\widetilde{c}_k = (-1)^k \widetilde{S}_k$ and this implies that

$$\begin{aligned}\widetilde{c}_k = (-1)^k(-1)^k \Bigg(& C_{2n+1}^{k-1} K \psi_W^{k+1} r_G^{k+1} + C_{2n}^{k-2} K \psi_W^k r_G^{k-1} + \\ & + \sum_{\ell=1}^{n} C_{2n-(2\ell-1)}^{k-(2\ell+1)} K \psi_W^{k+1-\ell} r_G^{k-\ell} (-1)^\ell \sum_{\mathbb{S}\in\mathscr{P}_\ell(\{1,2\ldots,n\})} \prod_{m\in\mathbb{S}} r'_m \Big(r_G \prod_{m\in\mathbb{S}} \psi_m + \sum_{m\in\mathbb{S}} (\psi_m r_m - \sigma_m) \prod_{j\in\mathbb{S}\setminus m} \psi_j \Big) + \\ & + \sum_{\ell=1}^{n} C_{2n-2\ell}^{k-(2\ell+2)} K \psi_W^{k-\ell} r_G^{k-\ell-1} (-1)^\ell \sum_{\mathbb{S}\in\mathscr{P}_\ell(\{1,2\ldots,n\})} \prod_{m\in\mathbb{S}} \psi_m r'_m \Bigg) .\end{aligned}$$

which yields eqn (2.34). □

Lemma 1 has a consequence which will prove important in establishing stability of the equilibrium.

Corollary 1 (Positive coefficients) *The coefficients of the characteristic polynomial, eqn (2.32), are all positive for sufficiently large K.*

Proof. The coefficients c_k of the characteristic polynomial, eqn (2.32), are first-order polynomials in K. Therefore, for K is sufficiently large, the sign will agree with that of the terms $\propto K$, since all other terms in c_k are compound expressions made up of the model's parameters, which are all bounded. It therefore suffices to establish that the $\widetilde{c}_k$ are positive. We consider the terms on the right-hand side of eqn (2.34) in turn. The first two terms are positive since K, ψ_W, and r_G are all positive. To determine the sign of the third term we recall that $r'_m < 0$ by the assumed properties of r_m as a function of x_m (where $m \in \{1,\ldots,n\}$). Since $m \in \mathbb{S}$ and $|\,\mathbb{S}\,| = \ell$, we have $\prod_{m\in\mathbb{S}} r'_m = (-1)^\ell \prod_{m\in\mathbb{S}} |\, r'_m \,|$ which means that the third term can be rewritten as follows:

$$\sum_{\ell=1}^{n} C_{2n-(2\ell-1)}^{k-(2\ell+1)} K \psi_W^{k+1-\ell} r_G^{k-\ell} \sum_{\mathbb{S}\in\mathscr{P}_\ell(\{1,2\ldots,n\})} \prod_{m\in\mathbb{S}} |\, r'_m \,| \left(r_G \prod_{m\in\mathbb{S}} \psi_m + \sum_{m\in\mathbb{S}} (\psi_m r_m - \sigma_m) \prod_{j\in\mathbb{S}\setminus m} \psi_j \right) .$$

This quantity is positive since $\psi_m r_m - \sigma_m > 0$, which can be seen by re-arranging eqn (2.29) as

$$\psi_m r_m - \sigma_m = (1 + x_m)\, \psi_W r_G$$

and recalling that $x_m \geq 0$ at equilibrium. The final term can be rewritten in analogy to the third term, yielding

$$\sum_{\ell=1}^{n} C_{2n-2\ell}^{k-(2\ell+2)} K \psi_W^{k-\ell} r_G^{k-\ell-1} \sum_{\mathbb{S} \in \mathscr{P}_\ell(\{1,2\ldots,n\})} \prod_{m \in \mathbb{S}} \psi_m \mid r'_m \mid ,$$

which is positive for $m \in \{1, 2, \ldots, n\}$. Thus, all terms in eqn (2.34) are positive and therefore $\widetilde{c}_k > 0$ for $k \in \{1, 2, \ldots, 2n+2\}$. It follows that the coefficients of the characteristic polynomial, eqn (2.32), are all positive for sufficiently large K. □

Stability of the characteristic equation

Theorem 1 (Strelitz) *A monic polynomial with real coefficients is stable if and only if the coefficients of both this polynomial and its sum-of-roots polynomial are all positive.*

We omit the proof, which can be found in Strelitz [140], who also shows how to compute the coefficients of the sum-of-roots polynomial efficiently in terms of power-sums. This algorithm exploits the Newton-Girard formulae for power-sums of polynomial roots [137] and Strelitz's recurrence formula. Let

$$f = \lambda^{2n+2} + \widetilde{c}_1 \lambda^{2n+1} + \widetilde{c}_2 \lambda^{2n} + \cdots + \widetilde{c}_{2n+1} \lambda + \widetilde{c}_{2n+2} ,$$

where the coefficients $\widetilde{c}_i$, $i \in \{1, 2, \ldots, 2n+2\}$, are given by eqn (2.34). The sum-of-roots polynomial is

$$g = \lambda^m + b_1 \lambda^{m-1} + b_2 \lambda^{m-2} + \cdots + b_{m-1} \lambda + b_m ,$$

where $m = (2n+2)(2n+1)/2 = (n+1)(2n+1)$ and the b_m are to be determined by means of Strelitz's algorithm. Let $\{\alpha_i\}_{i \in \{1,\ldots,2n+2\}}$ be the set of all $2n+2$ roots of f, and $\{\beta_i\}_{i \in \{1,\ldots,m\}} = \{\alpha_i + \alpha_j\}_{1 \leq i < j \leq 2n+2}$ be the set of all m roots of g. The power sums of f and g will be denoted as

$$\zeta_j = \sum_{i=1}^{2n+2} \alpha_i^j, \qquad s_j = \sum_{i=1}^{m} \beta_i^j, \qquad j \in \{0, 1, \ldots, m\} ,$$

respectively. Strelitz's algorithm consists of three main steps:

Step 1 Express ζ_j in terms of $\widetilde{c}_i$, where $i \in \{0, 1, \ldots 2n+2\},\ j \in \{0, 1, \ldots, m\}$.

Step 2 For $k \in \{0,1,\ldots,m\}$, express s_k in terms of $\widetilde{c}_i$, where $i \in \{0,1,\ldots 2n+2\}$, via the ζ_j, $j \in \{0,1,\ldots,m\}$, which are obtained in Step 1.

Step 3 For $\ell \in \{0,1,\ldots,m\}$, express b_ℓ in terms of $\widetilde{c}_i$, where $i \in \{0,1,\ldots 2n+2\}$, via the s_k, $k \in \{0,1,\ldots,m\}$, which are obtained in Step 2.

Step 1 relies on the Newton-Girard formulae:

$$\begin{aligned}
\zeta_0 &= 2n+2 \\
\zeta_1 + \widetilde{c}_1 &= 0 \\
\zeta_2 + \zeta_1\widetilde{c}_1 + 2\widetilde{c}_2 &= 0 \\
&\vdots \\
\zeta_j + \zeta_{j-1}\widetilde{c}_1 + 2\zeta_{j-2}\widetilde{c}_2 + \ldots + j\widetilde{c}_j &= 0 \\
&\vdots \\
\zeta_{2n+2} + \zeta_{2n+1}\widetilde{c}_1 + 2\zeta_{2n}\widetilde{c}_2 + \ldots + (2n+2)\widetilde{c}_{2n+2} &= 0
\end{aligned} \tag{2.37}$$

where for $j > 2n+2$ we have

$$\zeta_j + \zeta_{j-1}\widetilde{c}_1 + \ldots + \zeta_{j-(2n+2)}\widetilde{c}_{2n+2} = 0\,. \tag{2.38}$$

We shall write $\bar{c}_i = \widetilde{c}_i/K$, so that $\widetilde{c}_i = K\bar{c}_i$. From system (2.37) we find the ζ_j:

$$\begin{aligned}
\zeta_0 &= 2n+2 \\
\zeta_1 &= -\widetilde{c}_1 = -K\bar{c}_1 \\
\zeta_2 &= -\zeta_1\widetilde{c}_1 - 2\widetilde{c}_2 = K^2\bar{c}_1^2 - 2K\bar{c}_2 \\
\zeta_3 &= -\zeta_2\widetilde{c}_1 - 2\zeta_1\widetilde{c}_2 - 3\widetilde{c}_3 = -K^3\bar{c}_1^3 + 2K^2\bar{c}_1\bar{c}_2 - 3K\bar{c}_3 \\
&\vdots
\end{aligned} \tag{2.39}$$

which shows that the ζ_j are polynomials in K. Let $\widetilde{\zeta}_j$ denote the term in the polynomial ζ_j with the leading power of K. If K is sufficiently large, we need only consider these polynomials to leading power of K, since the $\bar{c}_i$, $i \in \{1,2,\ldots,2n+2\}$, consist of model parameters, each of which is bounded.

Lemma 2 *For each polynomial ζ_j, where $j \in \{2,3,\ldots,m\}$ only the term $-\zeta_{j-1}\widetilde{c}_1$ contributes to the*

leading power of K, in particular,

$$\widetilde{\zeta}_j = (-1)^j K^j \bar{c}_1^j \,. \tag{2.40}$$

We remark that the case $j = 1$ is irrelevant since ζ_1 does not depend on ζ_0.

Proof. The proof is by induction. For $j = 2$ we have, from system (2.39):

$$\zeta_2 = -\zeta_1 \widetilde{c}_1 - 2\widetilde{c}_2 = K^2 \bar{c}_1^2 - 2K\bar{c}_2 \,,$$

so that $\widetilde{\zeta}_2 = K^2 \bar{c}_1^2$ which agrees with the claim, since it is derived from $-\zeta_1 \widetilde{c}_1$ and conforms to the formula $(-1)^j K^j \bar{c}_1^j$, eqn (2.40). For the induction step, we assume that eqn (2.40) holds for $j = k$, i.e., the term with leading power of K of the polynomial ζ_k is contributed by $-\zeta_{k-1}\widetilde{c}_1$ which is the first term in the general form

$$\zeta_k = -\zeta_{k-1}\widetilde{c}_1 - 2\zeta_{k-2}\widetilde{c}_2 - \ldots - k\widetilde{c}_k \tag{2.41}$$

and, moreover, it is true that

$$\widetilde{\zeta}_k = (-1)^k K^k \bar{c}_1^k \,. \tag{2.42}$$

By the induction hypothesis, ζ_{k-1} contributes a term $\propto K^{k-1}$ and all terms other than the first in the right-hand side of eqn (2.41) must contribute powers of K less than k, which in turn implies that ζ_{k-2}, ζ_{k-3}, …, ζ_1 contribute powers of K less than $k-1$ as $\widetilde{c}_i = K\bar{c}_i$ for $i \in \{1, 2, \ldots, 2n+2\}$. To prove that the claim is correct for $j = k+1$ we consider the polynomial ζ_{k+1}, which by the Newton-Girard recursion takes on the following form:

$$\zeta_{k+1} = -\zeta_k \widetilde{c}_1 - 2\zeta_{k-1}\widetilde{c}_2 - \ldots - (k+1)\widetilde{c}_{k+1} \,. \tag{2.43}$$

By induction hypothesis, ζ_k contributes the leading power k of K, while ζ_{k-1} contributes K^{k-1} and ζ_{k-2}, ζ_{k-3}, …, ζ_1 contribute powers of K less than $k-1$. Thus, the leading-power term in ζ_{k+1} can only be $-\zeta_k \widetilde{c}_1$. Since $-\zeta_k \widetilde{c}_1 = -\zeta_k K \bar{c}_1$, the leading term is $-\widetilde{\zeta}_k K \bar{c}_1$, which can be combined with eqn (2.42) to give $\widetilde{\zeta}_{k+1} = (-1)^{k+1} K^{k+1} \bar{c}_1^{k+1}$ which agrees with eqn (2.40) for $j = k+1$, as required. An entirely analogous argument using eqn (2.38) establishes the result for $j > 2n+2$. □

As we have $\zeta_1 = -K\bar{c}_1$ from eqn (2.39), we can claim that

$$\widetilde{\zeta}_0 = 2n+2 \quad \text{and} \quad \widetilde{\zeta}_j = (-1)^j K^j \bar{c}_1^j \quad \text{for } j = 1, 2, \ldots, m. \tag{2.44}$$

We proceed to Step 2 of Strelitz's algorithm, expressing s_k in terms of $\widetilde{c}_i$ by means of the formulae for $\widetilde{\zeta}_j$

which were obtained in the previous step. Strelitz's recurrence formulae relate power-sums for g to those of f:

$$2s_j = \sum_{p=0}^{j} C_j^p \zeta_p \zeta_{j-p} - 2^j \zeta_j \,, \qquad j \in \{0,1,\ldots,m\} \,.$$

As ζ_j are polynomials in K, the s_j are also polynomials in K. Letting $\widetilde{s}_j$ denote the term in the polynomial s_j with leading power of K, we have

$$2\widetilde{s}_j = \sum_{p=0}^{j} C_j^p \widetilde{\zeta}_p \widetilde{\zeta}_{j-p} - 2^j \widetilde{\zeta}_j \,, \qquad j \in \{0,1,\ldots,m\} \,.$$

By system (2.44), we have

$$\begin{aligned} 2\widetilde{s}_j &= C_j^0 \widetilde{\zeta}_0 \widetilde{\zeta}_j + C_j^j \widetilde{\zeta}_j \widetilde{\zeta}_0 + \textstyle\sum_{p=1}^{j-1} C_j^p \widetilde{\zeta}_p \widetilde{\zeta}_{j-p} - 2^j \widetilde{\zeta}_j = \\ &= 2(2n+2)(-1)^j K^j \bar{c}_1^j + \textstyle\sum_{p=1}^{j-1} C_j^p (-1)^j K^j \bar{c}_1^j - 2^j (-1)^j K^j \bar{c}_1^j = \\ &= 2(2n+2)(-1)^j K^j \bar{c}_1^j + (-1)^j K^j \bar{c}_1^j \left(\textstyle\sum_{p=1}^{j-1} C_j^p - 2^j \right) \,. \end{aligned}$$

The term between brackets can be written as $\sum_{p=0}^{j} C_j^p - C_j^0 - C_j^j - 2^j$ which can be simplified by means of the combinatoric equation $\sum_{p=0}^{j} C_j^p = 2^j$, yielding:

$$\widetilde{s}_j = (-1)^j K^j \bar{c}_1^j (2n+1) \,, \qquad j \in \{1,2\ldots,m\} \,. \tag{2.45}$$

To express the b_ℓ in terms of the $\widetilde{c}_i$ via the $\widetilde{s}_j$, we again use the Newton-Girard formulae, replacing m, b_ℓ, and $\widetilde{s}_j$ by n, $\widetilde{c}_i$, and ζ_j, respectively in system (2.37), which gives

$$\begin{aligned} \widetilde{s}_0 &= m \\ \widetilde{s}_1 + b_1 &= 0 \\ \widetilde{s}_2 + \widetilde{s}_1 b_1 + 2b_2 &= 0 \\ &\vdots \\ \widetilde{s}_\ell + \widetilde{s}_{\ell-1} b_1 + 2\widetilde{s}_{\ell-2} b_2 + \ldots + \ell b_\ell &= 0 \\ &\vdots \\ \widetilde{s}_m + \widetilde{s}_{m-1} b_1 + 2\widetilde{s}_{m-2} b_2 + \ldots + m b_m &= 0 \end{aligned} \tag{2.46}$$

By eqn (2.45) we have

$$\begin{aligned} b_1 &= -\widetilde{s}_1 = K\bar{c}_1(2n+1) \\ 2b_2 &= -\widetilde{s}_2 - \widetilde{s}_1 b_1 = K^2\bar{c}_1^2(2n+1)2n \\ 3b_3 &= -\widetilde{s}_3 - \widetilde{s}_2 b_1 - 2\widetilde{s}_1 b_2 = K^3\bar{c}_1^3(2n+1)(2n)^2 \\ &\vdots \end{aligned} \tag{2.47}$$

The pattern that is apparent from these first few terms holds in general, as asserted by the following lemma.

Lemma 3 *Each coefficient b_ℓ is given by the following formula*

$$b_\ell = \frac{1}{\ell} K^\ell \bar{c}_1^\ell (2n+1)(2n)^{\ell-1} , \qquad \ell \in \{1,2,\ldots,m\} . \tag{2.48}$$

Proof. The proof is by induction. The case $\ell = 1$ is immediate since the first equation of system (2.47) is of the form claimed. For the induction step, we assume that eqn (2.48) is correct for $\ell = k$, which implies

$$b_k = \frac{1}{k} K^k \bar{c}_1^k (2n+1)(2n)^{k-1} . \tag{2.49}$$

It follows from eqn (2.46) that

$$k b_k = -\widetilde{s}_k - \widetilde{s}_{k-1} b_1 - 2\widetilde{s}_{k-2} b_2 - \ldots - (k-1)\widetilde{s}_1 b_{k-1} ,$$

which means that

$$-\widetilde{s}_k - \widetilde{s}_{k-1} b_1 - 2\widetilde{s}_{k-2} b_2 - \ldots - (k-1)\widetilde{s}_1 b_{k-1} = K^k \bar{c}_1^k (2n+1)(2n)^{k-1} \tag{2.50}$$

by hypothesis, eqn (2.49). Multiplying both sides of eqn (2.50) by $(-1)^{k+1} K\bar{c}_1$, we have, with eqn (2.45):

$$(-1)^{k+1}\left(\widetilde{s}_{k+1} + \widetilde{s}_k b_1 + 2\widetilde{s}_{k-1} b_2 + \ldots + (k-1)\widetilde{s}_2 b_{k-1}\right) = (-1)^{k+1} K^{k+1} \bar{c}_1^{k+1} (2n+1)(2n)^{k-1} ,$$

whose left-hand side can be rewritten as $(-1)^{k+1}\left(-(k+1)b_{k+1} - k\widetilde{s}_1 b_k\right)$ by system (2.46), giving

$$-(k+1)b_{k+1} - k\widetilde{s}_1 b_k = K^{k+1} \bar{c}_1^{k+1} (2n+1)(2n)^{k-1} ,$$

which yields

$$-(k+1)b_{k+1} = k\widetilde{s_1}b_k + K^{k+1}\bar{c}_1^{k+1}(2n+1)(2n)^{k-1} =$$
$$= -kK\bar{c}_1(2n+1)b_k + K^{k+1}\bar{c}_1^{k+1}(2n+1)(2n)^{k-1} ,$$

whence

$$(k+1)b_{k+1} = kK\bar{c}_1(2n+1)k^{-1}K^k\bar{c}_1^k(2n+1)(2n)^{k-1} - K^{k+1}\bar{c}_1^{k+1}(2n+1)(2n)^{k-1} =$$
$$= K^{k+1}\bar{c}_1^{k+1}(2n+1)^2(2n)^{k-1} - K^{k+1}\bar{c}_1^{k+1}(2n+1)(2n)^{k-1} =$$
$$= K^{k+1}\bar{c}_1^{k+1}(2n+1)(2n)^{k-1}(2n+1-1) =$$
$$= K^{k+1}\bar{c}_1^{k+1}(2n+1)(2n)^k ,$$

which agrees with eqn (2.48) for $\ell = k+1$, as required. □

Corollary 2 *The coefficients of the sum-of-roots polynomial of the characteristic polynomial, eqn (2.32), are all positive for sufficiently large K.*

Proof. By Lemma 2, the coefficients of the sum-of-roots polynomial of the characteristic polynomial for sufficiently large K are given by

$$b_\ell = \frac{1}{\ell}K^\ell\bar{c}_1^\ell(2n+1)(2n)^{\ell-1} \qquad \ell \in \{1,2,\ldots,m\} ,$$

where $\bar{c}_1 = \widetilde{c}_1/K = \psi_W^2 r_G^2 > 0$ by Lemma (1). Since ℓ, n, and K are all positive, we conclude that $b_\ell > 0$ for $\ell \in \{1,2,\ldots,m\}$. □

The stability of the equilibrium point of system (2.8) has now been established for sufficiently large K, since the characteristic polynomial is stable. This follows from Theorem 1, together with Corollary 1 and Corollary 2, which show that the coefficients are all positive and real.

2.6 Discussion

We have presented and analysed an extension of a VIS-type model for microbial growth and metabolism, explicitly accounting for the dynamic allocation of cellular resources over various types of catalytic machinery. The analysis suggests that dynamic allocation may play a role in adaptive responses to changing environmental conditions. This allocation can be charted in detail as a function of time through experi-

mental approaches such as ribosome profiling and detailed proteomics, recent developments that prompt an extension of the VIS theory to incorporate such data.

The general approach is modular: our categorisation of machinery is comparatively coarse-grained, e.g., collecting all proteins involved in the uptake of glucose into a single component, an assumption bolstered by the 'proportional synthesis' principle [95]. However, the set-up of the model readily lends itself to a more fine-grained treatment.

Whereas the stoichiometric part of the theory relies on basic conservation principles and hence ought to be uncontroversial, the constitutive relations are more speculative. It is therefore important to emphasise that the latter can be reconstructed from observational data.

We closed the dynamics via the r-functions and a normalisation corresponding, broadly speaking, to the relative amount of 'ribosome time' devoted to the manufacture of the various types of machinery. These r-functions express the respective propensities for the various types of machinery to be synthesised, and, in somewhat anthropomorphic terms, indicate how urgently the cell requires the various types. The formalism presented here shares a mechanism of regulation of growth via machinery-making machinery (ribosomes) with the Scott-Hwa-model [134, 135, 136]); another point of agreement is the effective implementation of building block allocation via 'ribosome time.' In both cases, the formalisms are in keeping with well-established knowledge of microbial physiology; in particular, the steady-state relationship between RNA and growth rate [68] is fundamental to the feedback mechanism expressed here by eqn (2.11).

Even if the modelling of allocation variables via r-functions is rejected, there is merit in the general approach of reconstructing a 'regulatory map' from the state $\{m_0, \ldots, m_G, x_1, \ldots, x_n\}$. Provided that the numerical values of the stoichiometric coefficients can be determined, this map can be recovered from data on cell quota combined with bioproduction rates. Moreover, we anticipate that additional information can be gleaned by studying data obtained from step changes in environmental conditions imposed on a continuous-growth culture. Regulatory maps can thus be reconstructed from data obtained under a broad range of environmental conditions.

If these maps agree, this would instil confidence in this simple approach, and if not, more complex models are required, for instance incorporating additional state variables (e.g. signalling machinery, epigenetic status) as well as direct environmental input on gene expression, which in prokaryotes is primarily mediated by two-component systems [164]. It is not *a priori* obvious how a cell might integrate

feedforward (signals emanating from ambient conditions) and feedback (signals from internal status such as reserves) regulation. Ambient stimuli could be the main driver, with a modulatory role for reserve status. Alternatively, reserves transmit a message effectively expressing the urgency of requirements for certain building blocks, whilst the ambient signals are used to decide between alternative sources to replenish these reserves, that is, where the organism is capable switching between, e.g., alternative carbon sources, it would dispose of the genetic material encoding the assimilatory machineries that can handle these respective alternative nutrients, and feedforward-type signals could be key to driving changes in gene expression, corresponding in our formalism by the r-factors.

The shape of the function used to relate a reserve density to an r-factor dictates whether this reserve is subject to stringent homeostasis, or whether it is allowed to wax and wane along with changing nutrient availability, as demonstrated in qualitative terms in Section 2.4.3 (the mid-point slope parameter is particularly important in this respect). If homeostasis is stringent for all reserve densities, a strong version of balanced growth ensues, as the overall biomass composition is also kept constant or at least maintained within narrow margins of variation. It can be shown that this type of regulation maximises the specific growth rate μ [155] but it would be a mistake to equate μ to fitness outright, as has been done in the past [87, 94]; only under certain, quite restrictive, conditions on the manner in which the environment varies and on the types of competitors faced by the organism, does μ agree with the correct general expression for fitness [102, 158]. Thus, under different ecological circumstances, such as, for instance, a regular alteration of the availability of carbon and nitrogen sources, different reserve management strategies will be favoured by natural selection [117].

We have represented nutrient influx through the assimilatory machinery M_i by a term of the form $\widehat{\widehat{\phi}}_i f_i M_i$, where $\widehat{\widehat{\phi}}_i$ represents a maximum possible influx and f_i could be, for instance, the Michaelis-Menten hyperbola, or some other rational function according to the details of the work cycle of the uptake machinery [153]. This implies that a two-fold reduction in f_i can be compensated by a two-fold increase in M_i, which as we have seen is key to the attainability of balanced growth. Light-harvesting in photosynthetic bacteria provides a dramatic demonstration of the ability of increased M_i to compensate for low f_i [8]. However, if there is an unstirred layer around the bacterium, the probability that a nutrient particle that has reached the cell wall will diffuse toward one of the nutrient-uptake pores before returning to the bulk phase must be taken into account. This probability increases asymptotically towards 1 as the pore density (which is $\propto M_i$) increases, which means that a less than proportional increase in the total flux

is accomplished by increasing M_i [7]. Thus f_i is a function of both the bulk phase concentration of the nutrient and of M_i. The 'idle time fraction' $1 - f_i$ could therefore serve as a signal that is carried back to the genome, to modulate the expression of genes encoding the M_i-machinery.

According to the equations of Section 2.2.1, the distribution of building blocks among the machinery relaxes to that imposed by the allocation constants with a time constant of order μ^{-1}. This may be too slow for reserves where the organism cannot tolerate large excursions, as will be the case when the reserve is physically represented by a small metabolite which is chemically reactive, or when the reserve consists of a chemical moiety as part of a regenerative cycle, which limits the capacity of storage [122]. By contrast, reserves that occur as polymers or elemental crystals, often stored as cellular inclusions, tend to be chemically inert and large variations in the fraction of cellular dry weight they represent can be withstood without affecting the function of core metabolism [109]. More rapid-acting pathways act to regulate such critical narrow-range or narrow-capacity reserves; on the top-end, an additional feedback to the influx is needed. The nutrient influx formula $\widehat{\widetilde{\phi}}_i f_i M_i$ is then extended with an additional multiplier, close to 1 when the reserve density remains below the critical maximum or capacity and steeply decreasing to 0 when the reserve approaches the critical value. Such an additional multiplier is a natural way to represent the chemical-kinetic interactions that modulate the efficacy of such systems [30, 64, 122]. As reserves approach critical depletion, the organism may switch to a different metabolic mode, or slow down the overall rate of metabolism to suit the diminished supply [150]. We anticipate that this can be brought into the present theory by introducing 'sliding dynamics' to prevent reserve densities from assuming negative values.

At the microscopic level, biochemical reaction rates are governed by concentrations of both reactants and products, or possibly only by those of the reactants, but not by the products alone—lest reactant concentrations can become negative, which is physically impossible. Yet in the equations of the present theory, which represent the organisation of fluxes at the macro-chemical level, such reactant-control (supply-side or donor-control) is lacking, limiting the validity of the model to those situations where sufficient reserves are left to replenish the pools of core metabolites. Negative reserve densities are tantamount to a breach of the homeostasis of the structural component, as these core metabolites are depleted.

Metabolic slow-down (or even shut-down) is related to the energy charge of the cell [151], which can be conceptualised as a store of 'phosphorylation equivalents' (PEs) which are physically realised as

phosphate moieties on purines [24, 113]. Numerous cellular processes rely on the availability of PEs to proceed [109], and as a consequence the range of tolerable variation is narrow, with end points that are guarded by rapid-acting processes. At the upper end of the range, these processes include the use of ATP to generate polyphosphate reserves [120], as well as a reduction of the efficiency of the processes that generate proton-motive force—these may be driven by light-harvesting, or electron-transfer chains coupled to oxidation and reduction of external substrates; in the latter case the modulation is known as 'uncoupling' [113]. When the energy charge is low, these changes are reversed (redox coupling or light harvesting efficiency is maximised) and if this does not suffice, reserves such as polyphosphate, glucans, lipids, and poly-β-hydroxybutyrate are mobilised [24]. This endogenous reserve mobilisation flux is one for which we should represent the dependence on the donor (the reserve) explicitly. If, despite maximal up-modulation stimulated by the low energy charge, this donor limitation limits the mobilisation flux to below the level required to replenish the PE pool, the latter is gradually depleted, and these critically low levels are coupled to a reduction in all rates [24, 150].

The cellular management of the energy charge has not been represented explicitly in the present paper; such an extension is necessary to accommodate the processes that happen at zero (or very low) specific growth rates and starvation. Virtually all rate terms that figure explicitly in the present paper are dependent on PEs; to the list of energy requirements should be added maintenance requirements [24, 100] which have been ignored here for the sake of simplicity.

Reducing equivalents (REs) mediate coupling between energy and nutrient budgets and serve as a 'co-nutrient' when the external growth substrate must be reduced to form cellular constituents [113]. These REs physically exist as (e^-, H^+) pairs that are carried by specialised co-enzymes which in reduced form carry 1 RE and can transfer it on as they are oxidised [113]. REs can be derived from the oxidation of organic compounds, this being the sole source in organotrophs, or from the oxidation of inorganic substrates (in lithotrophs) [109]. REs are expended in respiration (reducing an inorganic substrate, called the terminal electron acceptor, via a chain of redox transfers of the REs, generating proton-motive force in the process), in fermentation or disproportionation (using organic compounds as electron acceptors), and (in autotrophs) to reduce the carbon in inorganic nutrients to the levels of the organic building blocks required for biosynthesis [109]. Not all of these sources and sinks occur simultaneously in every bacterium, although some organisms are remarkably versatile [127, 159].

The status of the RE pool is primarily governed by its kinetic coupling to physiological fluxes that re-

quire or produce REs, as well as environmental availabilities of light and redox substrates. However, only when a terminal electron acceptor is not available for respiration, are REs expended on the endogenous reduction of organic compounds in fermentation, which is energetically less favourable than respiration; this is the Pasteur effect [109]. Furthermore, the degradation of poly-β-hydroxybutyrate, a source of REs, is inhibited, provided there are exogenous carbon sources [120]. A related conditional redox mode switch ensures the avoidance of dissipative idle cycles; for instance, in photo- and litho-autotrophs formation of energy reserves requires an investment of REs and PEs which is at best recovered without net gain when these reserves are concomitantly used to replenish the energy charge. Thus in the absence of exogenous electron donors and/or light, such assimilatory processes should be halted [151]. This can be modelled by regarding these assimilatory fluxes to have f_i-factors which depend on the availabilities of both the building-block substrate and the energy-yielding substrate.

Chapter 3

Microbial metabolism and growth under conditions of starvation modelled as the sliding mode of a differential inclusion

3.1 Introduction

Systems of ordinary differential equations (ODEs) with discontinuous right-hand sides are called *piecewise smooth (PWS)* systems [32]. The state space of such systems is divided into regions, in each of which the vector field is smooth. The boundaries between these regions are called *switching surfaces* or *surfaces of discontinuity*.

Filippov and Utkin pioneered the mathematical treatment of PWS systems [45, 148], which have subsequently proven to be invaluable in engineering and biological applications. In particular, PWS systems arise in control theory [147, 148] and the study of complementary and hybrid systems [99, 132], as well as in several other applications [19, 76, 77]. In biology, genetic regulatory networks have profitably been treated as PWS systems [17, 25, 52, 119, 145]. In a recent paper on the modelling of such networks, Gouze and Sari [57] applied the Filippov theory [45] to investigate the behaviour of the system on its surfaces of discontinuity. This approach, which is also widely used in control theory, involves an extension of the discontinuous system into a *differential inclusion* [45]. The solutions of this extended system on the surfaces of discontinuity are called *sliding modes* [45].

Here, we analyse a PWS system that describes bacterial growth and growth cessation under conditions of nutrient shortage (starvation). The model we study is a *Variable-Internal-Stores (VIS)* model [35,

61, 165] accounting for changes in cellular composition under varying conditions of nutrient availability [24]. Our *VIS-with-reallocation* model [112], accounts explicitly for the regulation of the allocation of molecular building blocks among various types of catalytic machinery [10, 152]. The changes in the rates at which these building blocks are incorporated into machinery proteins correspond to changes in gene expression and allow the organism to respond to environmental variations [90].

We investigate the behaviour of the VIS-with-reallocation model when at least one of the internal stores in the cell is approaching the point of complete depletion. To this end, we apply the Filippov theory and derive the resulting dynamics in terms of sliding modes. These constitute the mathematical counterpart to the biological phenomenon of metabolic 'shut down,' the organism's response to nutrient shortage whereby the rate of metabolism slows down or even comes to a complete stop [24, 109, 150]. We argue that sliding modes provide a versatile and convenient formalism to represent such transitory behaviours in metabolic systems, where this might otherwise require a more cumbersome dynamical system representation, e.g. of higher dimension.

The paper is organised as follows. In Section 3.2 we discuss the Filippov theory, establish notation, and review the results required for our application to the problem of metabolic 'shut down.' In Section 3.3 we review the VIS-with-reallocation model. In Section 3.4 we formulate the model as a PWS system and apply the Filippov theory [45] to find the solution of the discontinuous system on the surface of discontinuity. Finally, we consider regularisations in Section 3.5.

3.2 Filippov solutions of differential equations with discontinuities

In this section we briefly review Filippov's approach to defining a solution for PWS systems [45]. We restrict ourselves to the simple case where the state space $\mathbb{R}^n$ is divided into two regions, S^+ and S^-, in each of which the vector field is smooth, and which are separated by a boundary Σ, so that $\mathbb{R}^n = S^+ \cup \Sigma \cup S^-$. We consider a point in state space $\mathbf{X} \in \mathbb{R}^n$ with discontinuous dynamics:

$$\dot{\mathbf{X}} = f(\mathbf{X}) = \begin{cases} f^+(\mathbf{X}), & \text{if } \mathbf{X} \in S^+ \\ f^-(\mathbf{X}), & \text{if } \mathbf{X} \in S^- , \end{cases} \qquad \mathbf{X}(0) = \mathbf{X}_0 \in \mathbb{R}^n , \tag{3.1}$$

where the dot indicates differentiation with respect to time and the dynamics $f(\cdot)$ is defined and smooth on each of the subspaces S^+ and S^-, but is not defined on the boundary Σ. In particular, $f^+(\cdot)$ is assumed to be at least once continuously differentiable on $S^+ \cup \Sigma$ but not defined on S^-, whereas $f^-(\cdot)$ is assumed to be at least once continuously differentiable on $S^- \cup \Sigma$ but not defined on S^+.

Since the right-hand side of system (3.1) is not defined on the boundary (surface of discontinuity) Σ, an extension of the vector field is required. To this end, the *Filippov convex method* [45] extends the discontinuous system to a convex *differential inclusion*:

$$\dot{\mathbf{X}} \in F(\mathbf{X}) = \begin{cases} f^+(\mathbf{X}), & \text{if } \mathbf{X} \in S^+ \\ f^F(\mathbf{X}), & \text{if } \mathbf{X} \in \Sigma \\ f^-(\mathbf{X}), & \text{if } \mathbf{X} \in S^- \ , \end{cases} \tag{3.2}$$

where $f^F(\mathbf{X}) \in \mathbb{R}^n$ is a minimal closed convex set containing $f^+(\mathbf{X})$ and $f^-(\mathbf{X})$:

$$f^F(\mathbf{X}) = (1-\lambda) f^-(\mathbf{X}) + \lambda f^+(\mathbf{X}) \ , \tag{3.3}$$

where $\lambda \in [0,1]$ is a convex 'mixing' coefficient.

The differential inclusion can be regarded as a *variable structure system* [147, 148] with *control input* $u(\mathbf{X}) \in [0,1]$ by defining

$$f(\mathbf{X},u) = (1-u) f^-(\mathbf{X}) + u f^+(\mathbf{X}) \ , \tag{3.4}$$

where $u \equiv u^+ = 0$ if $\mathbf{X} \in S^-$, $u \equiv u^- = 1$ if $\mathbf{X} \in S^+$, and $u = \lambda$ if $\mathbf{X} \in \Sigma$. On this approach, f is a regular smooth dynamics that acquires its sliding mode characteristics through the choice of the control u, i.e., for suitable u, we have $f \equiv F$.

3.2.1 Construction and nature of Filippov solutions

Let us formally state what we mean by a solution in the sense of Filippov [45].

Definition 1 (solution in the sense of Filippov) *An absolutely continuous function $\mathbf{X}(t)$ is said to be a solution of (3.1) in the sense of Filippov, or Filippov solution, if for almost all t,*

$$\dot{\mathbf{X}} \in F(\mathbf{X}(t)) \ ,$$

where $F(\mathbf{X}(t))$ is as described by the differential inclusion (3.2).

Such a solution is guaranteed to exist by the following theorem [4].

Theorem 2 (existence of Filippov solution) *Provided that $F(\mathbf{X})$ is upper semi-continuous and has a compact, convex image, the solution of the Filippov differential inclusion (3.2) always exists.*

Remark 1 *By construction, $F(\cdot)$ as stated in (3.2) satisfies the conditions of Theorem 2.*

Specification of the Filippov solution is facilitated by introducing a scalar *switching function* $h : \mathbb{R}^n \to \mathbb{R}$ which is at least twice continuously differentiable, and is such that $h(\mathbf{X})$ has a non-zero gradient on the surface of discontinuity Σ, with

$$S^+ = \{\mathbf{X} \in \mathbb{R}^n : h(\mathbf{X}) > 0\}\,, \qquad \Sigma = \{\mathbf{X} \in \mathbb{R}^n : h(\mathbf{X}) = 0\}\,,$$
$$S^- = \{\mathbf{X} \in \mathbb{R}^n : h(\mathbf{X}) < 0\}\,.$$

Let us consider a solution of eqn (3.1) starting in S^+ and reaching Σ in a finite time. At this point, the trajectory may either immediately exit the boundary and enter one of the subspaces, or stay on the boundary. This depends on the directional derivatives $(\nabla h(\mathbf{X}))^T f^+(\mathbf{X})$ and $(\nabla h(\mathbf{X}))^T f^-(\mathbf{X})$. The trajectory may either cross Σ or enter it in a sliding mode. A *crossing* occurs when

$$(\nabla h(\mathbf{X}))^T f^+(\mathbf{X})(\nabla h(\mathbf{X}))^T f^-(\mathbf{X}) > 0 \tag{3.5}$$

is satisfied for $\mathbf{X} \in \Sigma$. In this case the trajectory leaves the surface of discontinuity and enters S^+ if and only if $(\nabla h(\mathbf{X}))^T f^-(\mathbf{X}) > 0$ (otherwise it enters S^-). The system enters Σ in a *slide* when

$$(\nabla h(\mathbf{X}))^T f^+(\mathbf{X})(\nabla h(\mathbf{X}))^T f^-(\mathbf{X}) < 0$$

for $\mathbf{X} \in \Sigma$. This *sliding mode* can be either *attracting* or *repulsive*. The former requires

$$(\nabla h(\mathbf{X}))^T f^+(\mathbf{X}) < 0 \quad \text{and} \quad (\nabla h(\mathbf{X}))^T f^-(\mathbf{X}) > 0\,. \tag{3.6}$$

In this case the trajectory continues on the boundary with the vector field $f^F(\mathbf{X})$ defined by eqn (3.3) with the following specification for λ:

$$\lambda = \frac{(\nabla h(\mathbf{X}))^T f^-(\mathbf{X})}{(\nabla h(\mathbf{X}))^T f^-(\mathbf{X}) - (\nabla h(\mathbf{X}))^T f^+(\mathbf{X})}\,. \tag{3.7}$$

The attracting sliding mode solution thus defined exists and is unique [45]. On the other hand, when

$$(\nabla h(\mathbf{X}))^T f^+(\mathbf{X}) > 0 \quad \text{and} \quad (\nabla h(\mathbf{X}))^T f^-(\mathbf{X}) < 0\,,$$

the sliding mode is said to be *repulsive* and several further subcases arise which we need not discuss for the purposes of the present paper.

3.2.2 First-order exit conditions

As long as the attracting sliding mode conditions (3.6) are met, the system will remain confined to the switching surface Σ, either stationarily or moving along a trajectory contained in Σ. Either these conditions will remain satisfied as $t \to \infty$, or there is an earliest point in time after entering Σ when the conditions are no longer satisfied. In the latter case, the system may exit Σ, but this is by no means a necessity; the outcome depends on a set of criteria called the *exit conditions*, which have been studied in detail by Dieci and Lopez [32], who provided *first-order exit conditions* and discussed higher-order exit conditions which must be invoked when the first-order conditions are inconclusive. We restrict our discussion to the first-order exit conditions as they suffice for our purposes. Without loss of generality, we write $t = 0$ for the earliest point in time, after entry of Σ, when conditions (3.6) are violated, and $t = 0^-$ for a point in time immediately before $t = 0$. The first-order exit conditions state that the sliding trajectory leaves the surface of discontinuity Σ and enters the subspace S^+ along the vector field $f^+(\mathbf{X})$ if at $t = 0$ the following conditions are satisfied:

$$\begin{cases} (\nabla h(\mathbf{X}))^T f^-(\mathbf{X}) > 0 \\ (\nabla h(\mathbf{X}))^T f^+(\mathbf{X}) = 0 \\ \dfrac{\partial}{\partial \mathbf{X}} g(\mathbf{X}) \dot{\mathbf{X}}|_{t=0^-} > 0\,, \end{cases} \tag{3.8}$$

where $g(\mathbf{X}) = (\nabla h(\mathbf{X}))^T f^+(\mathbf{X})$ and $\mathbf{X} \in \Sigma$. Exit from Σ to S^- is, by symmetry, subject to analogous conditions.

3.3 Variable-Internal-Stores-with-reallocation model

In this section we present the VIS-with-reallocation model, which is a minor generalisation of the version in a companion paper [112]. Figure 3.1 shows a schematic diagram of the model, which is based on the standard principles of chemical conservation, expressed by stoichiometric equations detailed in Section 3.3.1. In addition, the VIS-with-reallocation model comprises so-called *regulatory laws* that govern the allocation of molecular building blocks among various types of catalytic molecular machinery; these are detailed in Section 3.3.2. A novel extension, accounting for nutrient starvation, is presented in Section 3.3.3.

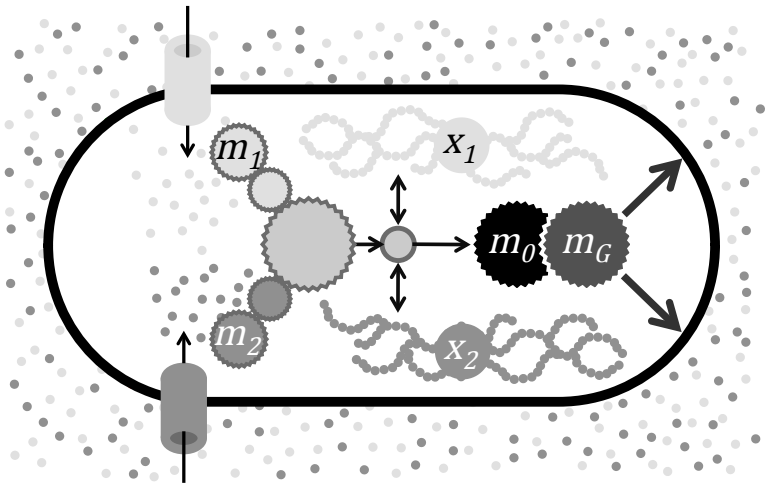

Figure 3.1: Schematic representation of the model described by system (3.14) for the case $n = 2$. Two types of nutrients are assimilated by dedicated pathways (m_1 and m_2) that feed into core metabolism from which building blocks are taken to machinery synthesis (m_0) and growth (m_G). Core metabolism also exchanges molecular building blocks with reserves (x_1 and x_2).

3.3.1 Stoichiometric equations

The model is based on the partitioning of a bacterial cell into three kinds of components: reserve polymers, machinery, and a structural component. The components each satisfy elemental homeostasis and thus have a fixed empirical formula which in most cases is normalised relative to carbon (C), giving C-molar quantities for each.

The reserve components serve as nutrient repositories and are mobilised by the cell to replenish the central pools of core metabolites. Many reserves (e.g. lipids, poly-β-hydroxybutyrate, polysaccharides, storage proteins) are expressible in terms of C-moles, whereas others (e.g. sulphur globules and polyphosphate inclusions) contain no carbon and have to be expressed in terms of their dominant element: if the primary element of the reserve of type j is X_j, the X_j-molar amount is used to quantify reserve j and this amount is denoted as X_j for $j \in \{1,\ldots,n\}$.

Molecular machinery is divided into $n+2$ components, where n is the number of different chemical species of essential nutrients that are accounted for in the model. Component 0 is the molecular machinery required to synthesise *de novo* machinery. Components 1 through n are machinery dedicated to the assimilation of the corresponding nutrients from the environment, and to the conversion of these nutrients into core metabolites. The last component $n+1$, given the special subscript G, is the machinery devoted to growth, which includes the synthesis of the cell envelope and the duplication of the genome. The C-molar amount of the molecular machinery of type i is denoted by M_i for $i \in \{0,1,\ldots,n,G\}$.

The structural component, whose C-molar amount will be denoted as W, comprises everything not covered by the first two categories. It includes the cell envelope, genetic material, and the small molecules of metabolism, which are maintained at nominal cellular concentrations via mechanisms that are not explicitly represented in this model.

Since all types of molecular machinery are synthesised by the machinery of type 0, we have:

$$\dot{M}_i = \alpha_i M_0 \widetilde{\phi}_i \,, \quad i \in \{0, 1, \ldots, n, G\} \,. \tag{3.9}$$

The stoichiometric coefficient $\widetilde{\phi}_i$ in eqn (3.9) shows the rate of production of the machinery of type i; the allocation coefficient α_i, discussed further in Section 3.3.2, defines the portion of zero-machinery that is dedicated for synthesis of the corresponding type i of machinery. The parameters α_i satisfy $\sum_{i\in\{0,1,\ldots,n,G\}} \alpha_i = 1$. Each reserve component is subject to uptake and expenditure fluxes:

$$\dot{X}_j = \sum_{i=1}^{n} \widetilde{\psi}_{ji} M_i - \widetilde{\sigma}_{jW} \dot{W} - M_0 \sum_{i\in\{0,1,\ldots,n,G\}} \widetilde{\sigma}_{ji} \alpha_i \widetilde{\phi}_i - \widetilde{c}_j W \,, i \in \{0, 1, \ldots, n, G\} \,, j \in \{1, \ldots, n\} \,, \tag{3.10}$$

where the first term represents an aggregated gain of reserve j from the influx through 1 to n types of assimilatory machinery, and the three remaining terms represent expenditures on, respectively, structural component growth, machinery production, and maintenance (which has not been included in the model in Chapter 2 for the sake of simplicity) [100, 118]. Accordingly, the stoichiometric parameters have the following biological interpretation: $\widetilde{\psi}_{ji}$ is the gain of reserve j per unit machinery of type i; $\widetilde{\sigma}_{jW}$ is the loss of reserve j per unit increase of W; $\widetilde{\sigma}_{ji}$ is the loss of reserve j per unit synthesis of machinery of type i; $\widetilde{c}_j$ is the loss of reserve j that is being catabolised per unit of structural biomass to maintain cellular integrity (even in the absence of growth and synthesis of machinery). The growth machinery is dedicated to the construction of the structural component:

$$\dot{W} = \widetilde{\psi}_W M_G \,, \tag{3.11}$$

where $\widetilde{\psi}_W$ is the rate of production of the structural component. The tilde over the stoichiometric parameters signifies that they are dimensional. Choosing suitable parameters as natural units, we can render the equations non-dimensional and we will let the corresponding symbols without tilde denote dimensionless (scaled) quantities. In particular, adopting $\widetilde{\phi}_0^{-1}$ as a unit of time, we define scaled state variables as

follows:

$$m_i = \frac{M_i \widetilde{\phi}_0}{W \widehat{m} \widetilde{\phi}_i} \; ; \qquad x_j = \frac{X_j}{W \widetilde{\sigma}_{jW}} \; , \tag{3.12}$$

where $\widehat{m}$ is a scaling parameter for M_0/W. Scaled stoichiometric parameters are defined as follows:

$$\psi_{ji} = \frac{\widetilde{\psi}_{ji} \widetilde{\phi}_i \widehat{m}}{\widetilde{\sigma}_{jW} \widetilde{\phi}_0^2} \; ; \qquad \psi_W = \frac{\widetilde{\psi}_W \widetilde{\phi}_G \widehat{m}}{\widetilde{\phi}_0^2} \; ; \qquad \sigma_{ji} = \frac{\widetilde{\sigma}_{ji} \widetilde{\phi}_i \widehat{m}}{\widetilde{\sigma}_{jW} \widetilde{\phi}_0} \; ; \qquad c_j = \frac{\widetilde{c}_j}{\widetilde{\sigma}_{jW} \widetilde{\phi}_0} \; . \tag{3.13}$$

This scaling gives $(W\widetilde{\phi}_0)^{-1}\dot{W} = \psi_W m_G$ for the specific growth rate which microbial physiologists usually denoted by μ [68, 109]. For the sake of simplicity, we assume that for every reserve j we have the same expenditure coefficient for each type of molecular machinery i: $\sigma_{ji} = \sigma_j$, which is reasonable when different types of machinery are biochemically similar, i.e. they require similar relative amounts of reserves for synthesis.

The final scaled system of differential equations takes on the following form:

$$\begin{cases} \dot{x}_j = \psi_j m_j - \mu\,(1 + x_j) - m_0 \sigma_j - c_j & \text{for } j \in \{1, \ldots, n\} \\ \dot{m}_i = \alpha_i m_0 - \mu m_i & \text{for } i \in \{0, 1, \ldots, n, G\} \; , \end{cases} \tag{3.14}$$

where the ψ_j denote stoichiometric coefficients whose derivation is detailed in a companion paper [112].

3.3.2 Constitutive relationships: regulatory laws

The allocation of molecular building blocks to the various types of catalytic machinery is expressed by the coefficients $\alpha_0, \alpha_1, \ldots, \alpha_n, \alpha_G$ which can be interpreted, in somewhat loose terms, as the fraction of time a ribosome will typically spend on each of these destinations. To close the equations, we require expressions for these coefficients in terms of the other model variables. Accordingly, we treat the allocation coefficients as functions of the internal state variables and/or environmental parameters. In keeping with the idea of 'ribosome time' we use the following expression:

$$\alpha_i = \widetilde{r}_i / \left(\widetilde{r}_0 + \widetilde{r}_1 + \cdots + \widetilde{r}_n + \widetilde{r}_G\right) \; , \tag{3.15}$$

where $\widetilde{r}_i$ is proportional to the concentration of translationally active mRNA for machinery of type i. For the sake of simplicity, we assume that $\widetilde{r}_0$ is a constant and use the scaling $r_i = \widetilde{r}_i / \widetilde{r}_0$ giving

$$\alpha_i = r_i \left(1 + r_1 + \cdots + r_n + r_G\right)^{-1} \; . \tag{3.16}$$

We assume that the r_j are decreasing sigmoid functions of corresponding reserve densities x_j, as follows:

$$r_j = \widehat{r}_j \left(1 + \exp\left\{\vartheta_j (x_j - \xi_j)\right\}\right)^{-1} , \tag{3.17}$$

where $\widehat{r}_j$, ϑ_j, and ξ_j are positive shape parameters. This arrangement creates a negative feedback loop in which the amount of machinery synthesised is 'counterskewed' to ambient nutrient availabilities and thus the reserve densities are regulated toward the mid-point ξ_j of the sigmoid curve.

Finally, r_G is an increasing function of m_0, which creates another feedback loop that adjusts the growth rate to overall resource availability:

$$r_G[m_0] = \begin{cases} 0 , & \text{if } m_0 \leq 1 - \delta \\ r_{G,\max}/2 + K(m_0 - 1) , & \text{if } 1 - \delta < m_0 \leq 1 + \delta \\ r_{G,\max} , & \text{if } m_0 > 1 + \delta , \end{cases} \tag{3.18}$$

where K is a positive parameter which can be estimated from the observed relationship between the cell's RNA content and relative growth rate [68] and $\delta = r_{G,\max}/(2K)$.

The coefficients ψ_j are dependent on environmental conditions and should generally be regarded as time-varying. Specifically, ψ_j is assumed to be a monotone increasing function of the ambient concentration of the jth essential nutrient. Under constant environmental conditions, we have $\dot{\psi}_j = 0$ for all j and the system has an equilibrium point which is unique and stable (the proof provided earlier assumed $c_j \equiv 0 \ \forall j$, but all its steps go through substantially unaltered under the notational change $\sigma_j \to \sigma_j + c_j/m_0$).

3.3.3 Starvation and metabolic 'shut down'

Starvation refers in general to a restricted environmental availability of one or more essential nutrients, or even the complete absence of one or several of them. However, in those cases where the cell has accumulated a substantial amount of reserves, it may be able to bridge periods of low or zero ambient nutrient concentration by mobilising these results. How long the cell is able to do this depends on the duration of the 'famine' and also on the levels of reserves it has built up; the latter depends in turn on the regulatory laws.

If the 'famine' endures for a sufficiently long period of time, one or more reserves will be depleted (i.e. one or more x_j will approach the value 0) and the cell will have to respond in some manner. Here we will use the general term 'shut down' to indicate a slowing down or even complete cessation of

metabolic rates; in reality microbial responses to nutrient stress are extraordinarily diverse as well as species-dependent [24] and we proffer the present treatment as a minimal general model of such responses.

The model as stated is not applicable to the shut-down situation, inasmuch as the expenditure fluxes are not donor-controlled. At a microscopic level, the rate of a biochemical reaction depends on the chemical activities of the reactants and the products and thus it may appear that the model as stated in Section 3.3.1 is fundamentally flawed. However, at the macro-chemical level, this model structure can be justified by appealing to the homeostasis of the structural component. In particular, this homeostasis includes a pool of small core metabolites which are the point of departure for all anabolic pathways [109]. As long as these metabolites are maintained at nominal levels, the expenditures behave as if demand-driven. It is precisely this assumption that breaks down when $x_j \downarrow 0$ for one or more reserve j.

Accordingly, we specify that the dynamics as stated in Section 3.3.1 is restricted to the case where all reserve densities are non-negative, and we require an additional set of equations to describe the dynamics when $x_j < 0$ for one or more j. From a biological perspective, negative reserve densities cannot exist, and they are to be interpreted as violations of the compositional homeostasis of the structural component. More specifically, negative reserve densities express excursions of one or more core metabolites below their nominal concentrations. We shall assume that the cell responds to this situation by shrinking at a relative rate $-\nu$ (where ν is a positive constant) to provide the materials to restore structural homeostasis. At the same time, we assume that anabolic and maintenance expenditures are stopped. These assumptions lead to the following ODEs (in scaled form):

$$\begin{cases} \dot{x}_j = \psi_j m_j + \nu(1 + x_j) & \text{for } j \in \{1, \ldots, n\} \\ \dot{m}_i = \nu m_i & \text{for } i \in \{0, 1, \ldots, n, G\} \end{cases} . \tag{3.19}$$

This extension is valid only in the near vicinity of the boundary of the region where the original model is valid. The pools of core metabolites, while crucial to the cell's physiology, are quantitatively minor. Therefore, only minute negative excursions of x_j can plausibly be interpreted as depletions of these pools. Moreover, the cell's physical scope for de-growth (structural shrinkage) is likely to be severely limited, given the chemical structure of the outer envelope [13, 109]. However, in anticipation of the Filippov solutions, we only require valid dynamics in close vicinity to the boundary which is the locus of $\prod_{j=1}^{n} x_j = 0$.

3.4 Sliding modes of the extended VIS-with-reallocation model

The previous section presented a PWS system of the following general form

$$\dot{\mathbf{X}} = f(\mathbf{X}) \,, \quad \mathbf{X} = (x_j \,;\, m_i)^T \qquad \text{for } i \in \{0,1,\ldots,n,G\} \,, j \in \{1,\ldots,n\} \,, \tag{3.20}$$

where superscript T denotes transposition, the dynamics $f(\cdot)$ is specified by two sets of ODEs, eqns (3.14) and (3.19), each with its own domain of validity. In this section we investigate the behaviour of this system under conditions of starvation that are sufficiently severe to drive one or more reserve densities down to zero, and show that metabolic 'shut down' corresponds to a sliding mode of the PWS system on the boundary defined by

$$\Sigma = \left\{ \mathbf{X} : \textstyle\prod_{j=1}^{n} x_j = 0 \right\} \,. \tag{3.21}$$

3.4.1 Filippov solution for single reserve

The state space $\mathbb{R}^4$ is divided into two regions, S^+ and S^-, according to the sign of x_1, which are separated by Σ, the locus of $x_1 = 0$. For $\mathbf{X} \in S^+$ we have $f(\mathbf{X}) = f^+(\mathbf{X})$ where f^+ is defined on S^+. Letting ξ_1^+ denote the dynamics of the reserve density x_1 and let η_i^+ denote the dynamics of the molecular machineries m_i for $i \in \{0,1,G\}$, we have the following dynamics for $\mathbf{X} \in S^+$:

$$\dot{\mathbf{X}} = f^+(\mathbf{X}) = (\xi_1^+ \,;\, \eta_i^+)^T \,, \quad \mathbf{X} = (x_1 \,;\, m_i)^T \quad \text{for } i \in \{0,1,G\} \,,$$

where ξ_1^+ and η_i^+ are defined in accordance with system (3.14), as follows:

$$\xi_1^+ = \psi_1 m_1 - \psi_W m_G (1+x_1) - \sigma_1 m_0 - c_1 \,, \quad \eta_i^+ = \alpha_i m_0 - \psi_W m_G m_i \tag{3.22}$$

for $i \in \{0,1,G\}$. Similarly, the dynamics for $\mathbf{X} \in S^-$ is as follows:

$$\dot{\mathbf{X}} = f^-(\mathbf{X}) = (\xi_1^- \,;\, \eta_i^-)^T \,, \quad \mathbf{X} = (x_1 \,;\, m_i)^T \quad \text{for } i \in \{0,1,G\} \,,$$

where f^- is defined on S^-, with the following definitions for ξ_1^- and η_i^-:

$$\xi_1^- = \psi_1 m_1 + \nu(1+x_1) \,, \quad \eta_i^- = \nu m_i \quad \text{for } i \in \{0,1,G\} \,, \tag{3.23}$$

in accordance with system (3.19). Combining the vector fields $f^+(\mathbf{X})$ and $f^-(\mathbf{X})$, we arrive at the following PWS system:

$$\dot{\mathbf{X}} = \begin{cases} f^+(\mathbf{X}) = (\xi_1^+ \; ; \; \eta_i^+)^T, & \text{if } \mathbf{X} \in S^+ \\ f^-(\mathbf{X}) = (\xi_1^- \; ; \; \eta_i^-)^T, & \text{if } \mathbf{X} \in S^- \; . \end{cases} \tag{3.24}$$

Filippov's approach requires that we characterise the surface of discontinuity Σ together with the subspaces S^+ and S^- by means of a suitably chosen scalar smooth function $h(\mathbf{X})$, $\mathbf{X} \in \mathbb{R}^4$, such that

$$S^+ = \{\mathbf{X} : h(\mathbf{X}) > 0\} \; , \qquad S^- = \{\mathbf{X} : h(\mathbf{X}) < 0\} \; , \qquad \Sigma = \{\mathbf{X} : h(\mathbf{X}) = 0\} \; .$$

These conditions are satisfied if we set $h(\mathbf{X}) = x_1$. The Filippov convex method leads us to consider a differential inclusion as stated in eqn (3.2) with the vector field $f^F(\mathbf{X})$ on the boundary Σ defined by eqn (3.3) with convex 'mixing' coefficient λ as given by eqn (3.7). In the case of system (3.24) we find

$$(\nabla h(\mathbf{X}))^T f^-(\mathbf{X}) = \xi_1^- \; ; \quad (\nabla h(\mathbf{X}))^T f^+(\mathbf{X}) = \xi_1^+ \; ,$$

and thus, by eqn (3.7),

$$\lambda = \xi_1^- / \left(\xi_1^- - \xi_1^+\right) \; ,$$

which allows us to calculate the boundary dynamics $f^F(\cdot)$. In particular, we have

$$f^F(x_1) = (1-\lambda)\xi_1^- + \lambda \xi_1^+ = \frac{-\xi_1^+}{\xi_1^- - \xi_1^+}\xi_1^- + \frac{\xi_1^-}{\xi_1^- - \xi_1^+}\xi_1^+ = 0 \, ,$$

which shows that a sliding mode with $x_1(t) \equiv 0$ is feasible. We recall from Section 3.2 that there are two principal ways for the trajectory to continue. The first is a crossing, subject to condition (3.5) which here takes on the form

$$(\psi_1 m_1 - \psi_W m_G(1+x_1) - \sigma_1 m_0 - c_1)(\psi_1 m_1 + \nu(1+x_1)) > 0 \, .$$

Since $\mathbf{X} \in \Sigma$ we have $x_1 = 0$, and thus this crossing condition becomes:

$$(\psi_1 m_1 - \psi_W m_G - \sigma_1 m_0 - c_1)(\psi_1 m_1 + \nu) > 0 \, .$$

Since ν is a positive constant and ψ_1 and m_1 are non-negative, the expression in the second pair of brackets is always positive, and the crossing condition can be further simplified to

$$\psi_1 m_1 > \psi_W m_G + \sigma_1 m_0 + c_1 \; . \tag{3.25}$$

Since ψ_1 is a monotone increasing function of the ambient concentration of the essential nutrient, this condition will be satisfied when the environmental level of this nutrient is sufficiently high. By contrast, if the nutrient concentration lies below a critical threshold, the crossing condition (3.25) is not met and the system is prevented from re-entering S^+. To establish that a sliding mode ensues, we turn to the attracting sliding mode conditions (3.6). These take on the following form for $\mathbf{X} \in \Sigma$:

$$\begin{cases} \psi_1 m_1 + \nu > 0 \\ \\ \psi_1 m_1 < \psi_W m_G + \sigma_1 m_0 + c_1 \ . \end{cases} \tag{3.26}$$

The first inequality is satisfied as ψ_1 and m_1 are non-negative and ν is a positive constant. The second inequality is just the opposite of the crossing condition. We may thus conclude that there is a critical value of the nutrient concentration, above which the crossing condition is met, and below which the attracting sliding condition is met. To this critical value of the nutrient concentration there corresponds a critical value of ψ_1 since ψ_1 is a monotone increasing function of the nutrient concentration. We shall write this critical value as $\psi_1^\star = (\psi_W m_G + \sigma_1 m_0 + c_1)/m_1$.

We anticipate that the system will exit the sliding mode when the ambient conditions improve and ψ_1 becomes equal to, or exceeds, the critical value $\psi_1^\star$. To verify this, we employ the first-order exit conditions (Section 3.2.2). The first condition from system (3.8) becomes

$$(\nabla h(\mathbf{X}))^T f^-(\mathbf{X}) = \psi_1 m_1 + \nu > 0 \, ,$$

which is satisfied, and the second condition from (3.8) takes on the form

$$(\nabla h(\mathbf{X}))^T f^+(\mathbf{X}) = \psi_1 m_1 - \psi_W m_G - \sigma_1 m_0 - c_1 = 0$$

which is satisfied when $\psi_1 = \psi_1^\star$. The third condition requires a bit more care. According to Dieci and Lopez [32], if the first two conditions from (3.8) are satisfied, we know that

$$\frac{\partial}{\partial \mathbf{X}} g(\mathbf{X}) \dot{\mathbf{X}}|_{t=0^-} \geq 0$$

(where $t = 0^-$ is the last point in time where attracting sliding mode conditions are satisfied) and if equality can be ruled out, the third exit condition in (3.8) will be satisfied. For this purpose, it suffices to establish strict inequality for at least one component which we choose to be x_1. We have

$$\frac{\partial}{\partial x_1} g(\mathbf{X}) \dot{x_1}|_{t=0^-} = -\psi_W m_G (\psi_1 m_1 - \psi_W m_G (1 + x_1) - \sigma_1 m_0 - c_1)|_{t=0^-} \ .$$

At $t = 0^-$ the trajectory is still on the surface of discontinuity and $x_1(0^-) = 0$. Hence

$$\frac{\partial}{\partial x_1} g(\mathbf{X}) \dot{x_1}|_{t=0^-} = \psi_W m_G(-\psi_1 m_1 + \psi_W m_G + \sigma_1 m_0 + c_1) .$$

The factor $\psi_W m_G$ is positive because both ψ_W and m_G are positive, as is the expression in brackets since $\psi_1 < \psi_1^\star$ at $t = 0^-$, which follows as $t = 0$ is by definition the first instant in time when $\psi_1 \geq \psi_1^\star$ becomes true. We conclude that

$$\frac{\partial}{\partial x_1} g(\mathbf{X}) \dot{x_1}|_{t=0^-} > 0$$

and thereby all first-order exit conditions are satisfied. We conclude that the dynamics 'unfreezes' as soon as ambient conditions become sufficiently favourable and the system will re-enter S^+. Whenever $\mathbf{X}$ attains the boundary Σ coming from S^+, it will follow sliding mode dynamics as long as $\psi_1 < \psi_1^\star$ and exit Σ to S^+ as soon as $\psi_1 \geq \psi_1^\star$. If ψ_1 is admitted as a state variable, this scenario can be classified as a *grazing-sliding* bifurcation of codimension 1 [75, 89].

The behaviour of the PWS system to a piecewise constant forcing function $\psi_1(t)$, representing an alternation of 'feast' and 'famine' conditions, is shown in Fig. 3.2. During the 'famines' the reserve runs down and the system enters a sliding mode with $x_1 \equiv 0$ from which it exits as soon as conditions improve.

The numerical solutions presented in Fig. 3.2 were obtained using *Mathematica*'s built-in tools to detect points in time at which discontinuity occurs, verify that the numerical value of the state at this time point lies within a pre-defined tolerance threshold, and perform either the switch to the adjacent vector field or enter a sliding manifold. This gives a reasonably accurate approximation to the system's trajectory right up to this point and employs these values as initial data for the next time segment. This is known as an *event-driven method* in which the discontinuous system is solved by treating it as a sequence of continuous systems [2].

3.4.2 Filippov solution for multiple reserves

Generalisation to systems with an arbitrary number of essential nutrients and corresponding reserves is straightfoward. The PWS system has the same form as (3.24), but the state variable $\mathbf{X}$ is extended to accommodate n reserves rather than just the one. This means that the regions S^+ and S^- are part of a space of higher dimension and we have to redefine the function $h(\mathbf{X})$ accordingly. Recall that h equals

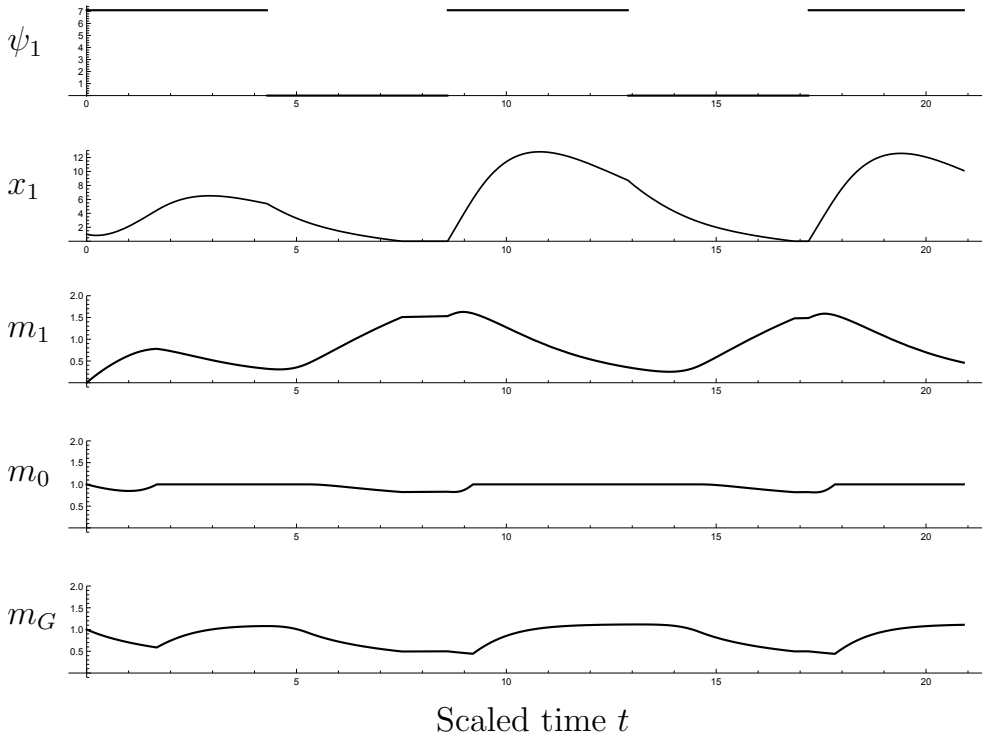

Figure 3.2: Numerical solutions of the PWS system (3.24) for $n = 1$. The imposed environmental conditions $\psi_1(t)$ are shown in the top panel and the remaining panels show the resulting solutions of the PWS system, as indicated by the labels. The function r_G is as in eqn (3.18) with $K = 10^4$ and $r_{G,\max} = 100$; $r_1 = 10/(1+\exp(x_1 - 1))$; $\psi_W = 0.42$; $\sigma_1 = 0.61$; $c_1 = 0.01$; and $\nu = 0.01$.

zero if and only if $\mathbf{X} \in \Sigma$ (eqn (3.21)). Let $s(\cdot)$ be defined as follows:

$$s(\mathbf{X}) = \begin{cases} +1, & \text{if } x_j > 0 \text{ for all } j \\ -1, & \text{otherwise .} \end{cases}$$

Then

$$\Sigma = \{\mathbf{X} \in \mathbb{R}^{2n+2} : h(\mathbf{X}) = 0\}$$

with

$$h(\mathbf{X}) = s(\mathbf{X}) \min(|x_1|, \ldots, |x_n|) \ .$$

Without serious loss of generality, we may consider only the case where the trajectory attains the boundary at a point where $x_j = 0$ for *exactly* one value of j, all other cases being non-generic (i.e. corresponding to a subset of initial conditions of measure zero). In the vicinity of such a generic crossing, all x_j but one (x_k, say) remain positive and x_k attains the value zero. Thus, in the neighbourhood of a generic crossing, we have

$$h(\mathbf{X}) = s(\mathbf{X}) \min(|x_1|, \ldots, |x_n|) \equiv \min(x_1, \ldots, x_n) \equiv x_k \ .$$

The regions S^+ and S^- correspond to the sign of the function $h(\mathbf{X})$, as in Section 3.4.1:

$$S^+ = \{\mathbf{X} \in \mathbb{R}^{2n+2} : h(\mathbf{X}) > 0\} , \qquad S^- = \{\mathbf{X} \in \mathbb{R}^{2n+2} : h(\mathbf{X}) < 0\} .$$

The dynamic flows in the two domains are

$$f^+(\mathbf{X}) = (\xi_j^+ \; ; \; \eta_i^+)^T , \qquad f^-(\mathbf{X}) = (\xi_j^- \; ; \; \eta_i^-)^T$$

for $j \in \{1,\ldots,n\}$, $i \in \{0,1,\ldots,n,G\}$, where

$$\xi_j^+ = \psi_j m_j - \psi_W m_G (1+x_j) - \sigma_j m_0 - c_j , \quad \eta_i^+ = \alpha_i m_0 - \psi_W m_G m_i$$

for $j \in \{1,\ldots,n\}$ and $i \in \{0,1,\ldots,n,G\}$. The vector field in the region S^- is defined in analogy to eqn (3.23):

$$\xi_j^- = \psi_j m_j + \nu(1+x_j) , \quad \eta_i^- = \nu m_i ,$$

where $j \in \{1,\ldots,n\}$, $i \in \{0,1,\ldots,n,G\}$ and ν is a positive constant. Calculations entirely analogous to those in Section 3.4.1 now yield $\lambda = \xi_k^- / (\xi_k^- - \xi_k^+)$. As before we find that the sliding mode is feasible, by virtue of stationarity on Σ:

$$f^F(x_k) = (1-\lambda)\xi_k^- + \lambda \xi_k^+ = \frac{-\xi_k^+}{\xi_k^- - \xi_k^+}\xi_k^- + \frac{\xi_k^-}{\xi_k^- - \xi_k^+}\xi_k^+ = 0 , \tag{3.27}$$

where k is the index of the 'limiting' reserve (i.e. $x_k = 0$). The arguments presented for $n = 1$ in Section 3.4.1 go through virtually unchanged. The overall behaviour of the solution of system (3.24) can be described as follows: it starts at an initial position $\mathbf{X}_0$ in the subspace S^+ and continues its motion along the vector field $f^+(\mathbf{X})$ until the trajectory reaches the surface of discontinuity Σ at some point in time, when one of the reserves is depleted ($x_k = 0$), whereas the other reserves can still furnish building blocks ($x_\ell > 0$, $\ell \neq k$). If the level of the corresponding nutrient k in the environment at this moment in time is such that the corresponding coefficient ψ_k is greater than its critical value $\psi_k^\star = (\psi_W m_G + \sigma_k m_0 + c_k)/m_k$, the solution will exit the boundary and return to S^+. Otherwise, the trajectory enters the sliding mode on the boundary until the level of the nutrient k increases sufficiently to ensure that the inequality $\psi_k \geq \psi_k^\star$ holds true.

3.5 Regularisation

The event-driven method used earlier to obtain numerical solution can be contrasted to the *regularisation* approach which attempts to approximate the trajectory of the PWS system with that of a system whose vector field is smooth over the entire domain of interest, such that the behaviour of the approximating system can be expected to converge to that of the PWS system as $\varepsilon \to 0^+$ for some suitable parameter $\varepsilon > 0$.

In *dynamic regularisation* [49], an auxiliary state $\mathbf{Z} \in \mathbb{R}^n$ is introduced to approximate solutions to the problem as stated, i.e.

$$\dot{\mathbf{X}} = f(\mathbf{X}) = \begin{cases} f^+(\mathbf{X}), & \text{if } h(\mathbf{X}) > 0 \\ f^-(\mathbf{X}), & \text{if } h(\mathbf{X}) < 0\,, \end{cases} \qquad \mathbf{X}(0) = \mathbf{X}_0 \in \mathbb{R}^n\,, \tag{3.28}$$

by the solutions of the following system of delay-differential equations:

$$\dot{\mathbf{X}}_\varepsilon = \mathbf{Z}\,; \quad \dot{\mathbf{Z}} = \varepsilon^{-1}\nabla_\varepsilon f(\mathbf{X}_\varepsilon)\,; \quad \mathbf{X}_\varepsilon(0) = \mathbf{X}_0\,; \quad \mathbf{Z}(t) = \boldsymbol{\zeta}(t)\,,\ t \in [-\varepsilon, 0]\,, \tag{3.29}$$

where ∇_ε is the backward difference operator with lag ε; provided that the continuous function $\boldsymbol{\zeta}(\cdot)$ satisfying certain regularity properties, the approximation $\mathbf{X}_\varepsilon(t)$ converges to the Filippov solution for $\mathbf{X}(t)$ as $\varepsilon \to 0^+$ [49].

In *flow field regularisation* [128, 138, 139], the discontinuous vector field $f(\cdot)$ is replaced by a smooth approximation which agrees with the original field except within distance $O(\varepsilon)$ of the surface of discontinuity:

$$\dot{\mathbf{X}}_\varepsilon = f_\varepsilon(\mathbf{X}_\varepsilon) = (1 - \theta_\varepsilon(h(\mathbf{X}_\varepsilon)))f^-(\mathbf{X}_\varepsilon) + \theta_\varepsilon(h(\mathbf{X}_\varepsilon))f^+(\mathbf{X}_\varepsilon)\,, \tag{3.30}$$

where $\theta_\varepsilon(\cdot)$ is a *regularisation function*, defined as follows:

$$\theta_\varepsilon(h) = \frac{1}{\varepsilon}\int_{-\infty}^{h} \rho\left(\frac{s}{\varepsilon}\right) ds\,, \tag{3.31}$$

where $\rho(\cdot)$ is a probability distribution function with support $[-1, 1]$. It follows that $\theta_\varepsilon(h)$ is non-decreasing on the interval $(-\varepsilon, \varepsilon)$ and agrees with the Heaviside function when $|h| \geq \varepsilon$:

$$\theta_\varepsilon(h) = 0 \ \text{ if } h \leq -\varepsilon\,; \qquad \theta_\varepsilon(h) = 1 \ \text{ if } h \geq \varepsilon\,. \tag{3.32}$$

The approximation $\mathbf{X}_\varepsilon(t)$ obtained by means of this regularisation converges uniformly to the Filippov solution of system (3.28) for $\varepsilon \to 0^+$ [128]. The concatenation of 'height' function h and regularisation θ_ε

is formally identical to the control input u in eqn (3.4). Thus, the flow field regularisation approach can be viewed as a continuous approximation to continuous control [147, 148].

3.5.1 Biological interpretation of the flow field regularisation

The regularisation, eqn (3.30), permits a natural interpretation in terms of the biological system at hand. In particular, let us consider the approximate dynamics of the reserve densities:

$$\dot{x}_{j,\varepsilon} = \psi_j m_{j,\varepsilon} + (1-\theta_\varepsilon)\nu(1+x_{j,\varepsilon}) - \theta_\varepsilon\left(\psi_W m_{G,\varepsilon}(1+x_{j,\varepsilon}) + \sigma_j m_{0,\varepsilon} + c_j\right) \tag{3.33}$$

and of the machinery densities:

$$\dot{m}_{i,\varepsilon} = (1-\theta_\varepsilon)\nu m_{i,\varepsilon} + \theta_\varepsilon\left(\alpha_i m_{0,\varepsilon} - \psi_W m_{G,\varepsilon} m_{i,\varepsilon}\right) . \tag{3.34}$$

In order to relate these equations to a physiologically plausible interpretation, we recall that the switching function h, the argument of θ_ε, is just the density of the 'limiting' reserve, and we consider these equations assuming that (i) we have $\nu \ll 1$ (in keeping with our earlier discussion); and (ii) almost all of the distribution ρ's probability mass is centered on the interval $[0,1]$. Under these assumptions, we may ignore the terms with $(1-\theta_\varepsilon)\nu$ and think of θ_ε as a dimensionless multiplicatory modification of the rates of metabolic expenditure. That latter is made up of fluxes through the various anabolic pathways, together with the endogeneous metabolism that generates the required Gibbs enthalpic driving force. This 'rate multiplier' θ_ε has a physiologically sensible behaviour: it remains at the value 1 as long as all reserve densities are bounded away from ε and no metabolic 'shut down' is required, and, furthermore, θ_ε traverses the interval $(0,1]$ from above as the limiting reserve density decreases through the value ε and lower. Intuitively, expenditures are 'pinched' as the limiting reserve density approaches complete depletion.

3.5.2 Convergence and robustness of the flow field regularisation

Let us apply the flow field regularisation to system (3.24) for the case $n = 1$. Assuming that

$$\rho(t) = \begin{cases} 1/2, & \text{if } t \in [-1,1] \\ 0, & \text{otherwise} , \end{cases}$$

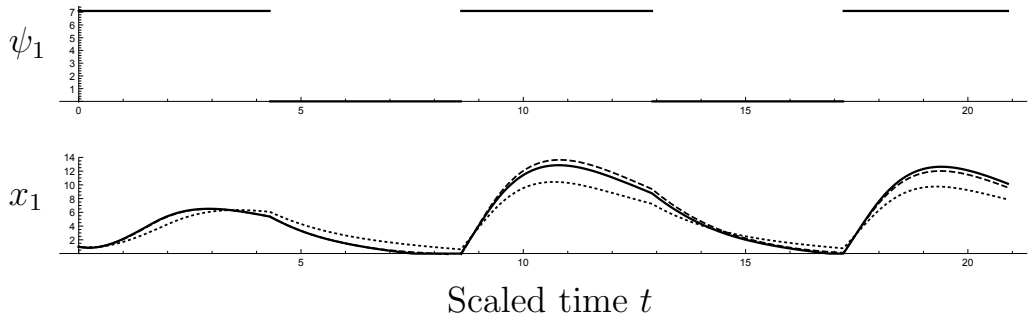

Figure 3.3: Numerical solutions of system (3.24) with its space regularisation with piecewise function θ defined by eqn (3.35) with parameter $\varepsilon = 0.1$ for $n = 1$. The function r_G is as in eqn (3.18) with $K = 10^4$ and $r_{G,\max} = 100$; $r_1 = 10/(1+\exp(x_1 - 1))$; $\psi_W = 0.42$; $\sigma_1 = 0.61$; $c_1 = 0.1$; and $\nu = 1$. The top panel shows the imposed environmental regime, whereas the bottom panel shows the reserve density for $\varepsilon = 10$ (dotted line); $\varepsilon = 1$ (dashed line); and $\varepsilon = 0.01$ (solid line); the latter is indistinguishable from *Mathematica*'s built-in event-driven method.

and recalling that $h(\mathbf{X}) = x_1$, we define the regularisation function θ_ε for system (3.24) as the following piecewise function:

$$\theta(x_1) = \begin{cases} 0, & \text{if } x_1 \leq -\varepsilon \\ (x_1/\varepsilon + 1)/2, & \text{if } x_1 \in (-\varepsilon, \varepsilon) \\ 1, & \text{if } x_1 \geq \varepsilon\,. \end{cases} \tag{3.35}$$

Numerical solutions of the regularised system (3.24) by means of the piecewise regularisation function θ defined by eqn (3.35) are shown in Fig. 3.3. For sufficiently small values of ε, the regularised numerical solution virtually coincides with the event-driven numerical solution, which, in tandem with the convergence result due to Schiller and Arnold [128], supports our confidence in both. Moreover, even if *Mathematica*'s built-in approximation to Filippov sliding mode solutions is admirably sophisticated, failure to exit the sliding mode occurs intermittently when ν is set to moderately small values (the intermittency is unpredictable for all intents and purposes and presumably due to round-off error). The regularisation does not suffer from this problem and thus appears to be a superior numerical method for the system at hand.

3.6 Discussion

We have analysed a Variable-Internal-Stores (VIS) model of microbial metabolism and growth that accounts for changes in cellular composition in response to fluctuations in nutrient availability in the environment. The model comprises stoichiometric balance equations together with constitutive equations that describe the adaptive allocation of molecular building blocks among various types of catalytic machinery; it has a unique, stable equilibrium point. Although the model may appear somewhat more

involved than the classical models [35, 88, 100, 107, 118, 150], it reduces to these models under suitable assumptions [112] and is the simplest mathematical framework in which these classical models can be made consistent with stoichiometric conservation principles and the principles of building block allocation (which in the biological system is effected by the regulatory interactions between transcription and translation); moreover, the formalism presented here is consistent with a mechanism of growth regulation featured in the Scott-Hwa-model [134, 135, 136].

We have considered the PWS system as consisting of the dynamics of the original model that deals with *intensive* variables only, i.e., density variables that do not scale with the overall size of the system (cell size, or, more generally, the size of a colony of cells described by the present model). However, there is one additional *extensive* variable, W. In the region S^+, we have the identities $\mu = (W\widetilde{\phi}_0)^{-1}\dot{W} = \psi_W m_G$, whereas $(W\widetilde{\phi}_0)^{-1}\dot{W} = -\nu$ in S^-. The intensive dynamics allowed us to avoid the question of what happens to the growth rate $\dot{W}$ on Σ, which we may not answer by noting that it is subject to the convex combination prescribed by Filippov:

$$\frac{\dot{W}}{W\widetilde{\phi}_0} = \frac{-\xi_k^+}{\xi_k^- - \xi_k^+}(-\nu) + \frac{\xi_k^-}{\xi_k^- - \xi_k^+}\psi_W m_G \tag{3.36}$$

(cf. eqn (3.27)) which evaluates to a much reduced relative rate of growth, vanishing in the double limit $\nu \to 0^+$, $\psi_k \to 0^+$ (where k is the index of the depleted reserve).

We studied the behaviour of the model under conditions of starvation, and considered, in particular, what happens when at least one of the reserves in the cell approaches a critical level of depletion, which forces the organism to switch to a 'survival' mode in which metabolic requirements are minimised. In the model, all reserve densities have to be bounded away from zero for metabolism and growth to proceed at normal rates. As long as this condition is satisfied, it is legitimate to treat the metabolic fluxes as demand-driven, at least on a macrochemical level. The microchemical justification of this assumption essentially resides in the homeostatic maintenance of an intracellular pool of small core metabolites, which are continually being replenished from the reserves, and which feed the anabolic pathways. It is precisely this assumption that breaks down under starvation conditions. Such conditions arise when there is an insufficient supply from the environment to keep the reserves bounded away from zero while they are being depleted at normal rates. In such cases, a supply-side modulation of the rates must be included explicitly in the equations.

Although we have argued here that sliding modes are the natural expression for such a supply-side

modification of the model, it is instructive to imagine a theoretical biologist who adopts an approach that perhaps comes more naturally to mathematical modellers, which is to modify the original model outright, along the following lines (we take $n = 1$ for the sake of simplicity):

$$\dot{x}_1 = \psi_1 m_1 - g(x_1)\left(\psi_W m_G(1+x_1) + \sigma_1 m_0 + c_1\right)$$

$$\dot{m}_i = g(x_1)\left(\alpha_i m_0 - \psi_W m_G m_i\right) \ ,$$

where $g(\cdot)$ is a function with the properties $g(0) = 0$, $g'(x) \geq 0$, and $g(x) \leq 1 \ \forall x$; for example

$$g(x_1) = x_1 / \left(\varkappa + x_1\right) \tag{3.37}$$

with positive parameter $\varkappa$. The theoretical biologist views $g(\cdot)$ as a 'throttle,' reducing metabolic expenditures when the reserve density runs low (cf. Section 3.5.1). Any such model can be cast as a regularisation by choosing a switching function $h(\cdot)$ and distribution $\rho(\cdot)$ so that the resulting function $\theta_\varepsilon(\cdot)$ provides a mock-up for the modeller's specification of $g(\cdot)$. Schiller and Arnold's theorem [128] guarantees that there is a corresponding Filippov dynamics that arises as a limiting case, (for eqn (3.37) this would be the limit $\varkappa \to 0$). This strongly suggests that sliding mode Filippov solutions are a natural, generic mathematical framework in which to express metabolic 'shut down.'

We suggest that mathematical models of metabolism and biochemical pathways will generically permit such a correspondence between smooth multiplier-type control models and regularisations of PWS systems. This could be exploited to furnish a systematic procedure to derive self-consistent PWS representations of biological processes, which is a non-trivial challenge in general. From the PWS point of view, starting with more complicated smooth dynamics may appear to be an unnecessary detour, but this approach is more intuitive and avoids the pitfalls associated with writing down PWS equations directly.

If the flow field regularisation has a counterpart in smooth models with natural biological interpretations, one may wonder if the same can be said for dynamic regularisation. At first blush this might seem a less promising avenue, not only because the required increase in state space dimension, but also because of the lack of an obvious biological counterpart for the backward difference operator ∇_ε that appears in eqn (3.29). The latter objection is somewhat alleviated by appealing to the 'linear chain trick' which can be regarded as a soft version of the hard non-linear delay, and which can be justified as a model of a multi-component signalling cascade [43].

A hybrid of the field and dynamic regularisations was proposed previously to model metabolic 'shut

down,' involving an auxiliary variable, as in the dynamic regularisation, but letting it act as a modulatory multiplier, as in flow field regularisation [150]. By way of definite example, let us replace θ_ε by a new state variable variable $z(t)$ that obeys the following ODE:

$$\dot{z} = \varsigma z \left((1 + \varepsilon/h)^{-1} - z \right) , \tag{3.38}$$

where $\varsigma > 0$ sets the time scale of z's dynamics and $\varepsilon > 0$ is, as before, a small parameter that governs the width of the transition layer near Σ. This approach can be extended considerably by having a dedicated dynamic modulatory multiplier for every individual metabolic flux or process, rather than a single one that controls the overall rate of metabolic 'shut down.' An extension of this form has been proposed as a generic approach to organismal homeostasis [157].

Chapter 4

Optimal management of nutrient reserves in micro-organisms under time-varying environmental conditions

4.1 Introduction

Many bacteria form intracellular reserves, in particular during so-called 'feast' periods of growth: when nutrients are available from the ambient environment at relatively high levels, bacterial cells accumulate polymers that can be degraded to fuel metabolism during subsequent periods of 'famine' when nutrients are absent from the environment or present at such low levels that they do not suffice to meet the cell's maintenance requirements [120]. In prokaryotes reserves occur as metabolite pools, reserve compounds, granules, and elemental inclusions [8, 109, 120]. Whether the organism can continue to meet the requirements of endogenous metabolism for the entire duration of the 'famine' depends on the amount of accumulated reserves. For instance, in experiments involving *Escherichia coli* growing on carbon as a limiting factor [72], the level of the carbon reserve compound glycogen accumulated by the cell was about 6–7% of the dry weight, which supported a cell during a starvation period of 15 hours. Similar results were obtained with *Rodospirillum ruborem* growing on acetate or butyrate and accumulating poly-β-hydroxybutyrate [34].

The accumulation of reserves can be viewed as an adaptation to fluctuating environmental conditions, which prompts us to ask at what rate the cell should allot core metabolites to the formation of reserves during the 'feast' periods. This question can be framed as an evolutionary one: what kind of reserve management strategy maximises fitness? Any attempt at an answer must presuppose that there is a sensible way to quantify fitness in the context of microbial ecology. The specific growth rate μ, defined as the

rate of change of the natural logarithm of the biomass, has long been viewed as a natural measure of fitness [94]. However, this is not valid in general [154]; in particular, the growth rate is generally a function of time t and it can be shown that the manner in which the function $\mu(t)$ should be 'discounted' over the long-term time integral strongly depends on ecological circumstances; for instance, if we consider an ecotype in which the need to outcompete competitors (in the short term, whenever the latter arrive) is paramount, we find that we should derive a different fitness measure as compared to an ecotype in which competition is not a dominant effect, but in which the cells form spores whenever they enter a spell of nutrient shortage [158]. Here, we consider an ecological setting in which one can assume as valid the definition proposed by Metz and co-workers [101, 102], namely that fitness is the eventual asymptotic growth rate of a colony that remains sufficiently small so as not to affect the state of the environment. To isolate the problem of interest, selective pressure is taken to derive solely from fluctuations in environmental availability of a nutrient; in particular, we assume that there are no competing types and the bacterial cell does not sporulate but has to survive periods of famine as a viable cell that has the ability to reduce endogenous metabolism under conditions of severe starvation.

To address the question of optimal (maximally adaptive) regulation of reserve accumulation and mobilisation we require, in addition to a quantitive measure of fitness, a suitable parametrisation of the regulatory phenotype. The biochemical and genetic particulars are intricate and highly variable between different species [24], suggesting that optimisation would be challenging in view of the high-dimensional parameter spaces of mathematical models at this level of detail. One solution is to tackle the problem at the higher, aggregated level of macro-chemical kinetics models, also known as Variable-Internal-Stores models [35, 61, 165]. We previously proposed that the regulation of internal stores in such models can be represented by so-called 'regulatory' functions that link the physiological state of the cell (in the case at hand: the reserve levels) to the allocation of molecular building blocks to various types of catalytic machinery [112]. At the biochemically detailed level, this allocation is mediated by regulation of transcription [90]: *ceteris paribus*, more of a given enzyme will be synthesised if the level of mRNA encoding that enzyme is increased (although numerous additional factors impinge on this causal connection [109]).

The aims of the present paper are, first, to support the notion of such regulatory functions, which we will call '*r*-functions' in what follows, by demonstrating how they can be explicitly reconstructed from experimental data; and second, to study the simplest example of an *r*-function, specifically a decreasing sigmoid, and determine the optimal-fitness combination of the shape parameters of this function faced

with an environment that switches between 'feast' and 'famine' in a predictable and regular fashion, and to understand the evolutionary optima we obtain in terms of the physiological dynamics of the cell.

The paper is organised as follows. In Section 4.2 we briefly review the theory of macro-chemical kinetics with variable internal stores. In Section 4.3 we describe and demonstrate the reconstruction of regulatory rules, represented as *r*-functions, from observational data. Finally, in Section 4.4, we address the problem of evolutionarily optimal regulation of reserve density.

4.2 Macro-chemical kinetics

Before describing the reconstruction of regulatory rules, implemented here as '*r*-functions,' we briefly review the basic model so as to render the present paper reasonably self-contained.

The model [111, 112] distinguishes $n+2$ types of molecular machinery, where n corresponds to the number of different chemical species of nutrients in the environment. In addition to *synthetic* machinery (RNA transcriptase, ribosomes, and the associated molecular components) and *growth* machinery (DNA replicase and machinery involved in cell envelope synthesis) there is a dedicated type of machinery for the *uptake* of each of the n nutrients. The C-molar amounts of these $n+2$ types of machinery are denoted as M_i for $i \in \{0, 1, \ldots, n, G\}$, where the index 0 stands for synthetic machinery, G for growth machinery, and 1 through n for assimilatory machineries. *Reserve* components are likewise expressed in C-moles, or, if carbon is not part of their chemical composition, in terms of the molar amount of their dominant element X_j. These amounts are denoted as X_j for $j \in \{1, \ldots, n\}$.

The *structural* component, finally, includes the cell envelope, as well as the genetic material and the small molecules of metabolism, the intermediates of catabolic and anabolic pathways which are maintained at appropriate cellular concentrations. The C-molar amount of the structural component is denoted by W. Table 4.1 characterises the components in terms of the major classes of proteins that are assigned to them.

Table 4.1: Assignment of major classes of proteins, grouped according to function, to macro-chemical components in a typical *E. coli* cell

Synthetic M_0	Uptake $M_1, \ldots, M_n$	Growth M_G	Structural W
Ribosome-related	Nutrient uptake	Agmatine synthesis	Catabolism
Ribosomal	Core metabolism	Amino-acid synthesis	Chaperones/folding
RNA-related		Cell division	Chemotaxis
Transcriptional		Cell envelope synthesis	Defense
Translational		Cofactor synthesis	Metabolic intermediates
		DNA replication	Repair

Table 4.1: Assignment of major classes of proteins, grouped according to function, to macro-chemical components in a typical *E. coli* cell

Synthetic M_0	Uptake $M_1,\ldots,M_n$	Growth M_G	Structural W
		Fatty acid synthesis	RNA degradation
		Glutamate synthesis	RNA modification
		Glutamine synthesis	Secretion
		Glutathione synthesis	Storage-related
		Protein synthesis	Transcriptional repressors
		Protoporphyrin synthesis	Cell envelope
		Selenophosphate synthesis	Redox reactions
		Spermidine synthesis	
		Sulfide synthesis	

See Table 4.2 in Section 4.5 for a detailed account assigning all known individual proteins.

The dynamics of each component is given by the following expression:

$$\dot{M}_i = \alpha_i M_0 \widetilde{\phi}_i \,, \quad i \in \{0,1,\ldots,n,G\} \,, \tag{4.1}$$

where α_i is the allocation coefficient describing which portion of (the time of) the basic catalytic machinery M_0 is dedicated to the synthesis of the ith component, and $\widetilde{\phi}_i$ is a stoichiometric coefficient (a tilde is used to mark parameters prior to scaling). The allocation coefficients α_i are all non-negative and satisfy $\sum_{i\in\{0,1,\ldots,n,G\}} \alpha_i = 1$. In principle, these coefficients should be treated as time-varying; they depend on the 'regulatory state' of the organism. A particularly simple feedback model for the α_i is used in the present study, eqn (4.7) below.

Growth (or more precisely, structural growth) is the rate of change of W and is proportional to M_G, as follows:

$$\dot{W} = \widetilde{\psi}_W M_G \,. \tag{4.2}$$

Summing over all gain and loss terms we obtain the dynamics of reserve component j:

$$\dot{X}_j = \sum_{i=1}^{n} \widetilde{\psi}_{ji} M_i - \widetilde{\sigma}_{jW} \dot{W} - M_0 \sum_{i\in\{0,1,\ldots,n,G\}} \widetilde{\sigma}_{ji} \alpha_i \widetilde{\phi}_i - \widetilde{c}_j W \,, \quad i \in \{0,1,\ldots,n,G\} \,, j \in \{1,\ldots,n\} \,. \tag{4.3}$$

Here the first term represents gains due to uptake; the second term represents expenditure on structural growth (increase of W); the third term represents investment in catalytic machinery; and the final term represents 'maintenance,' dissimilatory expenditure on endogenous metabolism [67, 100, 118]. Thus, $\widetilde{\psi}_{ji}$ is the gain of reserve j per unit machinery of type i; $\widetilde{\sigma}_{jW}$ is the loss of reserve j per unit increase of W; $\widetilde{\sigma}_{ji}$ is the loss of reserve j per unit synthesis of machinery of type i; $\widetilde{c}_j$ is the maintenance cost of reserve j that is being catabolised per unit of W. The specific growth rate $\widetilde{\mu}$ equals $\frac{d}{dt}\ln W(t)$ by definition.

Choosing $\widetilde{\phi}_0^{-1}$ as a unit of time, we render the equations dimensionless, by defining the following scaled variables:

$$m_i = \frac{M_i \widetilde{\phi}_0}{W \widehat{m} \widetilde{\phi}_i} \; ; \qquad x_j = \frac{X_j}{W \widetilde{\sigma}_{jW}} \; , \tag{4.4}$$

where $\widehat{m}$ is chosen such that $m_0 \equiv M_0/W$ is maintained at the dimensionless value 1 via the *r*-function for growth [112]. Scaled stoichiometric parameters are defined as follows:

$$\psi_{ji} = \frac{\widetilde{\psi}_{ji} \widetilde{\phi}_i \widehat{m}}{\widetilde{\sigma}_{jW} \widetilde{\phi}_0^2} \; ; \qquad \psi_W = \frac{\widetilde{\psi}_W \widetilde{\phi}_G \widehat{m}}{\widetilde{\phi}_0^2} \; ; \qquad \sigma_{ji} = \frac{\widetilde{\sigma}_{ji} \widetilde{\phi}_i \widehat{m}}{\widetilde{\sigma}_{jW} \widetilde{\phi}_0} \; ; \qquad c_j = \frac{\widetilde{c}_j}{\widetilde{\sigma}_{jW} \widetilde{\phi}_0} \; . \tag{4.5}$$

We assume $\sigma_{ji} = \sigma_j$ for every reserve j, which is reasonable as different types i of machinery can be taken to be biochemically similar. Also, for the sake of simplicity we assume $\psi_{ji} = 0$ whenever $j \neq i$ and write $\psi_{jj} \equiv \psi_j$. The scaled system of differential equations is as follows:

$$\begin{cases} \dot{x}_j = \psi_j m_j - \mu \, (1 + x_j) - m_0 \sigma_j - c_j & \text{for } j \in \{1, \ldots, n\} \\ \dot{m}_i = \alpha_i m_0 - \mu m_i & \text{for } i \in \{0, 1, \ldots, n, G\} \; . \end{cases} \tag{4.6}$$

The link between reserve densities and synthesis of catalytic machinery is encoded by allocation coefficients α_j which are given by the following expressions:

$$\alpha_0 = (1 + r_1 + \cdots + r_n + r_G)^{-1} \; ; \quad \alpha_j = r_j \alpha_0 \quad \text{for } 1 \leq j \leq n \; , \quad j = G \; , \tag{4.7}$$

where $r_1, \ldots, r_n, r_G$ are the *r*-functions. These are functions that are in general assumed to depend on the (intensive) state of the cell (i.e. the variables $\{m_0, m_1, \ldots, m_n, m_G, x_1, \ldots, x_n\}$, perhaps augmented with whatever additional state variables are required to describe the regulatory behaviour of the organism). In the present (simplest) incarnation of the model, r_j is assumed to be a decreasing sigmoid function of the reserve density x_j for $1 \leq j \leq n$ and r_G is assumed to be a steeply increasing sigmoid function of m_0, with a mid-point at $m_0 = 1$. The latter is consistent with observations on the relationship between the cell's RNA content and the specific growth rate [68].

Under constant and growth-sufficient environmental conditions (i.e., the coefficients ψ_j are constant in time and permit growth at a strictly positive rate), the system (4.6) has a unique and stable equilibrium

point [112], characterised by the following equations:

$$\mu = \alpha_0 = \left(1 + \sum_{i \in \{1,\ldots,n,G\}} r_i\right)^{-1} , \tag{4.8}$$

$$m_i = r_i m_0 \quad \text{for } i \in \{1,\ldots,n,G\} , \tag{4.9}$$

$$\psi_j r_j = \psi_W r_G (1 + x_j) + \sigma_j + c_j/m_0 \quad \text{for } j \in \{1,\ldots,n\} , \tag{4.10}$$

where $\mu = (W\widetilde{\phi}_0)^{-1}\dot{W} = \psi_W m_G$ is the specific growth rate expressed in scaled time.

Numerical estimates for the scaled parameters can be obtained by considering the stoichiometry of a typical prokaryotic cell, as described in detail in Section 4.5. We usually focus on *intensive* scaled state variables $\{m_0, m_1, \ldots, m_n, m_G, x_1, \ldots, x_n\}$, which represent densities, rather than the corresponding *extensive* variables $\{M_0, M_1, \ldots, M_n, M_G, X_1, \ldots, X_n\}$, which are proportional to the structural biomass W; it is the intensive variables that can plausibly be assumed to be represented by intracellular signals.

4.3 Data-driven reconstruction of the r-function

In the context of macro-chemical kinetics models such as described in the foregoing section, r-functions serve as linker functions that connect the physiological state of the cell to the relative rates of synthesis of new catalytic machinery [112]. We here focus on what is perhaps the most elementary specification for the r-function, namely one that links reserve density to the allocation of molecular building blocks to the machinery devoted to the uptake of the nutrient that is stored.

The steady-state solution leads to the following pair of equations for $n = 1$:

$$x_1 = \psi_1 \left(\mu^{-2} - \mu^{-1} - {\psi_W}^{-1}\right) - (1 + \sigma_1/\mu + c_1/\mu) \tag{4.11}$$

$$r_1 = \mu^{-1} - 1 - \mu/\psi_W \tag{4.12}$$

[112]. Thus, given a set of observations performed at various values of $\widetilde{\mu}$ under steady-state conditions, we can calculate x_1 and r_1 and plot them as pairs (x_1, r_1), obtaining a scatter plot that gives a graphical representation of the regulatory law $r_1(x_1)$. For the purposes of subsequent analysis, it is usually convenient to fit a suitable empirical function to these data; we shall employ the following sigmoid function:

$$r_1 = \zeta_1 + \widehat{r}_1 \left(1 + \exp\{\vartheta_1 (x_1 - \xi_1)\}\right)^{-1} , \tag{4.13}$$

which has two shape parameters, a mid-point location parameter ξ_1 and a mid-point slope parameter ϑ_1,

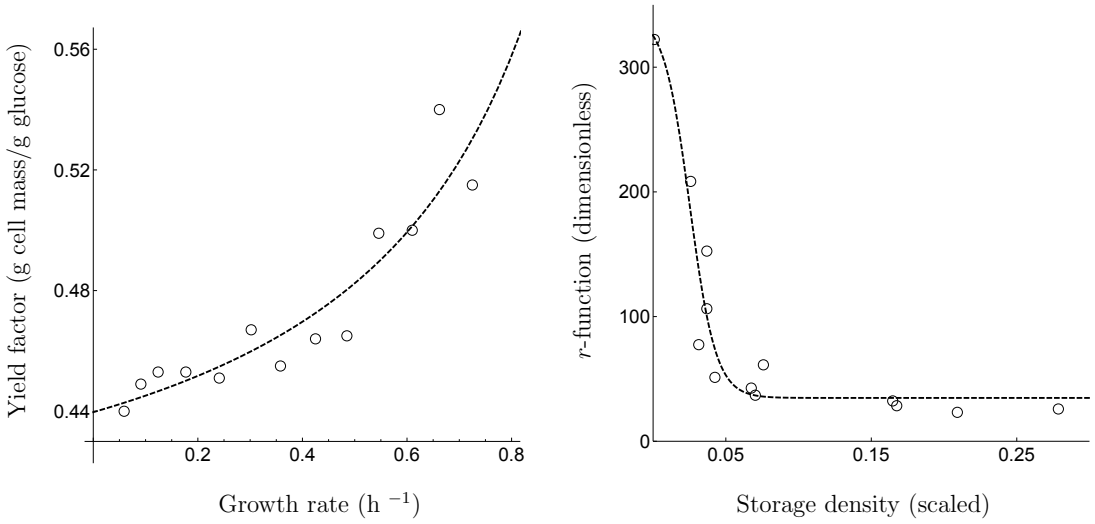

Figure 4.1: Reconstruction of the r-function for *Escherichia coli* grown under carbon-limited conditions (the limiting nutrient is glucose). Left: original data taken from [131], together with the optimal non-linear least-squares fit of eqn $y = c + a/(b-x)$ with parameters $a = 0.074$; $b = 1.2$; $c = 0.38$. Right: transformed data, together with the optimal non-linear least-squares fit of eqn (4.13) with parameters $\widehat{r}_1 = 307.84$; $\vartheta_1 = 111.65$; $\xi_1 = 0.025$; $\zeta_1 = 34.76$.

as well as a scaling parameter $\widehat{r}_1$ and an offset parameter ζ_1.

As eqns (4.11) and (4.12) make clear, the essential challenge is to estimate the scaled reserve density x_1 from the data, inasmuch as r_1 is readily deduced from the scaled specific growth rate μ (along with the scaled parameter ψ_W, which is estimated in Section 4.5). Different strategies must be adopted, depending on the type of data available. For instance, [131] provide data on the yield of *E. coli* grown on glucose, defined as the amount of biomass Y gained per unit of glucose taken up by the cell mass (Fig. 4.1, left panel). If we assume that the yield at $\widetilde{\mu} = 0$ corresponds to lean cells devoid of glycogen surplus, we can regard the difference between $Y(\widetilde{\mu})$ and $Y_0 = Y(\widetilde{\mu})|_{\widetilde{\mu}=0} = W + M_0 + M_G + M_1$ as a measure for the glycogen surplus present at $\widetilde{\mu}$. Taking 0.45 as the weight fraction occupied by structural biomass W within this lean cell composition (since $W/(W + M_0 + M_G + M_1) = 0.45$, see Section 4.5), we are able to estimate the structural weight W^* corresponding to $Y - Y_0$ as $0.45Y_0$. The scaled reserve density x_1 can then be calculated using eqn (4.4) as $x_1 = X_1/(W^*\widetilde{\sigma}_{1,W})$, where the numerical value of $\widetilde{\sigma}_{1,W}$ is provided by the calculations outlined in Section 4.5. The transformed data (x_1, r_1) together with the best-fitting empirical form, eqn (4.13), are shown in Fig. 4.1, right panel.

Direct observations on the reserve density are available in some cases. For instance, Rhee [123] estimated phosphate reserves in the green alga *Scenedesmus sp.*, grown under phosphorus-limited conditions, by means of two different analytical methods ('surplus P' and 'total polyphosphates'). The scaled reserve density x_1 can then be directly calculated, using the estimate for the mass of structural biomass per cell

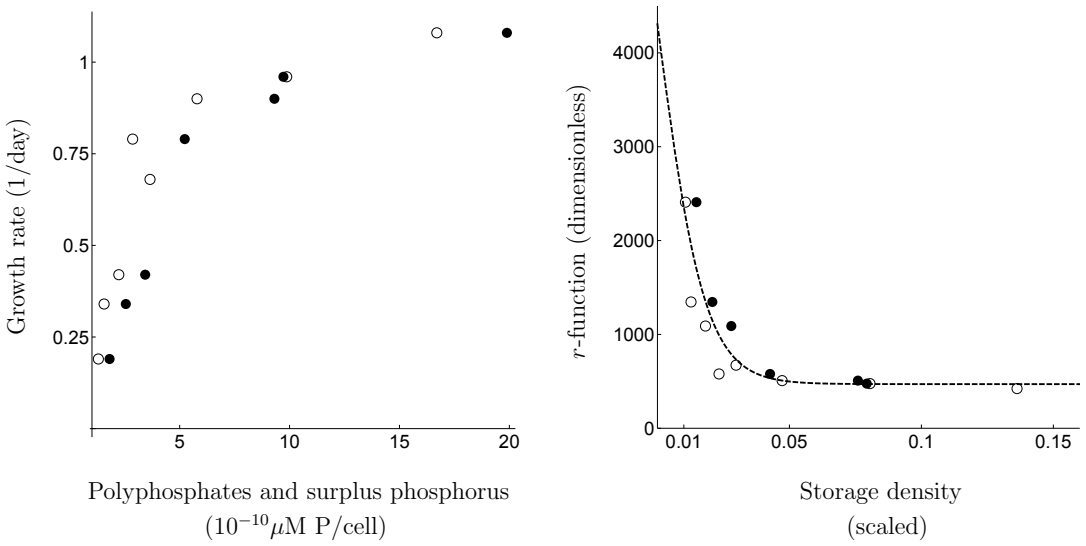

Figure 4.2: Reconstruction of the r-function for *Scenedesmus sp.* grown under phosphorus-limited conditions (the limiting nutrient is phosphate). Left: original data taken from [123]. Right: transformed data, together with the optimal non-linear least-squares fit of eqn (4.13) with parameters $\widehat{r}_1 = 7668.8$; $\vartheta_1 = 112.1$; $\xi_1 = 2.25 \times 10^{-9}$; $\zeta_1 = 470.3$. Open and filled circles correspond, respectively, to the values of surplus P and total polyphosphates taken from [123].

(Section 4.5). The results are shown in Fig. 4.2.

More generally, however, the available chemical-analytical methods do not permit a specific assignment of the particle species of interest to reserve versus non-reserve biomass, or do so only imperfectly. In these instances, the *cell quota* concept introduced by Droop [35] is useful: one simply states the total over all components and reports this figure on a per-cell basis. Calculating x_1 and r_1 on the basis of cell quota data is more involved but it has the advantage that it is applicable for general $n \geq 1$.

Let $\widetilde{\widehat{\phi}}_j f_j M_j$ denote the flux of the corresponding nutrient through the assimilatory machinery of type j, where $\widetilde{\widehat{\phi}}_j$ corresponds to a maximum rate per unit of machinery (e.g. when the latter is fully saturated by excess of substrate in the environment) and $f_j \in [0,1]$ expresses ambient conditions (e.g. eqn (4.15) below). In view of the scaling for M_j, eqn (4.4) and the equilibrium conditions, eqns (4.8)–(4.10), we have the following expression for the nutrient uptake flux via machinery of type j:

$$\widetilde{\widehat{\phi}}_j f_j \frac{\widetilde{\phi}_j}{\widetilde{\phi}_0} r_j W \widehat{m} \,.$$

At steady state, an alternative and equally valid expression for the flux is available in terms of the cell quota Q_j, a concept introduced by Droop [35], who expressed the nutrient uptake through assimilatory machinery of type j as $Q_j W \widetilde{\mu}$, where $\widetilde{\mu} = \frac{d}{dt} \ln W(t)$ is the unscaled specific growth rate. Equating these

two expressions and solving for the r-function we find:

$$r_j = \frac{\widetilde{\phi}_0 \widetilde{\mu} Q_j}{\widetilde{\widetilde{\phi}}_j \widetilde{\phi}_j \widehat{m} f_j} \,, \tag{4.14}$$

which can be viewed as a product of two factors: $\widetilde{\mu} Q_j / f_j$, composed of three quantities that can be estimated from empirical data, and a proportionality constant which is a compound parameter condensing stoichiometric coefficients; numerical estimates of the latter on the basis of independent data are discussed in Section 4.5.

An often-employed model is the Michaelis-Menten hyperbola [153] that relates f_j to ambient conditions:

$$f_j = (1 + K_j / [\mathrm{N}_j])^{-1} \,, \tag{4.15}$$

where $[\mathrm{N}_j]$ denotes the ambient concentration of the nutrient and K_j is the saturation constant. On this relationship, eqn (4.14) becomes:

$$r_j = \frac{Q_j \widetilde{\mu} \widetilde{\phi}_0 (1 + K_j / [\mathrm{N}_j])}{\widetilde{\widetilde{\phi}}_j \widetilde{\phi}_j \widehat{m}} \,. \tag{4.16}$$

The cell quota is given by the following equation:

$$Q_j = \kappa_W + \kappa_{m,0} m_0 + + \kappa_{m,G} m_G + \sum_{\ell=1}^{n} \left(\kappa_{m,\ell} m_\ell + \kappa_{x,\ell} x_\ell \right) \,, \tag{4.17}$$

where $\kappa_\star$ accounts for the amount of nutrient that is incorporated per scaled unit of the corresponding component $\star$; numerical estimates of these coefficients, on the basis of independent data, are discussed in Section 4.5. In general, we thus obtain a linear system which can be solved for $x_1, \ldots, x_n$.

In practice, it is convenient to begin by estimating the parameters K_j and $\widetilde{\widetilde{\phi}}_j$ by means of the least-squares criterion, on the basis of the experimental data of the form $\{u_j, [\mathrm{N}_j]\}$, where $u_j = Q_j \widetilde{\mu}$ is the uptake rate of the corresponding nutrient N_j. According to the Michaelis-Menten relationship, eqn (4.15), u_j depends on N_j as follows:

$$u_j = \widetilde{\widetilde{\phi}}_j (1 + K_j / [\mathrm{N}_j])^{-1} \,. \tag{4.18}$$

Applying this procedure to data pertaining to the diatom *Skeletonema costatum* grown under nitrogen-limited conditions, we obtain the result shown in Fig. 4.3. It should be noted that these data do not fix the maximum parameter $\widehat{r}_1$ well and equally good fits can be obtained by letting this parameter be free or fixing it at a plausible value. However, from the perspective of the present theory, the precise value of this parameter is not critical. This stands in contrast to the midpoint parameter ξ_1, which governs the

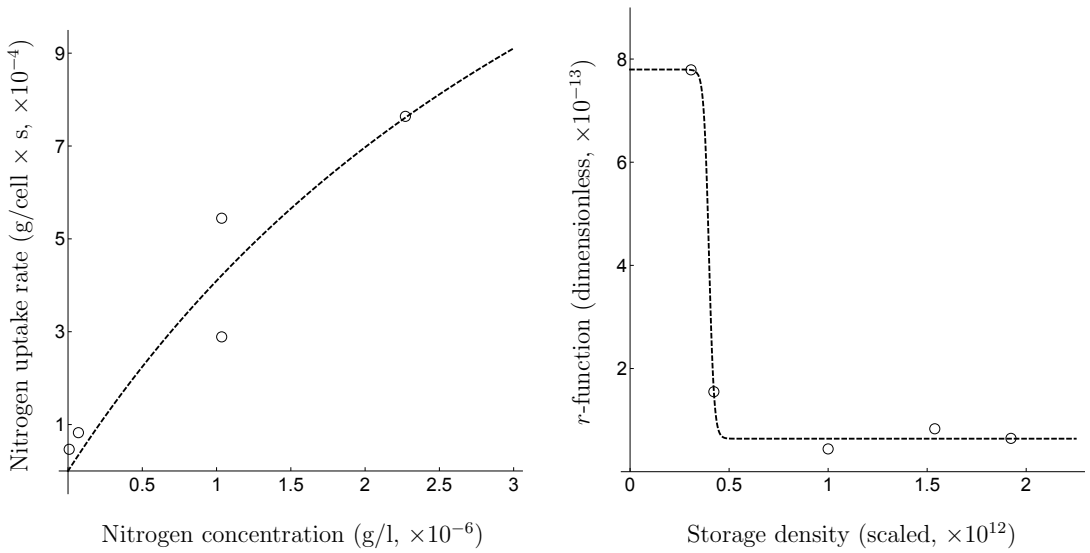

Figure 4.3: Reconstruction of the *r*-function for *Skeletonema costatum* grown under nitrogen-limited conditions (the limiting nutrient is ammonium). Left: original data taken from [65], together with the optimal non-linear least-squares fit of eqn (4.18) with parameters $K_1 = 4.7 \times 10^{-6}$ g/l; $\widehat{\widetilde{\phi}}_1 = 3.3 \times 10^9$ g per g of uptake machinery per second. Right: transformed data based on cell quota data from [65], together with the optimal non-linear least-squares fit of eqn (4.13) with parameters (best estimate $\pm$ standard deviation) $\widehat{r}_1 = (7.2 \pm 0.32) \times 10^{-13}$; $\vartheta_1 = (78.1 \pm 0.0002) \times 10^{-12}$; $\xi_1 = (0.4 \pm 0.005) \times 10^{12}$; $\zeta_1 = (0.64 \pm 0.16) \times 10^{-13}$.

behaviour of the *r*-function within the framework of the control loop underpinning the present theory. Estimates for this parameter are consistent irrespective of how the parameter $\widehat{r}_1$ is treated.

Despite these caveats, it can be seen that the sigmoid function, eqn (4.13), is adequate for the three data sets considered here. The good agreement with the data in all cases suggest that the *r*-function, which might otherwise be dismissed as a mere conceptual device to provide mathematical closure for the macro-chemical kinetics equations, can be regarded as reified by the data to some extent. It is best thought of as a *grosso modo* description of the regulatory feedback mechanisms in the organism.

A striking difference between the three examples shown is the relative steepness of the sigmoid which corresponds to how stringently the reserve is regulated to the mid-point value ξ_1. Provided that the range of *r*-values allowed by ζ_1 and $\widehat{r}_1$ is great enough, the variation in r_1 is translated into an adapative re-allocation of molecular building blocks toward the corresponding uptake machinery. If the range is great enough and the sigmoid is steep, even small variations will translate into large swings in how building blocks are allocated to the various types of machinery, and thus the growth rate is rapidly adjusted to a value commensurate with maintaining the reserves at level ξ_1 under the prevailing ambient conditions. If the steepness is smaller (and also if the range between ζ_1 and $\widehat{r}_1$ is smaller), the cell allows a certain range of variation of the reserve density, i.e. reserve homeostasis is less stringent.

From a biological point of view, it is almost self-evident that the shape parameters of the *r*-function,

which express how the organism manages its reserves, assume values in response to selective pressure. In other words, the parameter values that characterise a particular organism, for a given type of nutrient reserve, are presumed to constitute an evolutionary optimum. In the remainder of this paper, we explore the hypothesis that this is the case, and investigate in particular the problem of optimality in the face of ambient fluctuations in nutrient availability.

4.4 Evolutionary adaptation of the *r*-function

In order to assess evolutionary optimality of the design parameters in any given biological system, a suitable criterion of optimality is required. This is the fitness (or more precisely, the *marginal* fitness) associated with the parameter set $\{\xi_j, \vartheta_j, \widehat{r}_j, \zeta_j\}_{j=1,\ldots,n}$. For micro-organisms, the specific growth rate $\widetilde{\mu}(t) \equiv \frac{d}{dt} \ln W(t)$ is an obvious candidate: if two competing types are characterised by the values $\widetilde{\mu}_A$ and $\widetilde{\mu}_B$, the relative abundance of type A with respect to B is expected to grow as $\exp\{\widetilde{\mu}_A - \widetilde{\mu}_B\}$ and thus the condition $\widetilde{\mu}_A > \widetilde{\mu}_B$ amounts to the statement that A is fitter than B. Although this argument seems to have gained currency among microbiologists (e.g. [94]) it is readily shown by means of elementary counterexamples that instantaneous fitness can be problematic and, in particular, that the ecophysiology of the organism dictates which regime of discounting $\widetilde{\mu}(t)$ over time t is the appropriate measure of fitness [158].

A suitable definition of fitness in this context is the long-time average specific growth rate, defined as follows:

$$\rho = \lim_{t\to\infty} \frac{\ln W(t)}{t} \tag{4.19}$$

(cf. [102]). For the practical purposes of estimating fitness via numerical simulations, we use a sufficiently large averaging time to approximate this limit.

4.4.1 Optimal regulation in a constant environment

Consider the model with $n \geq 1$ types of reserves, subjected to a time-constant environment characterised by the parameters $\{\psi_1, \ldots, \psi_n\}$ with all constants ψ_j strictly positive and growth-sufficient. In such an environment, the optimal *r*-function for all reserves j is characterised by the double limit $\vartheta_j \to \infty$; $\xi_j \to 0\ \forall j$. To see this, first observe that this condition is equivalent to $x_j \equiv 0\ \forall j$, eventually as $t \to \infty$, as a result of the adaptive re-allocation property of the model; in other words we are disregarding any transient behaviour for small t and consider the model in steady state, eqns (4.8)–(4.10).

We thus have to establish optimality of the condition $x_j \equiv 0 \,\forall\, j$, which, in view of the fact that $x_j < 0$ is not permitted in the theory for any j (cf. [111]), amounts to showing that any set of non-negative reserve density values $\{x_1, \ldots, x_n\}$ is sub-optimal whenever at least one element is strictly positive. Without loss of generality, relabelling reserves and corresponding nutrient species if necessary, we may assume that x_1 is strictly positive.

Consider the ray emanating from the origin and passing through the point $(x_1, \ldots, x_n)$. The distance between this point and the origin is

$$R = x_1 \sqrt{1 + \eta_2^2 + \cdots + \eta_n^2}\,, \tag{4.20}$$

where the parameters $\eta_j = x_j/x_1$, $1 < j \leq n$, are fixed along the ray. We consider the rate of change of the steady-state value of μ as we move along this ray. From eqns (4.20) and (4.8)–(4.10) we find:

$$\frac{d\mu}{dR} = \frac{-\mu\left(\psi_1^{-1} + \eta_2\psi_2^{-1} + \cdots + \eta_n\psi_n^{-1}\right)}{\sqrt{1 + \eta_2^2 + \cdots + \eta_n^2}\left(\psi_W^{-1} + \psi_1^{-1} + \cdots + \psi_n^{-1} + \mu^{-2}\right) + R\left(\psi_1^{-1} + \eta_2\psi_2^{-1} + \cdots + \eta_n\psi_n^{-1}\right)}\,, \tag{4.21}$$

which shows that $d\mu/dR < 0$ and thus any steady state in which not all x_j are zero (i.e., one or more are strictly positive) can be improved upon by choosing any point, closer to the origin, along the ray connecting this state to the origin. It follows that the optimal steady state is at the origin, that is, μ is maximal when $x_j = 0$ for all j. This steady state with all reserve densities at zero can be characterised as the 'lean growth' or 'balanced growth' condition [152]; 'lean' because the cells in this state consist entirely of structural components and machinery, 'balanced' as re-allocation due by the r-functions effectively 'counter-skews' stoichiometric imbalances in the environment (cf. [155]).

This lean regulatory regime is optimal only if the environment is unchanging and growth is sufficient, for in that case the steady-state value of μ becomes identical to the fitness ρ as defined by eqn (4.19), as ultimately $W(t) \sim \exp\{\mu t\}$ or $\ln\{W(t)\}/t \sim \mu$. We can tentatively extend this conclusion to environments that do fluctuate, but remain growth-sufficient in perpetuity: provided that the long-term increase in biomass is not affected too strongly by the transients during which the cells 're-balance' through adaptive re-allocation, μ will be close to the optimum dictated by environmental conditions most of the time. Moreover, steep r-functions (i.e. $\vartheta_j \gg 1$) offer the most reactive response to the changing conditions, minimising the losses that accompany such transients.

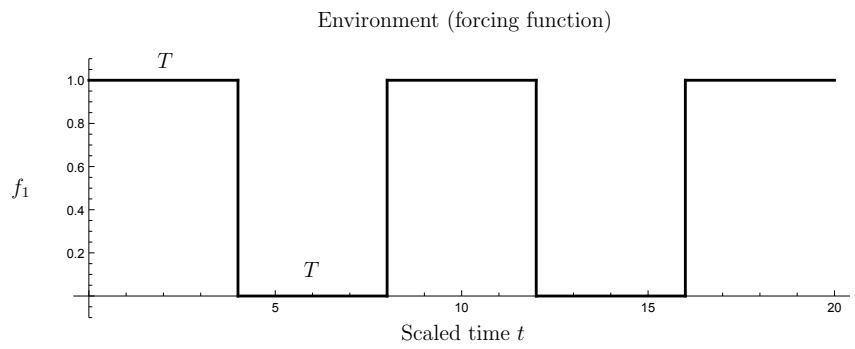

Figure 4.4: The time-varying environment: a 'feast' of duration T alternates with a 'famine' also of duration T.

4.4.2 Optimal regulation in a 'feast-or-famine' environment

If the environment intermittently imposes conditions which do not support growth at a positive rate (i.e. periods of 'famine'), the possibility arises that reserve management is no longer optimal when it is geared to balanced growth, characterised by low ξ_j and high ϑ_j, which promote $x_j \approx 0 \; \forall j$. Whereas these parameter settings maximise fitness in a constant, growth-sufficient environment, as shown in Section 4.4.1, permitting a certain reserve surplus to build up during times of plenty may allow the organism to maintain growth during times of nutrient shortage. Such a strategy could increase fitness in the sense of eqn (4.19), in view of the down-time losses incurred when the cell enters a state of metabolic shut-down with zero growth. A cell which maintains reserves close to zero at all times (even during 'feast' periods) will spend essentially the entire famine period in this shut-down state, in which the metabolic rate has slowed down to virtually zero, and this may depress fitness ρ. The behaviour of the present model as it enters such shut-down states has been treated in detail in a previous paper [111]; essentially, this extreme starved state corresponds to a *sliding mode* of the dynamical system.

To explore this hypothesis, we subject the model, with $n = 1$, to periodic environmental forcing that simulates feast-or-famine conditions in a basic fashion: a piecewise constant function that alternates between periods of feast ($f_1(t) \equiv 1$) and of famine ($f_1(t) \equiv 0$). Feast and famine both have duration T (in scaled time units); thus the period of the entire cycle is $2T$ (Fig. 4.4). We set $\zeta_1 = 0$ in the analysis that follows. Numerical results were obtained via simulations performed by means of a stand-alone server application written in *Java 8* by Oleg A. Nev. In view of the stiffness properties of the equations, the Gear implicit fourth-order method [20] was employed to calculate a numerical solution of the system of ODEs. Furthermore, a random-restart hill-climbing approach [126] was used to maximise fitness ρ.

Let us first fix $\widehat{r}_1$ and ϑ_1 and consider the variation of the ρ-maximizing value of ξ_1, the mid-point

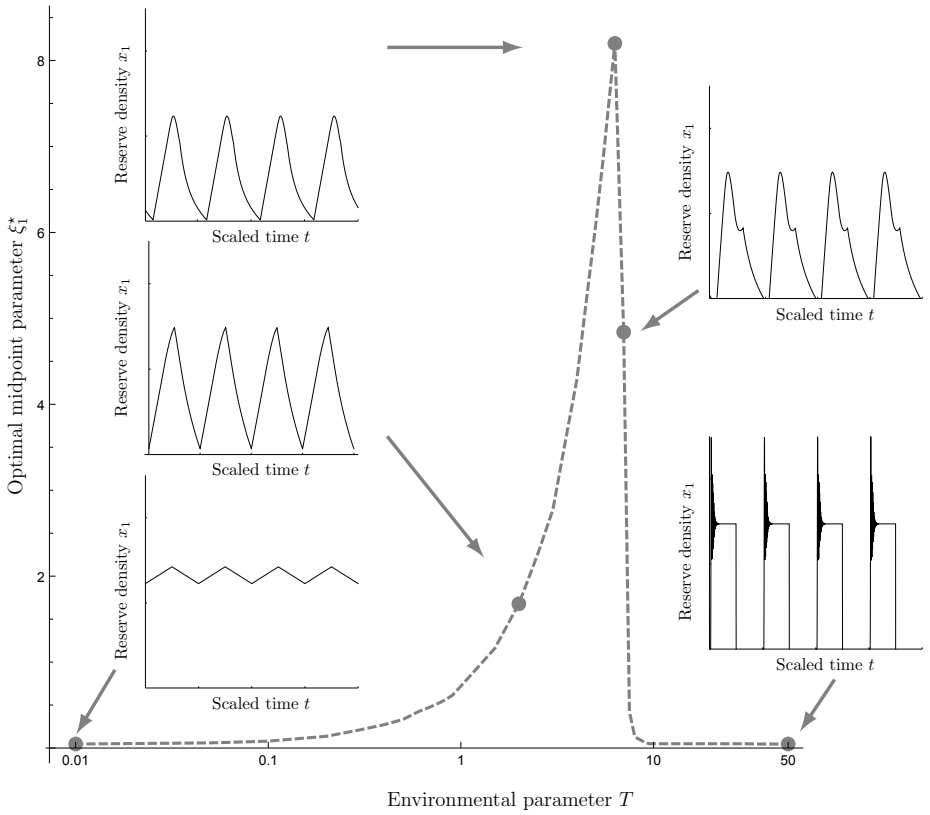

Figure 4.5: Fitness-optimal mid-point shape parameter $\xi_1^*(T)$ of the regulatory function $r_1(x_1)$ as a function of the environmental parameter T. Insets show each four stationary cycles at the optimal parameter value; the abscissa thus has width $8T$ and the ordinate runs from 0 to 2.5$\times$ the optimal value $\xi_1^*(T)$. The parameter $\widehat{r}_1$ was fixed at the value 10 and the parameter ϑ_1 was fixed at the value 100.

parameter which may be interpreted as the *setpoint* of the reserves, as a function of the environmental parameter T, denoted $\xi_1^*(T)$. As shown in Fig. 4.5, $\xi_1^*(T)$ is close to zero for both $T \ll 1$ and $T \gg 1$. The non-dimensionalisation of the model is such that the typical time scale of the dynamics is of order 1. Thus the case $T \ll 1$ can be viewed as an environment that fluctuates much more rapidly than the inherent physiological dynamics. The latter effectively average out these fluctuations, and the system behaves as if exposed to a *constant* environment with $f_1 \equiv \frac{1}{2}$ and the results of Section 4.4.1 can be applied. The case $T \gg 1$ is somewhat more delicate. In this limiting case, the system spends most of its time in the eventual state belonging to the prevailing conditions, i.e. the growth state for $f_1 = 1$ and the sliding mode for $f_1 = 0$. The transients between the two phases become less important as T increases. Thus the fitness ρ is dominated by the biomass gains made during the feast periods, and hence the optimal parameter regime accords with the results of Section 4.4.1. This leaves the intermediate case where $T \sim 1$. Here transient dynamical behaviour following the changes in environmental conditions dominates the outcome. These transients are associated with the depletion of reserves during famines and reserve replenishment during

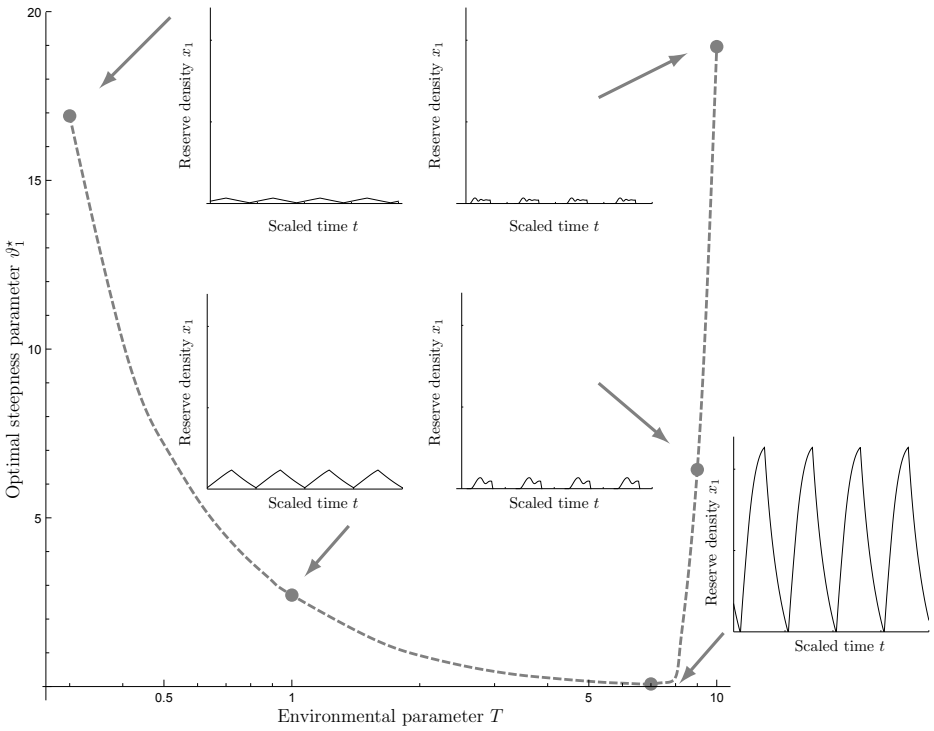

Figure 4.6: Fitness-optimal steepness parameter $\vartheta_1^*(T)$ of the regulatory function $r_1(x_1)$ as a function of the environmental parameter T. Insets each show four stationary cycles at the optimal parameter value; the abscissa thus has width $8T$ and the ordinate runs from 0 to 12. The parameter $\widehat{r}_1$ was fixed at the value 10 and the parameter ξ_1 was fixed at the value 0.1.

feasts. The optimal reserve level $\xi_1^*(T)$ appears to be such that the reserve density just attains the sliding mode at the end of the feast period.

Next, we fix $\widehat{r}_1$ and ξ_1 and consider the variation of the ρ-maximizing value of ϑ_1, the steepness parameter which may be interpreted as the *regulatory reactivity* of the control system, as a function of the environmental parameter T, denoted $\vartheta_1^*(T)$. Again we can observe agreement with the results of Section 4.4.1 in the cases $T \ll 1$ and $T \gg 1$, with much reduced optimal steepness in the intermediate case $T \approx 7$ (Fig. 4.6). This lower value of $\vartheta_1^*(T)$ allows for a greater amplitude of reserve density fluctuation over the stationary cycle, again with the reserve density just attaining the sliding mode at the end of the feast period.

More generally, we should treat ρ as a function of the three parameters $\{\xi_1, \vartheta_1, \widehat{r}_1\}$. The latter variable, $\widehat{r}_1$, is fitness-limiting when it is too small, since the operating range of the control system is then constrained by this variable; for $\widehat{r}_1 \gg 10$, optimal fitness ρ becomes insensitive to this parameter. Accordingly, we fix $\widehat{r}_1$ at the sufficiently large value 10 and determine the maximum fitness ρ with respect to ξ_1 and ϑ_1. We observe that the optimal stationary cycles again display the greatest variation in reserve density x_1 for $T \approx 6$, with smaller amplitude variations for both $T \ll 1$ and $T \gg 1$ (Fig. 4.7). For large T,

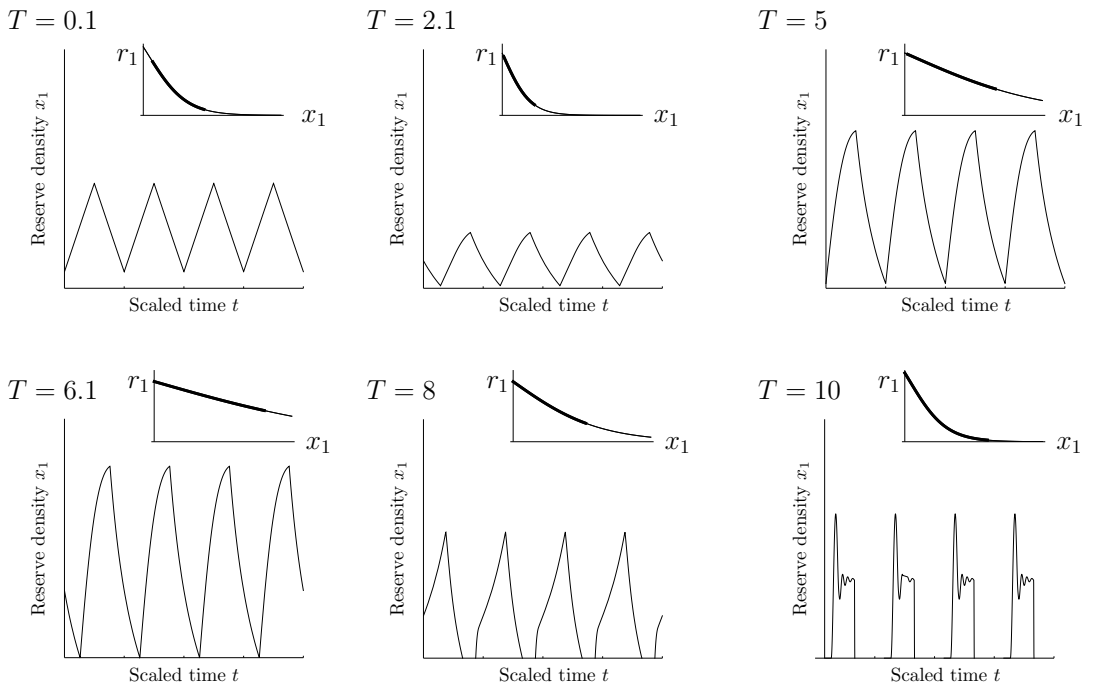

Figure 4.7: Stationary cycles for fitness-optimal *r*-functions. Each panel shows four stationary cycles of the reserve density, total duration $8T$ with T as indicated, with ordinate running from 0 to 0.25 for $T = 0.1$ and $T = 10$ and 12 for all other values of T. The parameter $\widehat{r}_1$ was fixed at the value 10 and the parameters ξ_1 and ϑ_1 were simultaneously optimised for maximal ρ. Insets show the corresponding optimal *r*-functions, with abscissa running from 0 to 0.25 for $T = 0.1$ and $T = 10$ and 12 for all other values of T and ordinate from 0 to 6 in all cases. The heavy-lined portion of the inset graphs corresponds to the working range of the stationary cycle.

the sliding mode behaviour at the end of famine intervals can be seen. The optimal *r*-functions, shown in the insets of Fig. 4.7, exhibit a 2- to 3-fold variation of r_1 over the stationary cycle for the intermediate regime, with a greater variation at the extremes ($T \ll 1$, $T \gg 1$).

4.5 Stoichiometric calculations and estimates

A wealth of data is available for the species *Escherichia coli*, which we will here take as our model for a 'typical' prokaryotic cell, using these data to estimate the various stoichiometric parameters.

4.5.1 Assignment of proteins to components

The first step is to assign the proteins expressed, or potentially expressed, by an *E. coli* cell to the macro-chemical components as distinguished within the context of the mathematical model described in Section 4.2. Proteins dedicated to transcription and translation are shared between the machinery that generates catalytic machinery (i.e., the macro-chemical component denoted M_0) and the machinery that generates more structural biomass (i.e., machinery M_G generating structural biomass W), since both types of machinery produce proteins. In addition, the machinery for growth M_G comprises proteins involved

in the synthesis of the cell envelope, proteins involved in DNA replication and cell division, genomic maintenance and duplication, as well as biosynthetic pathways. Uptake machinery (denotes $M_1, \ldots, M_n$) comprises proteins that underlie the assimilation of nutrients from the ambient environment, such as transporters and binding proteins, as well as the machinery required to transform these nutrients into core metabolites. Guided by these general principles, we obtain the assignment of all currently known and functionally identified *E. coli* proteins to components, as detailed in Table 4.2. Valgepea et al. [149] give quantitative estimates for the cellular abundance of each of these proteins. Summing the totals for each component, we find that the structural component (W) accounts for $\sim 39.4\%$ of the protein dry weight, synthetic machinery (M_0) for $\sim 19.6\%$, growth machinery (M_G) for $\sim 33.8\%$, and assimilatory (or 'uptake') machinery ($M_1, \ldots, M_n$) for $\sim 7.2\%$. Among the latter, machinery devoted to the assimilation of glucose, nitrogen, and phosphorus, accounting for, respectively, 0.563%, 0.44%, and 0.1% of the total cellular protein mass.

The structural component W comprises $\sim 39.4\%$ of the protein mass, which means that the fraction of RNA- and ribosome-related proteins belonging to the growth machinery is about 0.394, since the growth machinery is dedicated to the synthesis of the structural component. It follows that machinery M_0 synthesising catalytic machinery accounts for $\sim 60.6\%$ of all RNA- and ribosome-related proteins in the cell. Let $\beta_0 = 0.606$ denote the portion of RNA- and ribosome-related proteins that appertain to the synthetic machinery, and $1 - \beta_0 = 0.394$ for the remainder.

Assuming equal protein sizes on average across the components, we can convert these estimates into allocation coefficients, as follows:

$$\alpha_0 = 0.323, \quad \alpha_G = 0.558, \quad \alpha_{\mathrm{Gl}} = 0.0093, \quad \alpha_{\mathrm{N}} = 0.0073, \quad \alpha_{\mathrm{P}} = 0.0017\,, \tag{4.22}$$

where the subscripts Gl, N, and P stand for glucose, nitrogen, and phosphorus, respectively.

According to [109], one gram of *E. coli* contains 0.55 g of protein and 0.2053 g RNA. This gives

$$0.55 \times 0.196 + 0.2053 \times \beta_0 = 0.232 \text{ g synthetic machinery per gram-cell ;}$$

$$0.55 \times 0.338 + 0.2053 \times (1 - \beta_0) = 0.267 \text{ g growth machinery per gram-cell ;}$$

$$0.55 \times 0.072 = 0.0396 \text{ g assimilatory machinery per gram-cell .}$$

The structural component comprises every molecule not assigned to catalytic machinery or reserves; the

latter comprise ~ 0.025 g per gram-cell [109]. Thus, by subtraction, we have

$$1-(0.232+0.267+0.0396+0.025)=0.436 \text{ g structural component per gram-cell}\,.$$

4.5.2 Rates of production

Protein elongation The rate of elongation attained by a single ribosome is 18 amino acids per second [12]; multiplying this by the total of $\sim 26,300$ ribosomes per cell [12], we have for the whole-cell protein synthesis elongation rate:

$$18\times 26,300 = 473,400 \text{ amino acids per second per cell}\,.$$

Equivalently, using a dry weight of one cell of $\sim 2.8\times 10^{-13}$ grams [109],

$$473,400/(2.8\times 10^{-13}) = 1,690.7\times 10^{15} \text{ amino acids/(s·gram-cell)}\,.$$

With 550 mg of protein, equivalent to $5,081\times 10^{-6}$ mol amino acid residues, for every gram-cell [109], we finally calculate

$$1,690.7\ \times\ 10^{15}\ \times\ 550\ \times\ 10^{-3}/(5,081\ \times\ 10^{-6}\ \times\ N_A)\ =\ 0.0003039 \text{ g protein/(s·gram-cell)}\ \ ,$$

where $N_A = 6.02214129\times 10^{23}$.

Scaled parameters Using eqn (4.22) and the value of β_0, we can now calculate estimates for the stoichiometric coefficients $\widetilde{\phi}_k$ from eqn (4.1), which express the rate of production of the machinery of type k:

$$\widetilde{\phi}_0 = \frac{0.0003039\times\beta_0\times(1+\text{g RNA in } M_0/\text{g of proteins in } M_0)}{\alpha_0\times \text{ g of } M_0} = \frac{0.0003039\times\beta_0\times(1+0.124/0.108)}{0.323\times 0.232} = 0.0053 \text{ per second}\,,$$

$$\widetilde{\phi}_G = \frac{0.0003039\times\beta_0\times(1+\text{g RNA in } M_G/\text{g of proteins in } M_G)}{\alpha_G\times \text{ g of } M_0} = \frac{0.0003039\times\beta_0\times(1+0.081/0.186)}{0.558\times 0.232} = 0.002 \text{ per second}\,,$$

$$\widetilde{\phi}_{\mathrm{Gl}} = \frac{0.0003039\times\beta_0}{\alpha_{\mathrm{Gl}}\times \text{ g of } M_0} = \frac{0.0003039\times\beta_0}{0.0093\times 0.232} = 0.085 \text{ per second}\,,$$

$$\widetilde{\phi}_{\mathrm{N}} = \frac{0.0003039\times\beta_0}{\alpha_{\mathrm{N}}\times \text{ g of } M_0} = \frac{0.0003039\times\beta_0}{0.0073\times 0.232} = 0.109 \text{ per second}\,,$$

$$\widetilde{\phi}_{\mathrm{P}} = \frac{0.0003039\times\beta_0}{\alpha_{\mathrm{P}}\times \text{ g of } M_0} = \frac{0.0003039\times\beta_0}{0.0017\times 0.232} = 0.5 \text{ per second}\,.$$

The specific growth rate prior to scaling $\widetilde{\mu}$ is equal to $\frac{d}{dt}\ln W(t) \equiv \dot{W}/W$ by definition where $\dot{W} = \widetilde{\psi}_W M_G$ in the present model. Over a period of time in which $\widetilde{\mu}$ is not time-varying, this parameter is related to the doubling time $\widetilde{T}_2$ by the formula $\widetilde{\mu} = \ln\{2\}/\widetilde{T}_2$. Hence, using $\widetilde{T}_2 = 2{,}400$ sec [109], we have $\widetilde{\mu} = 0.00029$ sec^{-1}, which leads us to

$$\widetilde{\psi}_W = \frac{\widetilde{\mu}}{M_G/W} = \frac{0.00029 \text{ per second}}{0.267 \text{ g } M_G \text{ per gram-cell}/0.436 \text{ g } W \text{ per gram-cell}} = 0.00047 \text{ per second} .$$

Applying the scaling, eqn (4.5), and considering the cell in homeostasis for synthetic machinery (i.e., $m_0 = 1 \Leftrightarrow M_0/W = \hat{m}$), we obtain:

$$\psi_W = \frac{\widetilde{\psi}_W \widetilde{\phi}_G}{\widetilde{\phi}_0^2}\hat{m} = \frac{\widetilde{\psi}_W \widetilde{\phi}_G}{\widetilde{\phi}_0^2}\frac{M_0}{W} = \frac{0.00047 \text{ per s} \times 0.002 \text{ per s}}{0.0053^2 \text{ per s}^2} \times \frac{0.232 \text{ g of } M_0 \text{ per gram-cell}}{0.436 \text{ g of } W \text{ per gram-cell}} = 0.018 .$$

4.5.3 Stoichiometric coefficients related to glucose

Glucose as a building block Neidhardt et al. [109] indicate that *E. coli* is 50% carbon by dry weight (d/w). Since glucose ($C_6H_{12}O_6$, molar mass 180 g/mol) is the only source of carbon for *E. coli* when grown in a minimal medium, it follows that one gram of cell d/w requires $0.5 \times 180/(12 \times 6) = 1.25$ g of glucose (i.e. $180/(12 \times 6) = 2.5$ g glucose is required for each g C). Protein per g d/w requires 0.29 g of carbon [109]; therefore protein synthesis requires

$$0.29 \text{ g of C per gram-cell} \times 2.5 \text{ g glucose per g of C} = 0.73 \text{ g glucose per gram-cell} ,$$

since we consider the glucose to be the sole source of carbon. RNA requires 0.072 g of carbon per gram-cell [109], and thus

$$0.072 \text{ g C per gram-cell} \times 2.5 \text{ g glucose per g C} = 0.18 \text{ g glucose per gram-cell}$$

is required for RNA synthesis. According to [109], glycogen (the main glucose reserve in the cell of *E. coli*) accounts for 0.028 g glucose per gram-cell, and the energetic cost of forming the glycogen polymer out of glucose is negligible.

Glucose as a source of energy The maximum ATP yield per molecule of glucose is ~ 29.38 ATP molecules [124], thus $1/29.38 = 0.034$ molecules of glucose must be completely catabolised to produce one molecule of ATP. The total energy required for polymerisation of all essential macromolecules to create one gram d/w equals 0.023 mol ATP per gram-cell [109]; accordingly, the energetic requirement

to render all macromolecules in their polymeric form is

$$0.023 \text{ mol ATP per gram-cell} \times 0.034 \text{ molecules of glucose per molecule ATP} \times 180 \text{ g/mol} =$$
$$0.14 \text{ g glucose per gram-cell}.$$

In terms of protein synthesis, 0.022 mol ATP per g d/w is required to drive the processes of activation and incorporation, as well as to provide the cell with the energy for proofreading, assembly, and modification reactions [109]. This is equivalent to

$$0.022 \text{ mol ATP per gram-cell} \times 0.034 \text{ molecules of glucose per molecule ATP} \times 180 \text{ g/mol} =$$
$$0.13 \text{ g glucose per gram-cell}.$$

In terms of RNA synthesis, a similar calculation yields:

$$0.00026 \text{ mol ATP per gram-cell} \times 0.034 \text{ molecules of glucose per molecule ATP} \times 180 \text{ g/mol} =$$
$$0.0016 \text{ g glucose per gram-cell}.$$

In addition, glucose must be expended to fuel the synthesis of the monomeric building blocks that are assembled into the macromolecules; these include amino acids, nucleotides, lipid components, peptidoglycan monomers, and polyamines [109]. All the building blocks are derived from a central pool of a dozen core metabolites comprising glucose-6-phosphate, fructose-6-phosphate, ribose-5-phosphate, erythrose-5-phosphate, triose-phosphate, 3-phosphoglycerate, phosphoenolpyruvate, pyruvate, acetyl-CoA, α-ketoglutarate, succinyl CoA, and oxaloacetate [109]. The combined cost of synthesis for all required monomers from these twelve metabolites to generate one gram-cell d/w equals 0.018 mol ATP, -0.0035 mol NADH, and 0.017 mol NADPH [109]. Generation of NAD(P)H from NAD(P)$^+$ requires 1.5 ATP molecules [114, 142]. Thus, the glucose equivalent of the energetic requirement of 1 g d/w cell is as follows:

$$\begin{aligned}&(0.018 \text{ mol ATP} - 0.0035 \text{ mol NADH} \times 1.5 \text{ ATP per NADH} + \\ &0.017 \text{ mol NADPH} \times 1.5 \text{ ATP per NADPH}) \times \\ &(0.034 \text{ molecules of glucose per ATP}) \times 180 \text{ g/mol} = 0.23 \text{ g glucose per gram-cell}.\end{aligned}$$

Similar calculations yield that energetic requirements for glucose are 0.13 g/(gram-cell) to synthesise the

precursors for protein production, 0.034 g/(gram-cell) to synthesise precursors for RNA production, and 0.0009 g/(gram-cell) to synthesise precursors for glycogen production.

Glucose investment in macro-chemical components Synthetic machinery (M_0) contains both RNA and proteins. Accordingly, we estimate the total amount of the glucose required for these purposes in the following way:

$$
\begin{aligned}
& \beta_0 \times (0.18 \text{ g glucose as a building block for RNA production} \\
+\ & 0.036 \text{ g glucose to fuel RNA production}) \\
+\ & 0.196 \times (0.73 \text{ g glucose as a building block for protein production} \\
+\ & 0.26 \text{ g glucose as to fuel protein production}) \\
=\ & 0.33 \text{ g glucose per gram-cell for synthetic machinery .}
\end{aligned}
$$

A similar calculation for growth machinery (M_G) yields:

$$
\begin{aligned}
& (1-\beta_0) \times (0.18 \text{ g glucose as a building block for RNA production} \\
+\ & 0.036 \text{ g glucose to fuel RNA production}) \\
+\ & 0.338 \times (0.73 \text{ g glucose as a building block for protein production} \\
+\ & 0.26 \text{ g glucose to fuel protein production}) \\
=\ & 0.42 \text{ g glucose per gram-cell for growth machinery .}
\end{aligned}
$$

A similar calculation for assimilatory machinery ($\sum_{i=1}^{n} M_i$) yields:

$$
\begin{aligned}
& 0.072 \times (0.73 \text{ g glucose as a building block for protein production} \\
+\ & 0.26 \text{ g glucose to fuel protein production}) \\
=\ & 0.071 \text{ g glucose per gram-cell for uptake machinery .}
\end{aligned}
$$

To estimate the amount of glucose invested in the structural component, we subtract, from the total glucose requirement for 1 gram-cell, the requirements for the catalytic machinery components as well

as the glycogen reserves as found in a cell grown under standard conditions. This gives:

$$
\begin{aligned}
&(1.25 \text{ g glucose as a building block for production of 1 gram-cell} \\
&+\ 0.37 \text{ g glucose to fuel production of 1 gram-cell}) \\
&-\ 0.33 \text{ g glucose for } M_0 \\
&-\ 0.42 \text{ g glucose for } M_G \\
&-\ 0.071 \text{ g glucose for } (M_1 + \cdots + M_n) \\
&-\ 0.0289 \text{ g glucose fueling synthesis of glycogen reserves} \\
&=\ 0.77 \text{ g glucose per gram-cell to produce the structural component .}
\end{aligned}
$$

Rate of glucose reserve consumption By the scaling relations outlined in Section 4.2 we have

$$\sigma_{ji} = \frac{\widetilde{\sigma}_{ji}\widetilde{\phi}_i}{\widetilde{\sigma}_{jW}\widetilde{\phi}_0}\hat{m} \, .$$

Since we assume that $\sigma_{ji} = \sigma_j$ for $i \in \{0, 1, \ldots, n, G\}$, for $i = 0$ we have:

$$\sigma_j = \frac{\widetilde{\sigma}_{j0}\widetilde{\phi}_0}{\widetilde{\sigma}_{jW}\widetilde{\phi}_0}\hat{m} = \frac{\widetilde{\sigma}_{j0}}{\widetilde{\sigma}_{jW}}\hat{m} \, ,$$

and we therefore calculate the stoichiometric coefficient σ_{Gl} as follows:

$$\sigma_{\mathrm{Gl}} = \frac{\widetilde{\sigma}_{\mathrm{Gl},0}}{\widetilde{\sigma}_{\mathrm{Gl},W}}\hat{m} \, , \tag{4.23}$$

where $\hat{m} = M_0/W$. The coefficients $\widetilde{\sigma}_{\mathrm{Gl},0}$ and $\widetilde{\sigma}_{\mathrm{Gl},W}$ in eqn (4.23) denote the amounts of glucose required to produce a unit of, respectively, synthetic machinery or structural component. Accordingly, we have

$$
\begin{aligned}
\widetilde{\sigma}_{\mathrm{Gl},0} &= \frac{0.33 \text{ g glucose per gram-cell for } M_0 \text{ production}}{0.232 \text{ g of } M_0 \text{ per gram-cell}} = 1.4 \text{ g glucose per g } M_0 \, , \\
\widetilde{\sigma}_{\mathrm{Gl},W} &= \frac{0.77 \text{ g glucose per gram-cell for } W \text{ production}}{0.436 \text{ g of } W \text{ per gram-cell}} = 1.8 \text{ g glucose per g of } W \, ,
\end{aligned}
$$

and using $\hat{m} = M_0/W = 0.53$ g of M_0 per g of W, we find

$$\sigma_{\mathrm{Gl}} = \frac{1.4 \text{ g glucose per g } M_0 \times 0.53}{1.8 \text{ g glucose per g } W} = 0.4 \, .$$

4.5.4 Stoichiometric coefficients related to nitrogen

Nitrogen requirements A single gram dry weight of cellular mass contains 0.097 g nitrogen dispersed over its proteinaceous contents, and 0.035 g nitrogen contained in its RNA [109]. Accordingly, nitrogen

requirements for the production of each type of machinery are as follows:

$$\beta_0 \times 0.035 \text{ g nitrogen per gram-cell for RNA}+$$

$$0.196 \times 0.097 \text{ g nitrogen per gram-cell for protein} =$$

$$0.04 \text{ g nitrogen per gram-cell for synthetic machinery production ;}$$

$$(1-\beta_0) \times 0.035 \text{ g nitrogen per gram-cell for RNA}+$$

$$0.338 \times 0.097 \text{ g nitrogen per gram-cell for protein} =$$

$$0.047 \text{ g nitrogen per gram-cell for growth machinery production ;}$$

$$0.072 \times 0.097 \text{ g nitrogen per gram-cell for protein} =$$

$$0.007 \text{ g nitrogen per gram-cell for assimilatory machinery production .}$$

According to [166], glutamate ($C_5H_9NO_4$, 147 g/mol, the main nitrogen reserve in *E. coli*) comprises 100.55×10^{-6} mol per gram-cell. In terms of stoichiometric reckoning, only the nitrogen atoms in these glutamate molecules are assigned to the reserve, whereas the glutamine body is assigned to the structural component, in accordance with the biochemical notion of transaminase reactions to store the cell's temporary nitrogen surplus onto these bodies [109]. We have

$$100.55 \times 10^{-6} \text{ mol per gram-cell} \times 14 \text{ g/mol} =$$

$$0.0014 \text{ g nitrogen per gram-cell attributed to nitrogen reserve .}$$

An *E. coli* cell contains 14% nitrogen d/w [109] and thus

$$0.14-(0.04+0.047+0.007+0.0014) = 0.045 \text{ g nitrogen per gram-cell in the structural component .}$$

Rate of nitrogen reserve consumption To estimate the stoichiometric coefficient σ_N we use the following scaling equation:

$$\sigma_N = \frac{\widetilde{\sigma}_{N,0}}{\widetilde{\sigma}_{N,W}} \hat{m} \,, \tag{4.24}$$

where $\hat{m} = M_0/W$. The coefficients $\widetilde{\sigma}_{N,0}$ and $\widetilde{\sigma}_{N,W}$ denote the nitrogen amount needed to produce a unit of synthetic machinery or structural component, respectively. Accordingly,

$$\widetilde{\sigma}_{N,0} = \frac{0.04 \text{ g N per gram-cell for } M_0 \text{ production}}{0.232 \text{ g of } M_0 \text{ per gram-cell}} = 0.17 \text{ g N per g } M_0 \,,$$
$$\widetilde{\sigma}_{N,W} = \frac{0.045 \text{ g N per gram-cell for } W \text{ production}}{0.436 \text{ g of } W \text{ per gram-cell}} = 0.1 \text{ g N per g } W \,,$$

and using $\hat{m} = M_0/W = 0.53$ g of M_0 per g of W, we find

$$\sigma_N = \frac{0.17 \text{ g N per g } M_0 \times 0.53}{0.1 \text{ g N per g } W} = 0.8 \,.$$

Nitrogen cell quota By definition, the nitrogen cell quota is its intracellular density (amount per cell, which can roughly be thought of as an average concentration [35]). In terms of the state scaled variables of the macro-chemical model we have the following linear stoichiometric equation (assuming $n = 1$):

$$Q_N = \kappa_{m,0} m_0 + \kappa_{m,G} m_G + \kappa_{m,N} m_N + \kappa_{x,N} x_N + \kappa_W \,, \tag{4.25}$$

where κ_* is the amount of nitrogen attributed to the corresponding component $*$ in gram per cell. Following this definition of κ_*, we express $\kappa_{x,N} x_N$ as follows

$$\kappa_{x,N} x_N = \frac{X_N}{\gamma_W W} \,,$$

where γ_W is the number of cells that corresponds to one gram of structural component W. Therefore together with scaling from eqn (4.4) we have

$$\kappa_{x,N} x_N = \frac{W \widetilde{\sigma}_{N,W} x_N}{\gamma_W W} = \frac{\widetilde{\sigma}_{N,W} x_N}{\gamma_W} \,,$$

whence

$$\kappa_{x,N} = \frac{\widetilde{\sigma}_{N,W}}{\gamma_W} = 1.25 \times 10^{-14} \text{ g N per cell attributed to the nitrogen reserve} \,.$$

Reasoning similarly, we represent $\kappa_{m,i} m_i$ for $i \in \{0, N, G\}$ in the following form:

$$\kappa_{m,i} m_i = \frac{\text{g N}}{\text{g } M_i} \times \frac{\text{g } M_i}{\text{cell}} = \frac{\text{g N}}{\text{g } M_i} \times \frac{\text{g } M_i}{\text{g } W} \times \frac{\text{g } W}{\text{cell}} = \frac{\text{g N}}{\text{g } M_i} \times \frac{m_i \widehat{m} \widetilde{\phi}_i}{\widetilde{\phi}_0} \times \frac{\text{g } W}{\text{cell}} \,,$$

whence

$$\kappa_{m,i} = \frac{\text{g N}}{\text{g } M_i} \times \frac{\widehat{m} \widetilde{\phi}_i}{\widetilde{\phi}_0} \times \frac{\text{g } W}{\text{cell}} \,.$$

Using this expression, we obtain the following values for the weighting coefficients:

$$\kappa_{m,0} = 1.13 \times 10^{-14} \text{ g N per cell attributed to the synthetic machinery ,}$$

$$\kappa_{m,G} = 4.39 \times 10^{-15} \text{ g N per cell attributed to the growth machinery ,}$$

$$\kappa_{m,N} = 2.38 \times 10^{-13} \text{ g N per cell attributed to the nitrogen assimilatory machinery .}$$

The last coefficient κ_W can be expressed as follows:

$$\kappa_W = \frac{\text{g N}}{\text{g } W} \times \frac{\text{g } W}{\text{cell}} = 1.25 \times 10^{-14} \text{ g N per cell attributed to the structural component .}$$

In these units, eqn (4.25) takes on the following form:

$$Q_{\text{N}} = 1.13 \times 10^{-14} m_0 + 4.39 \times 10^{-15} m_G + 2.38 \times 10^{-13} m_N + 1.25 \times 10^{-14} x_N + 1.25 \times 10^{-14} =$$
$$1.13 \times 10^{-14} m_0 + 4.39 \times 10^{-15} \widetilde{\mu} (\widetilde{\phi}_0 \psi_W)^{-1} + 2.38 \times 10^{-13} m_N + 1.25 \times 10^{-14} x_N + 1.25 \times 10^{-14} , \tag{4.26}$$

since it follows from the scaling (Section 4.2) and the definition of the specific growth rate that $\widetilde{\mu} = \mu \widetilde{\phi}_0 = m_G \psi_W \widetilde{\phi}_0$.

4.5.5 Stoichiometric coefficients related to phosphorus

Phosphorus requirements for the cell components production According to [110], polyphosphate, which constitutes the main phosphorus reserve, accounts on average for ~ 0.003 g per gram-cell d/w. Since PO_3H unit weighs 80 g/mol and phosphorus weighs 31 g/mol, we should assign $0.003 \times 31/80 = 0.001$ g of P per gram-cell to the phosphorus reserve.

Assuming that the four bases guanine, adenine, cytosine, and uracil are equally abundant [125], we find that an RNA unit weighs $80 + 115 + (150 + 134 + 110 + 111)/4 = 321.25$ g/mol, which implies that RNA requires $31/321.25 = 0.096$ g P per gram-cell. Accordingly, phosphorus requirements for the production of synthetic and growth machineries are as follows:

$$\beta_0 \times 0.096 \text{ g P per g of RNA} \times 0.2053 \text{ g of RNA per gram-cell} =$$
$$0.012 \text{ g P per gram-cell for synthetic machinery .}$$
$$(1 - \beta_0) \times 0.096 \text{ g P per g of RNA} \times 0.2053 \text{ g RNA per gram-cell} =$$
$$0.008 \text{ g P per gram-cell for growth machinery .}$$

An average *E. coli* cell is about 3% phosphorus d/w [109], whence we conclude that

$$\begin{aligned}
\text{0.03 g P per gram-cell} - \ & (\text{0.012 g P per gram-cell in the synthetic machinery} \\
& + \ \text{0.008 g P per gram-cell in the growth machinery} \\
& + \ \text{0.001 g P per gram-cell in the reserve}) \\
& = \ \text{0.009 g P per gram-cell in the structural component .}
\end{aligned}$$

Rate of phosphorus reserve consumption We estimate the stoichiometric coefficient σ_P in accordance with the following scaling equation:

$$\sigma_P = \frac{\widetilde{\sigma}_{P,0}}{\widetilde{\sigma}_{P,W}} \hat{m} \tag{4.27}$$

with $\hat{m} = M_0/W$. The coefficients $\widetilde{\sigma}_{P,W}$ and $\widetilde{\sigma}_{P,0}$ express, respectively, how much phosphorus is required to synthesise one unit of the structural component and of the synthetic machinery. Thus we obtain:

$$\begin{aligned}
\widetilde{\sigma}_{P,0} &= \frac{\text{0.012 g of P per gram-cell for } M_0 \text{ production}}{\text{0.232 g of } M_0 \text{ per gram-cell}} = \text{0.052 g of P per g of } M_0 \text{ ,} \\
\widetilde{\sigma}_{P,W} &= \frac{\text{0.009 g of P per gram-cell for } W \text{ production}}{\text{0.436 g of } W \text{ per gram-cell}} = \text{0.02 g of P per g of } W \text{ .}
\end{aligned}$$

Therefore we have:

$$\sigma_P = \frac{\text{0.052 g of P per g of } M_0 \times \text{0.53 g of } M_0 \text{ per g of } W}{\text{0.02 g of P per g of } W} = 1.4 \text{ .}$$

4.5.6 Maintenance

To estimate the maintenance coefficients c_j we use the scaling equation (Section 4.2):

$$c_j = \frac{\widetilde{c}_j}{\widetilde{\sigma}_{jW}\widetilde{\phi}_0} \text{ ,} \tag{4.28}$$

where the coefficient $\widetilde{c}_j$ expresses the amount of substrate j per unit of structural component per unit of time required by the cell to maintain essential processes and structures that are not related to its growth. This parameter can be estimated by means of the following definition of the maintenance coefficient [118]:

$$m = a/Y \text{ ,} \tag{4.29}$$

where a denotes the specific maintenance rate, a typical value for *E. coli* being $\sim$ 0.03 h $^{-1}$ [109]. The parameter Y is the yield coefficient for a substrate used for growth, which is estimated as 0.25 g of cell

dry weight per g glucose for *E. coli* growing on glucose [66]. Therefore we can calculate the maintenance coefficient $\widetilde{c}_{\mathrm{Gl}}$ for *E. coli* growing on glucose as follows:

$$\begin{aligned}\widetilde{c}_{\mathrm{Gl}} &= \frac{0.03/3600 \text{ per second}}{0.25 \text{ gram-cell per g glucose} \times 0.436 \text{ g } W \text{ per gram-cell}} \\ &= 7.6 \times 10^{-5} \text{ g glucose per g } W \text{ per second} ,\end{aligned}$$

whence the scaled coefficient takes on the following form:

$$c_{\mathrm{Gl}} = \frac{7.6 \times 10^{-5} \text{ g glucose per g } W \text{ per second}}{1.8 \text{ g glucose per g } W \times 0.0053 \text{ per second}} = 0.008 .$$

4.5.7 Adjustments for eukaryotes

Inasmuch as *E. coli* is much more extensively documented than almost any other micro-organism, it is tempting to treat the *E. coli*-based estimates as quasi-universal. This can be expected to be warranted to some extent, the more so as the parameters express intrinsic, biochemically universal properties. For instance, the storage compounds that are accumulated in the cells can probably be regarded as comparable, as many algal species accumulate glycogen [163], amino acids [33], and polyphosphate [123]. Nonetheless, eukaryotic unicellular organisms are quite distinct from the prokaryote *E. coli*, and therefore this porting of stoichiometric estimates must be considered with some care, and adjusted wherever data are available for the eukaryotic species analysed in the main text. Since the cell quota is calculated on a per cell basis rather than g d/w, the weighting coefficients (κ-type parameters) need to be revised, using the reported dry weight of 2.9×10^{-10} g/cell for *Skeletonema costatum* [116].

Adjustments for nitrogen cell quota for *Skeletonema costatum* The weighing coefficients for the nitrogen cell quota equation are adjusted as follows:

$$\kappa_{x,N} = 1.3 \times 10^{-11} \text{ g N per cell attributed to the nitrogen reserve} ,$$

$$\kappa_{m,0} = 1.2 \times 10^{-11} \text{ g N per cell attributed to the synthetic machinery} ,$$

$$\kappa_{m,G} = 4.5 \times 10^{-12} \text{ g N per cell attributed to the growth machinery} ,$$

$$\kappa_{m,N} = 2.45 \times 10^{-10} \text{ g N per cell attributed to the nitrogen assimilatory machinery} ,$$

$$\kappa_{W} = 1.3 \times 10^{-11} \text{ g N per cell attributed to the structural component} .$$

Table 4.2: Assignment of *E. coli* proteins to macro-chemical components

Synthetic M_0	Uptake $M_1, \ldots, M_n$	Growth M_G	Structural W
Ribosome-associated	Path to core metabolism	Agmatine biosynthesis	Catabolism
Rlml	AnsA	SpeA	AsnB
RlmN	AspA	SpeB	ClpP
RluB	CysQ	Amino-acid biosynthesis	DacA
RluD	DadA	ArgA	DacC
RmsA	GadA	ArgB	Dcp
Rnc	GcvP	ArgC	DegQ
RsgA	LtaE	ArgD	Ggt
RsmB	ManA	ArgE	GlmS
RsmC	MtlD	ArgG	GuaA
RsuA	TreA	ArgH	HslV
SrmB	Nutrient uptake	ArgI	LdcA
Yfif	AlsB	AroA	LexA
TypA	AraF	AroB	Lon
RimM	ArgT	AroC	Map
RaiA	ArtI	AroG	OmpT
RbfA	ArtJ	AroK	PepA
YchF	ArtP	Asd	PepB
YbcJ	ChbB	AspC	PepD
YibL	Crr	CysE	PepE
RoxA	CysA	CysK	PepN
YjgA	CysP	CysM	PepP
Der	Dppa	DapB	PepQ
RimP	DppD	DapD	PepT
YihI	DppF	DapE	PmbA
YjeE	FepB	DapF	Prc
HflX	FruA	DkgA	PrlC
RsmI	FruB	HisB	PurF
Era	GalE	HisC	SohB
RlmM	GatA	HisD	TldD
Ribosomal	GlnH	HisF	YajL
RplA	GlnQ	HisG	YegQ
RplB	GltI	HisH	YggG
RplC	GsiB	HisI	YhbO
RplD	HisJ	IlvB	Chaperones/folding
RplE	HisP	IlvC	CbpA
RplF	KgtP	IlvD	ClpA
RplI	LivF	IlvE	ClpB
RplJ	LivG	IlvH	ClpX
RplK	LivJ	IlvI	CspC
RplL	LivK	LeuA	CspD
RplM	LolD	LeuC	CspE

Table 4.2: Assignment of *E. coli* proteins to macro-chemical components

Synthetic M_0	Uptake $M_1,\ldots,M_n$	Growth M_G	Structural W
RplN	LptB	LeuD	DegP
RplO	LptF	LysA	DnaJ
RplP	LptG	LysC	DnaK
RplQ	LsrB	MetA	DsbA
RplR	MalE	MetB	DsbC
RplS	MalK	MetC	DsbG
RplT	ManX	MetE	FklB
RplU	ManY	MetK	FkpA
RplV	ManZ	MetL	FkpB
RplW	MetN	Mtn	FtsH
RplX	MetQ	PheA	GroL
RplY	MglA	ProA	GroS
RpmA	MlaD	ProB	GrpE
RpmB	MlaF	ProC	GrxB
RpmC	ModA	RidA	GrxC
RpmD	ModF	SerA	GrxD
RpmE	MppA	SerC	HdeB
RpmF	MsbA	ThrA	HscA
RpmG	MtlA	ThrB	HscB
RpmH	NagE	ThrC	HslO
RpsA	NlpA	TrpA	HslU
RpsB	OmpA	TrpB	HtpG
RpsC	OmpC	TrpC	NfuA
RpsD	OmpF	TrpD	PpiA
RpsE	OppA	TrpE	PpiB
RpsF	OsmF	TyrA	PpiC
RpsG	PhoP	TyrB	PpiD
RpsH	PotA	Usg	SecB
RpsI	PotD	Cell division	Skp
RpsJ	PotF	Fic	SlyD
RpsK	PstS	FtsA	SurA
RpsL	PtsG	FtsE	Tig
RpsM	PtsH	FtsZ	TrxA
RpsN	PtsI	MinC	TrxC
RpsO	PtsN	MinD	YbbN
RpsP	PtsP	MinE	ProQ
RpsQ	RbsD	MreB	YcdY
RpsR	SapA	MukE	BepA
RpsS	SufC	RodZ	Chemotaxis
RpsT	ThiB	Slt	FliY
RpsU	UgpB	ZapA	RbsB
Sra	YadG	ZapB	Defense
YqjD	YdcS	ZipA	Ahpc
Hpf	YecC	ObgE	ArcA

Table 4.2: Assignment of *E. coli* proteins to macro-chemical components

Synthetic M_0	Uptake $M_1,\ldots,M_n$	Growth M_G	Structural W
RNA-related	YgiS	EngB	ArcB
AlaS	YtfQ	FtsP	Bcp
ArgS	MscS	DamX	DcyD
AsnS	TolB	ZapD	Dps
AspS	MlaC	MatP	FrdA
CysS	DcrB	NlpI	FrdB
Fmt	EfeO	RlpA	GlnB
GlnS	AroP	Cell envelope synthesis	KatE
GltX	TolQ	AccA	KatG
GlyQ	CorC	AccB	LuxS
GlyS	Tsx	AccC	NarL
HisS	PhoU	AccD	NarP
IleS	GadC	AcpP	OtsA
LeuS	CorA	AnmK	SodA
LysS	ChaB	BtuE	SodB
LysU	SstT	Cld	SodC
MetG	TrkA	DhaK	SolA
MnmA	LamB	DhaL	SpeG
PheS	FadL	FabA	Tpx
PheT		FabB	WrbA
ProS		FabD	Yfid
RpoA		FabF	Yqhd
RpoB		FabG	Metabolic intermediates
RpoC		FabH	AceA
RpoD		FabI	AceB
RpoE		FabZ	AceE
RpoN		FadA	AceF
RpoS		FadB	AckA
RpoZ		FadE	AcnA
SerS		FadI	AcnB
ThrS		FadJ	Acs
TrpS		FadM	AdhE
TyrS		Ffh	Agp
ValS		FtsY	ArnC
YihD		GalF	AtpA
YhbY		Glf	AtpC
YgfZ		GlpK	AtpD
RraA		GpsA	AtpF
LepA		KdsA	AtpG
YceD		KdsB	AtpH
YciO		KdsC	BglA
CmoA		LpcA	CobB
RseB		LpxA	CydA

Table 4.2: Assignment of *E. coli* proteins to macro-chemical components

Synthetic M_0	Uptake $M_1,\ldots,M_n$	Growth M_G	Structural W
RimN		LpxB	CydB
MnmE		LpxD	CyoA
RapZ		Mpl	CyoB
Transcription		MrcB	DeoC
AllR		MurA	Dld
ArgP		MurC	Eda
Crl		MurD	Eno
Crp		MurE	FbaA
CysB		MurF	FbaB
DksA		PlsB	Fbp
FadR		Psd	FolA
Fnr		PssA	FolD
FruR		RfaD	FrmA
Fur		RfaE	FucO
GlpR		TesA	FumA
GntR		TesB	GabD
HupA		UgpQ	GabT
HupB		YidC	GalM
IscR		YbiS	GapA
Lrp		MdoG	GarR
MalT		LolA	Gcd
MetJ		LptA	GcvH
MhpR		BamC	GcvT
MprA		CpoB	GhrA
NadR		BamB	GhrB
NagC		BamD	GlcB
NikR		BamA	Glk
NrdR		YnhG	GlmM
OsmE		LpoB	GlmU
OxyR		MipA	GloA
PdhR		WbbI	GloB
PurR		LpoA	GltA
SlyA		LolB	GlyA
TrpR		MdoD	Gnd
TyrR		YcjG	Gor
YqgE		ErfK	GpmA
Zur		LptD	GpmM
NusG		LapB	Gst
BolA		Cofactor biosynthesis	HchA
YebC		BioD	Icd
Cra		CoaA	KdgK
KdgR		Dxs	LdhA
YehT		FolE	LldD

Table 4.2: Assignment of *E. coli* proteins to macro-chemical components

Synthetic M_0	Uptake $M_1, \ldots, M_n$	Growth M_G	Structural W
YciT		Fre	Lpd
YhgF		FtnA	MaeA
RapA		HemB	MaeB
Translation		HemD	Mdh
Efp		HemE	MetF
Frr		HemG	MetH
FusA		HemX	MgsA
InfA		Iscs	MurQ
InfB		IspA	NagB
InfC		IspB	NagZ
PrfC		IspG	Ndh
Tsf		IspH	NuoA
TufA		LipA	NuoB
YeiP		MenB	NuoC
EttA		MoaC	NuoF
YbaK		MoaD	NuoG
SelB		MoaE	NuoI
		NadA	Pck
		NadC	PfkA
		NadE	PfkB
		NadK	PflB
		PanB	Pgi
		PanC	Pgk
		PdxB	Pgl
		PdxH	Pgm
		PdxJ	PoxB
		PncA	Ppa
		PncB	Ppc
		PntA	PpsA
		PntB	Prs
		QueC	Pta
		RfbA	PurH
		RfbB	PurN
		RfbC	PurT
		RfbD	PykA
		RibB	PykF
		RibC	RbsK
		RibD	Rpe
		RibE	RpiA
		SthA	SdhA
		SufS	SdhB
		ThiC	SdhD
		ThiD	SseA
		ThiE	SucA

Table 4.2: Assignment of *E. coli* proteins to macro-chemical components

Synthetic M_0	Uptake $M_1, \ldots, M_n$	Growth M_G	Structural W
		ThiF	SucB
		ThiG	SucC
		ThiL	SucD
		ThiM	TalA
		UbiB	TalB
		UbiD	ThyA
		UbiE	TktA
		UbiF	TktB
		UbiG	TpiA
		MoaB	YccX
		MoeA	YdbK
		UbiJ	YeaD
		DNA replication	YtjC
		DnaA	Zwf
		DnaN	IscU
		DnaX	YeeX
		GyrA	HinT
		GyrB	YdgH
		IhfA	YdhR
		IhfB	YgiN
		LigA	ErpA
		PolA	Ivy
		Purine metabolism	GstB
		Pyrimidine metabolism	Fdx
		Rob	ElbB
		SeqA	YdjN
		Ssb	SgcQ
		TopA	AzoR
		YbaB	MioC
		GreA	NagD
		YdaM	MenI
		Fatty acid biosynthesis	RcnB
		Cfa	IscA
		GnsB	Dtd
		Glutamate biosynthesis	FdhE
		GdhA	UcpA
		Glutamine biosynthesis	YgiF
		GlnA	EutL
		GltB	YcbX

Table 4.2: Assignment of *E. coli* proteins to macro-chemical components

Synthetic M_0	Uptake $M_1, \ldots, M_n$	Growth M_G	Structural W
		GltD	FrsA
		Glutathione	CsdE
		biosynthesis	
		GshB	MpaA
		Protein	CpdA
		biosynthesis	
		Def	PaaY
		FolX	GutQ
		PncC	Pka
		Protoporphyrin	Repair
		biosynthesis	
		HemL	Dut
		HemY	HelD
		Selenophosphate	Mfd
		biosynthesis	
		SelD	MsrA
		Spermidine	MsrB
		biosynthesis	
		SpeE	Mug
		Sulfide	MutL
		biosynthesis	
		CysH	NrdA
		CysI	NrdB
		CysJ	RdgC
			RecA
			UvrA
			UvrB
			UvrD
			XseB
			XthA
			RNA degradation
			Pnp
			Ppk
			RhlB
			Rho
			Rnb
			Rne
			Rnr
			RraB
			Ydfg
			Orn
			RNA modification
			Tgt
			TrmJ

Table 4.2: Assignment of *E. coli* proteins to macro-chemical components

Synthetic M_0	Uptake $M_1, \ldots, M_n$	Growth M_G	Structural W
			Secretion
			AcrA
			CopA
			CusB
			CusC
			CusF
			SecA
			SecD
			SecG
			SecY
			TolC
			YajC
			YebF
			MsyB
			AcrB
			Storage-related
			CsrA
			GlgA
			GlgB
			GlgC
			GlgP
			MalP
			Bfr
			Transcriptional repressors
			BaeR
			BasR
			CpxR
			Hns
			OmpR
			RcsB
			RcsD
			RstA
			StpA
			SuhB
			UvrY
			NusA
			NusB
			Rof
			Rsd
			RcnR
			YjdC
			FrmR
			MtfA
			ExuR

Table 4.2: Assignment of *E. coli* proteins to macro-chemical components

Synthetic M_0	Uptake $M_1, \ldots, M_n$	Growth M_G	Structural W
			FabR
			LrhA
			Defence
			UspA
			OsmY
			YajQ
			OsmC
			YifE
			HdeA
			SspA
			YggX
			UspG
			YfbU
			YggE
			ElaB
			PspA
			IbaG
			ChrR
			UspE
			AhpF
			UspF
			Tas
			YbgI
			CueO
			Slp
			SspB
			YiiM
			MscL
			SlyX
			UspD
			SbmC
			TehB
			YmdB
			YfcF
			CstA
			MobA
			PspB
			Blc
			Cell envelope
			Lpp
			YbaY
			YhcB
			Pal
			Redox reactions

Table 4.2: Assignment of *E. coli* proteins to macro-chemical components

Synthetic M_0	Uptake $M_1,\ldots,M_n$	Growth M_G	Structural W
			MsrC
			CyaY
			MdaB
			FldA
			YgjR
			YdgJ
			QorB

4.6 Discussion

Intracellular reserves, also known as variable internal stores [61] are a conspicuous feature of microbial organisms, sometimes occupying a significant portion of the volume of the cell and often present in the form of inclusion bodies [8, 24, 120]. Our results suggest that we should expect to find such features predominantly in fluctuating environments, since the optimal management strategy regarding reserves in stable growth-supporting environments is to maintain minimal reserve densities. Moreover, the time scale of the environmental fluctuations is important: very rapid fluctuations are irrelevant, and very slow fluctuations are essentially equivalent to constant environments, since stores that would allow the cells to tide them over the entire famine period would have to be unfeasibly large, and thus such periods become dead losses. Thus optimal reserve management is governed primarily by fluctuations that happen at a time scale comparable to that of the cell's physiology; this might be termed 'eco-physiological resonance.'

At the height of this eco-physiological resonance regime, the optimal parameter setting appears to be such that the stores just suffice to tide the cell over. In other words, the system reaches the sliding-mode regime just as the next feast period commences. This observation is in keeping with the results obtained by Parnas and Cohen [117] who used a similar, if slightly more coarse-grained, model of macro-chemical kinetics.

The limitations and possible extensions of the present study are readily apparent if we consider the more general definition of fitness proposed by Metz et al. [102]: the fitness of a given type Y is the asymptotic exponential growth rate $\rho_{E(C)}(Y)$ of the biomass of Y in an ergodic environment E in which the type is present in vanishingly small proportions relative to resident types $C \equiv \{X_1,\ldots,X_n\}$. This definition implies that $\rho_{E(C)}(X_i) = 0$ for $i = 1,\ldots,n$, since the biomasses of resident types cannot go to zero (this is what it means to be *resident*; so $\rho_{E(C)}(X_i) < 0$ is ruled out) and none of those masses can

go to infinity either (so $\rho_{E(C)}(X_i) > 0$ is ruled out as well). By contrast, for the non-resident type Y, interest centres on the case $\rho_{E(C)}(Y) > 0$ since its extinction is otherwise assured. The definition we have employed, eqn (4.19), accords for the particular eco-evolutionary scenario we have studied with the general one, but the latter encompasses *ergodic environments* and *multiple (competing, mutant) types*.

As regards multiple types, what we have studied here is optimality of reserve management *tout court*, as it were from an engineering perspective, isolating the role of reserves as stored supplies for times of scarcity. The presence of variant types in the environment would change the analysis since another role of reserves would come into play, namely that of capturing nutrients before a competitor can: short-term rapid uptake of peaks in ambient availability may then become a major factor.

Moreover, the spatial ordering of the environment may be important in how these competitive effects are transmitted. In a well-mixed environment, such as a high-turbidity lake, cells may be expected to be exposed to competing type cells *pro rata*, but by the same token, the effects are averaged out as the nutrient concentration tends to be uniform across the ecological system. By contrast, in a more static diffusion-limited environment, such as a biofilm-like system (cf. [159]), most cells may be surrounded by cells of like type, and competition is confined to the interfaces between subpopulations, which may allow polymorphisms to persist which would otherwise not be available (e.g. [62]).

As regards ergodic environments, the deterministic alteration studied here, with fixed time scale T, can be generalised to stochastic environments in which the duration of a feast or a famine is realised from a suitable statistical distribution, such as a Gaussian or exponential distribution. (In more advanced variations, the level f could itself be treated as a random variable, but still piecewise constant, or alternatively $f(t)$ could be the subject of an SDE.) We surmise that the present results would still go through in a qualitative sense. In particular, the average duration of a famine would have to be order 1 to evoke ξ_1^* bounded away from zero, as a consequence of the eco-physiological resonance effect described above, but the effect would be tempered by the extent to which feast periods allow the requisite storage levels to accumulate; if the feasts are relatively short, we do not expect the stores at the start of a typical famine period to be sufficient to keep the model away from the sliding mode for the entire duration of that famine. On the other hand, we do not expect long feast periods to negate the need to accumulate stores (cf. [117]).

Of special interest is the extension to stochastic (ergodic) environments for multiple nutrient limitation (i.e. the case $n > 1$). Let us consider the simplest version of such a model, in which each of the n environmental factors f_j can occur in either the state 0 or 1. Thus 2^n distinct joint environmental states

are possible, and the transitions between these states can be described as a continuous-time Markov chain. The key quantity in this setting is the correlation between the feast states for the various factors (and thus also between the famine states). We conjecture that negative correlation would result in higher reserve 'setpoints' ξ_j. For instance, for $n = 2$, strong negative correlation would imply that at most points in time, one is high while the other is low, with strict alternation between which one is feast and which is famine. In that case the storage serves not so much to survive bad times, but to carry on growing while only one factor is readily available. In contrast to the 'survival' aspect which is associated with providing energy to sustain the needs of endogenous metabolism, this second role is also important with regard to building blocks (e.g., N, P, S, trace metals,...). Strong positive correlation, on the other hand, would effectively reduce the dimensionality of the model back to $n = 1$, as the various environmental factors behave as though they were a single, more complex, nutrient compound. To conclude our conjecture on correlation, we surmise that eco-physiological resonance would be negated, or only possible for a limited range of environmental parameter values, as n increases when there is weak or no correlation between the environmental factors.

In terms of physiological realism, the present model implicitly assumes that the pool of core intermediary metabolites is kept under strict homeostasis, which allow the rates of synthesis of macromolecules to be treated as acceptor-driven. This assumption breaks down under metabolic shutdown conditions, and here the model can be extended with explicit donor-controlled rate multipliers, or equivalently, as we have shown elsewhere [111], by postulating a sliding mode for the dynamics. The model is based on $n+1$ feedback loops, one between each reserve density and the allocation of molecular building blocks towards the machinery dedicated to the assimilation of that nutrient, in addition to a basic growth-control loop that is based on homeostasis of the density of synthetic (zero-type, i.e. machinery-making) machinery; the latter may be referred to as the M_0/M_G-loop. The nutrient loops are expressed by the r-functions reconstructed from experimental data in Section 4.3, whereas the M_0/M_G-loop is consistent with the findings by [68]. In its present form, all nutrients are treated as essential; when nutrients can be exchanged for one another, the phenomenon of metabolic switching must be taken into account, and the regulatory laws become more involved than the ones considered here. Finally, we have not taken into account here the possibility of endogenous rhythmic processes, which may supply important timing cues to the control system. Such processes would effectively constitute clocks that govern (a subset of) the parameters of the r-functions.

Chapter 5

Future work

In this final chapter, I will discuss several limitations of the present theory as well as prospects for future work.

5.1 Relationship between types of nutrients and types of reserves. Diauxic growth

In the general case, we consider n different nutrients in the environment, each of which is converted into one of m types of reserves in the cell, where $m \leq n$. If we are dealing with a quadratic and diagonal matrix Ψ which describes the conversion of nutrients to reserves (see Chapter 2), then each ambient nutrient is essential, and is dedicated to one reserve. However, other scenarios are possible. For instance, nutrients can be chemically decomposed and thereby feed more than one type of reserve compound in the cell, which implies that the matrix $\mathbf{\Psi}$ contains non-zero off-diagonal elements. Several nutrients can also be substitutional [47] and converted into the same reserve type. For example, the organism may be able to utilise several different sugars in the environment (e.g. glucose and lactose); it is then often observed that they control gene expression in such way that a preferred substrate is used first (e.g. glucose) [46]. Micro-organisms typically 'prefer', i.e. give precedence to, the nutrient source on which they grow faster [109]. This phenomenon is called catabolite repression; it results in biphasic exponential growth, as shown in Fig. 5.1. This is also called diauxic growth. The first phase, during which the organism grows on glucose, is followed by the second phase, during which the organism grows on another sugar, which is lactose in the case of the lactose regulatory system [109]. In the situation where the cell has to switch between two essential nutrients, the regulatory laws are more complicated. One way to implement such switching is to postulate nutrient sensing [60]: the regulatory functions become dependent not only on the corresponding

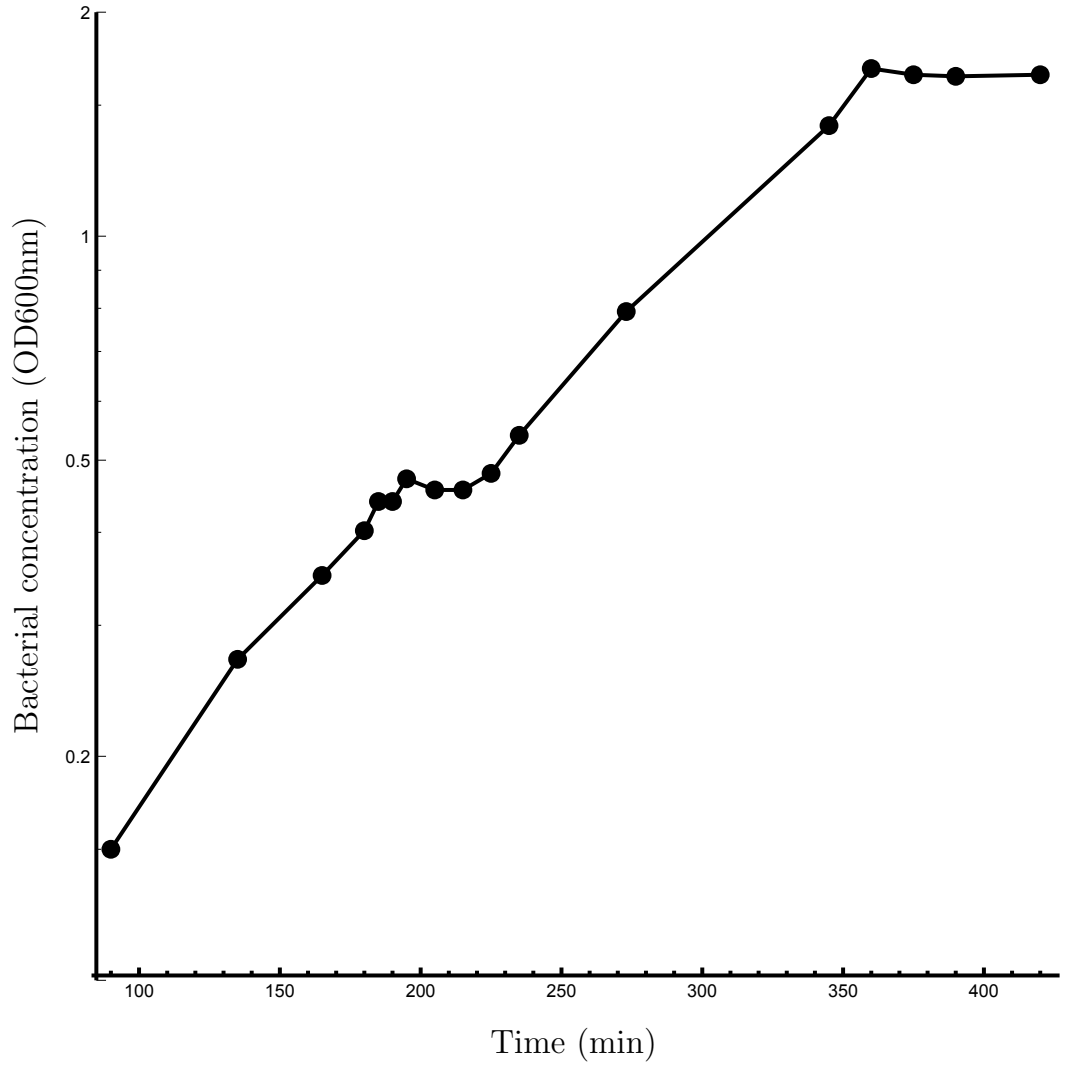

Figure 5.1: Glucose-lactose diauxic growth of *E. coli*. The first stage of a constant relative growth rate (i.e., exponential growth), where glucose is used as a main carbon source, is followed by a short stationary stage of a zero growth rate, after which a constant relative growth rate is resumed with lactose as a main carbon source. Data taken from [18].

reserve density, but also on the concentrations of the two nutrients in the environment. In particular, these functions can be modelled as shown in Fig. 5.2, where we are considering the situation of two alternative substrates, both of which are converted into reserve type 1. Let us call their ambient concentrations $[\mathrm{N}]_{1,A}$ and $[\mathrm{N}]_{1,B}$ and their r-functions $r_{1,A}$ and $r_{1,B}$, where the latter depend on the ratio $[\mathrm{N}]_{1,A}/[\mathrm{N}]_{1,B}$ as well as on the reserve density x_1. Both regulatory functions decrease as a function of x_1, as before, but in addition they are small when uptake and processing of the other substrate is preferred (e.g. more efficient in terms of building blocks invested in their uptake, energetic cost of processing, and so on [46]).

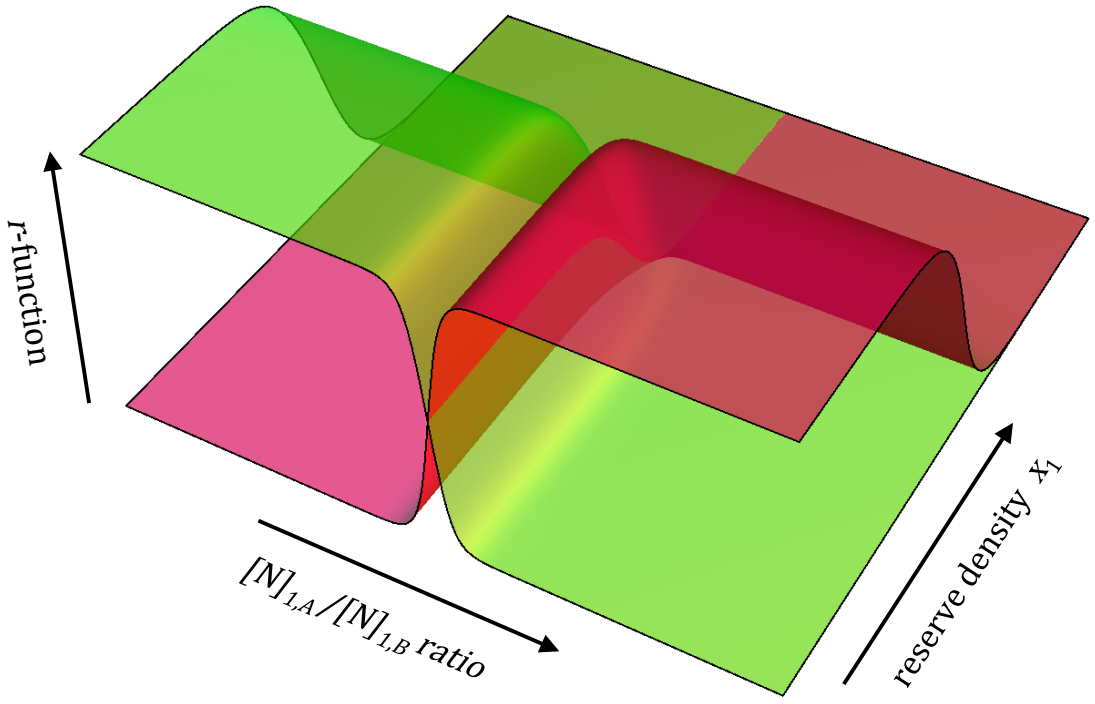

Figure 5.2: Diauxic growth. Two substitutional nutrients with ambient concentrations $[\mathrm{N}]_{1,A}$ and $[\mathrm{N}]_{1,B}$ are converted into reserve type 1. The corresponding r-functions $r_{1,A}$ and $r_{1,B}$ are functions of $[\mathrm{N}]_{1,A}/[\mathrm{N}]_{1,B}$ and of x_1. The red surface is a graph of $r_{1,A}$ and the green surface is a graph of $r_{1,B}$.

5.2 Diffusion limitation

The influx of the nutrient of type i was represented in this thesis as proportional to the density of the uptake machinery dedicated to its assimilation M_i in the form $\widehat{\widehat{\phi}}_i f_i M_i$, where $\widehat{\widehat{\phi}}_i$ is the maximum possible influx per unit of uptake machinery, and f_i is a dimensionless factor that indicates the degree of saturation of the uptake machinery. The latter can be expressed, for instance, by the Michaelis-Menten hyperbola [104] in the following form:

$$f_i = \frac{u_i(r_0)}{K_m + u_i(r_0)} ,$$

where $u_i(r)$ is the concentration of nutrient of type i at the distance r from the center of a spherical cell with radius r_0, and K_m is a saturation constant, as before (see Chapter 1). If we consider a Gram-positive bacterium growing in the well-mixed environment, then such a representation is reasonable, so we have the following expression for the influx of the nutrient of type i:

$$\Phi_i = \widehat{\widehat{\phi}}_i \frac{u_i(r_0)}{K_m + u_i(r_0)} M_i . \tag{5.1}$$

In this case balanced growth can be achieved via proportional increase in the density of membrane transporters in response to decrease in nutrient concentration in the bulk phase. However, when there is an

unstirred layer around the cell, diffusion limitation has to be taken into account, which leads to a more complicated definition for the nutrient influx. Since in this case diffusion can be described by means of the Laplace equation [31, 40], we obtain the following expression for the concentration of the nutrient of type i:

$$u_i(r) = \hat{u}_i - a/r \,,$$

where $\hat{u}_i = \lim_{r\to\infty} u_i(r)$, and a is a positive constant. Since at the surface of the cell ($r = r_0$) the diffusive flux must match the nutrient uptake by transporters, we can determine the constant a from the following equation:

$$\frac{Da}{r_0^2} = \widehat{\widetilde{\phi}}_i \frac{\hat{u}_i - a/r_0}{K_m + \hat{u}_i - a/r_0} \,, \tag{5.2}$$

where D is the diffusion constant. We also obtain an expression for the nutrient bulk concentration as follows:

$$\hat{u}_i = \frac{\Phi_i r_0}{D} + \frac{K_m}{M_i \widehat{\widetilde{\phi}}_i/\Phi_i - 1} \,. \tag{5.3}$$

If the first term on the right-hand side of this equation dominates, so that $\Phi_i \approx D\hat{u}_i/r_0$ and $u(r_0) \ll \hat{u}_i$, the flux is diffusion-limited; in the opposite situation, when the second term dominates, so that $\Phi_i \ll D\hat{u}_i/r_0$ and $u(r_0) \approx \hat{u}_i$, the flux is transport machinery-limited. Equation (5.3) indicates that every increase in uptake machinery moves the system towards the diffusion-limited regime. In Chapter 4 I showed that optimal regulation in constant environments is achieved when reserves are negligibly small, that is μ is maximal when $x_j = 0$ for all j. I conjecture that this is also true when diffusion limitation is taken into account. However, the behaviour of micro-organisms in fluctuating environments that was investigated in Chapter 4 might not longer show the same dynamics under diffusion-limited environmental conditions, though I would expect that the extreme regimes that are characterised by rapid and slow fluctuations again dictate the regulatory mode of the cell, similar to the case of constant environments.

Furthermore, in Gram-negative bacteria, a nutrient particle needs to traverse an outer membrane and a periplasm in addition to the cytoplasmic membrane (cf. Fig. 1.2 in Chapter 1). In this case, the flux will depend in general on the densities of the three types of machinery: porins in the outer membrane, binding proteins in the periplasm, and transporters in the inner membrane.

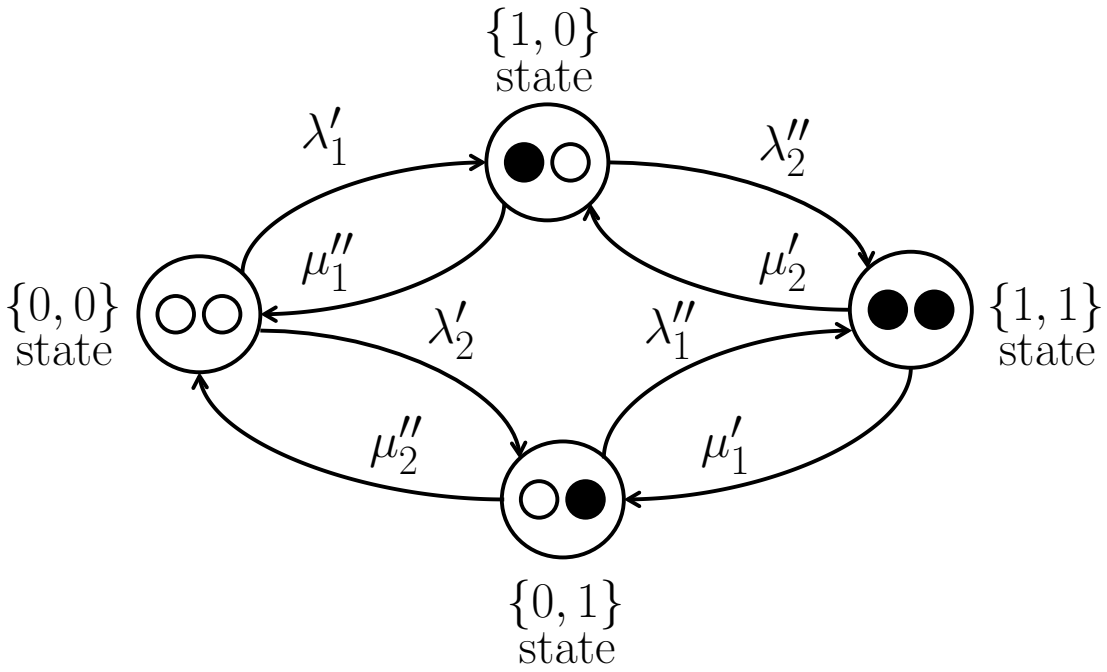

Figure 5.3: Schematic representation of the environment with two environmental factors as a Markov chain. Each of two environmental factors takes on the value 0 or 1, and therefore the environment is modelled as a four-state Markov chain with eight distinct transition rates as indicated. If the factors are not correlated, these transition rates depend on four parameters λ_1 , λ_2 , μ_1 , μ_2, as follows, $\lambda_1' = \lambda_1'' = \lambda_1$, $\lambda_2' = \lambda_2'' = \lambda_2$, $\mu_1' = \mu_1'' = \mu_1$, $\mu_2' = \mu_2'' = \mu_2$.

5.3 Modelling of the environment

Assuming that the factor f_i depends on the nutrient bulk concentration, we can model the latter either deterministically or stochastically. I studied the deterministic environment for the case $n = 1$ in Chapter 4, where the duration of feast and famine periods is fixed. The representation of the environment for $n > 1$ is challenging, since the correlation between different environmental factors has to be taken into account. Preliminary work shows that correlations are expected to have a profound influence on the cell's adaptive strategies affecting, for instance, the optimal density of surplus reserves which the cell maintains, how quick the cell is to re-allocate molecular building blocks to the assimilation of a nutrient when its sub-cellular stores are being depleted, and how the cell decides to switch to a new mode of metabolism (e.g. change to a new carbon source, a new donor of reducing equivalents, etc.).

The simplest approach to model a higher-dimension environment is to consider each of abiotic factors in a binary fashion, with zero being absence of the factor in the ambient environment and one corresponding to saturating levels (i.e. 'feast' and 'famine'). Thus, environmental conditions can be described as a positive recurrent Markov chain with 2^n states, where n is the number of environmental factors; the case $n = 2$ is shown in Fig. 5.3. Another approach is to consider them as real numbers bounded by certain

limits that set the finite range for each factor. The Lévy processes might be a suitable choice for this modelling purpose as they have been used in modelling stochastic environments, such as daily average temperature variations [6] or storm rainfall [105].

Bibliography

[1] `http://www.algaebase.org`.

[2] V. Acary and B. Brogliato. *Numerical Methods for Nonsmooth Dynamical Systems. Applications in Mechanics and Electronics. Lecture Notes in Applied and Computational Mechanics*. Springer-Verlag, 2008.

[3] H. M. Alvarez. Triacylglycerol and wax ester-accumulating machinery in prokaryotes. *Biochimie*, 120:28–39, 2016.

[4] J.-P. Aubin and A. Cellina. *Differential Inclusions*. Springer-Verlag, 1984.

[5] D. A. Beard. A biophysical model of the mitochondrial respiratory system and oxidative phosphorylation. *PLoS Comput. Biol.*, 1:e36, 2005.

[6] F. E. Benth and J. Šaltytė-Benth. Stochastic modelling of temperature variations with a view towards weather derivatives. *Applied Mathematical Finance*, 12:53–85, 2005.

[7] H. C. Berg and E. M. Purcell. Physics of chemoreception. *Biophysical J.*, 20:193–219, 1977.

[8] T. J. Beveridge. The structure of bacteria. In J. S. Poindexter and E. R. Leadbetter, editors, *Bacteria in Nature III: Structure, Physiology, and Genetic Adaptability*, pages 1–65. Plenum, 1989.

[9] F. R. Blattner, G. Plunkett, C. A. Bloch, N. T. Perna, V. Burland, M. Riley, J. Collado-Vides, J. D. Glasner, C. K. Rode, G. F. Mayhew, J. Gregor, N. W. Davis, H. A. Kirkpatrick, M. A. Goeden, D. J. Rose, B. Mau, and Y. Shao. The complete genome sequence of *Escherichia coli* K-12. *Science*, 277:1453–1469, 1997.

[10] S. Bleecken. Model for the feedback control system of bacterial growth I. Growth in discontinuous culture. *J. Theor. Biol.*, 133:37–65, 1988.

[11] W. Boos. Bacterial transport. *Annu. Rev. Biochem.*, 43:123–146, 1974.

[12] H. Bremer and P. P. Dennis. Modulation of chemical composition and other parameters of the cell by growth rate. In F.C. Neidhardt and et al., editors, *Escherichia coli and Salmonella typhimurium: Cellular and Molecular Biology*, chapter 97. ASM Press, 1996.

[13] C. Broughton, H. A. van den Berg, A. M. Wemyss, D. I. Roper, and A. Rodger. Beyond the discovery void: New targets for antibacterial compounds. *Science Progress*, 99:153–182, 2016.

[14] D. K. Button. Biochemical basis for whole-cell uptake kinetics: Specific affinity, oligotrophic capacity, and the meaning of the Michaelis constant. *Appl. Environ. Microbiol.*, 57:2033–2038, 1991.

[15] J. Caperon. Population growth in micro-organisms limited by food supply. *Ecology*, 48:715–722, 1967.

[16] J. Caperon. Population growth response of *Isochrysis galbana* to nitrate variation at limiting concentration. *Ecology*, 49:866–872, 1968.

[17] R. Casey, H. de Jong, and J.-L. Gouze. Piecewise-linear models of genetics regulatory networks: Equilibria and their stability. *J. Math. Biol.*, 52:27–56, 2006.

[18] D.-E. Chang, D. J. Smalley, and T. Conway. Gene expression profiling of *Escherichia coli* growth transitions: An expanded stringent response model. *Mol. Microbiol.*, 45:289–306, 2002.

[19] E. K. P. Chong, S. Hui, and S. H. Zak. An analysis of a class of neural networks for solving linear programming problems. *IEEE Trans. Autom. Control*, 44:1995–2006, 1999.

[20] L. O. Chua and P.-M. Lin. *Computer-Aided Analysis of Electronic Circuits: Algorithms and Computational Techniques*. Prentice-Hall, 1975.

[21] G. N. Cohen. Metabolism of bacteria. *Annu. Rev. Microbiol.*, 5:71–100, 1951.

[22] A. L. Davidson and J. Chen. ATP-binding cassette transporters in bacteria. *Annu. Rev. Biochem.*, 73:241–268, 2004.

[23] A. L. Davidson, E. Dassa, C. Orelle, and J. Chen. Structure, function, and evolution of bacterial ATP-binding cassette systems. *Microbiol. Mol. Biol. Rev.*, 72:317–364, 2008.

[24] E. A. Dawes. Growth and survival of bacteria. In J. S. Poindexter and E. R. Leadbetter, editors, *Bacteria in Nature III: Structure, Physiology, and Genetic Adaptability*, pages 67–187. Plenum, 1989.

[25] H. de Jong, J.-L. Gouze, C. Hernandez, M. Page, T. Sar, and J. Geiselmann. Qualitative simulation of genetic regulatory networks using piecewise-linear models. *Bull. Math. Biol.*, 66:301–340, 2004.

[26] R. de Wit, F. P. van den Ende, and H. van Gemerden. Mathematical simulation of the interactions among cyanobacteria, purple sulfur bacteria and chemotrophic sulfur bacteria in microbial mat communities. *FEMS Microbiol. Ecol.*, 17:117–136, 1995.

[27] K. B. Decker and D. M. Hinton. Transcription regulation at the core: Similarities among bacterial, archaeal, and eukaryotic RNA polymerases. *Annu. Rev. Microbiol.*, 67:113–139, 2013.

[28] T. den Blaauwen. Prokaryotic cell division: Flexible and diverse. *Cur. Opin. Microbiol.*, 16:738–744, 2013.

[29] T. den Blaauwen, M. A. de Pedro, M. Nguyen-Distèche, and J. A. Ayala. Morphogenesis of rod-shaped sacculi. *FEMS Microbiol. Rev.*, 32:321–344, 2008.

[30] J. Deutscher, F. M. Aké, M. Derkaoui, A. C. Zébré, T. N. Cao, H. Bouraoui, T. Kentache, A. Mokhtari, E. Milohanic, and P. Joyet. The bacterial phosphoenolpyruvate:carbohydrate phosphotransferase system: Regulation by protein phosphorylation and phosphorylation-dependent protein-protein interactions. *Microbiol. Mol. Biol. Rev.*, 78:231–256, 2014.

[31] E. DiBenedetto. *Partial Differential Equations*. Birkhauser, Boston, Second edition, 2010.

[32] L. Dieci and L. Lopez. Sliding motion in Filippov differential systems: Theoretical results and a computational approach. *SIAM J. Numer. Anal.*, 47:2023–2051, 2009.

[33] Q. Dortch, J. R. Clayton, S. S. Thoresen, and S. I. Ahmed. Species differences in accumulation of nitrogen pools in phytoplankton. *Marine Biology*, 81:237–250, 1984.

[34] M. Doudoroff and R. Y. Stanier. Role of poly-β-hydroxybutyric acid in the assimilation of organic carbon by bacteria. *Nature, Lond.*, 183:1440–1442, 1959.

[35] M. R. Droop. Vitamin B12 and marine ecology. IV. The kinetics of uptake, growth and inhibition in *Monochrysis lutheri*. *J. Mar. Biol. Assoc.*, 48:689–733, 1968.

[36] M. R. Droop. 25 years of algal growth kinetics – a personal view. *Botanica Marina*, 24:99–112, 1983.

[37] D. E. Dykhuizen. Experimental studies of natural selection in bacteria. *Annu. Rev. Ecol. Syst.*, 21:373–398, 1990.

[38] M. Ederer, S. Steinsiek, S. Stagge, M. D. Rolfe, A. T. Beek, D. Knies, M. J. T. de Mattos, T. Sauter, J. Green, R. K. Poole, K. Bettenbrock, and O. Sawodny. A mathematical model of metabolism and regulation provides a systems-level view of how *Escherichia coli* responds to oxygen. *Front. Microbiol.*, 5:124–135, 2014.

[39] A. J. Egan and W. Vollmer. The physiology of bacterial cell division. *Ann. N. Y. Acad. Sci.*, 1277:8–28, 2013.

[40] A. Einstein. Über die von der molekularkinetischen Theorie der Wärme geforderte Bewegung von in ruhenden Flüssigkeiten suspendierten Teilchen (in German). *Annalen der Physik*, 322:549–560, 1905.

[41] R. W. Eppley, J. N. Rogers, and J. J. McCarthy. Half-saturation constants for uptake of nitrate and ammonium by marine phytoplankton. *Limnology and Oceanography*, 14:912–920, 1969.

[42] W. Epstein and J. R. Beckwith. Regulation of gene expression. *Annu. Rev. Biochem.*, 34:411–436, 1968.

[43] C. P. Fall, E. S. Marland, J. M. Wagner, and J. J. Tyson. *Computational Cell Biology*. Springer-Verlag, 2002.

[44] A. M. Feist, M. J. Herrgård, J. L. Reed I. Thiele, and B. Ø. Palsson. Reconstruction of biochemical networks in microorganisms. *Nat. Rev. Microbiol.*, 7:129–143, 2009.

[45] A. F. Filippov. *Differential Equations with Discontinuous Right-Hand Side*. Kluwer Academic, 1988.

[46] S. H. Fisher and A. L. Sonenshein. Control of carbon and nitrogen metabolism in *Bacillus subtilis*. *Annu. Rev. Microbiol.*, 45:107–135, 1991.

[47] K. J. Flynn and A. Mitra. Building the "perfect beast": Modelling mixotrophic plankton. *J. Plankton Res.*, 31(9):965–992, 2009.

[48] P. Forterre. Looking for the most "primitive" organism(s) on Earth today: The state of the art. *Planet. Space Sci.*, 43:167–177, 1995.

[49] G. Fusco and N. Guglielmi. A regularization for discontinuous differential equations with application to state-dependent delay differential equations of neutral type. *J. Diff. Equations*, 250:3230–3279, 2011.

[50] D. Gangaiah, I. I. Kassem, Z. Liu, and G. Rajashekara. Importance of Polyphosphate Kinase 1 for *Campylobacter jejuni* viable-but-nonculturable cell formation, natural transformation, and antimicrobial resistance. *Appl. Environ. Microbiol.*, 75:7838–7849, 2009.

[51] P. Ghazal, S. Watterson, K. Robertson, and D. C. Kluth. The *in silico* macrophage: Toward a better understanding of inflammatory disease. *Genome Med.*, 3:4–11, 2011.

[52] L. Glass and S. A. Kauffman. The logical analysis of continuous non-linear biochemical control networks. *J. Theor. Biol.*, 39:103–129, 1973.

[53] E. Gonçalves, J. Bucher, A. Ryll, J. Niklas, K. Mauch, S. Klamt, M. Rochad, and J. Saez-Rodriguez. Bridging the layers: Towards integration of signal transduction, regulation and metabolism into mathematical models. *Mol. Biosyst.*, 9:1576–1583, 2013.

[54] A. González, C. Chaouiya, and D. Thieffry. Logical modelling of the role of the Hh pathway in the patterning of the *Drosophila* wing disc. *Bioinformatics*, 24:i234–i240, 2008.

[55] D. S. Goodsell. *The Machinery of Life*. Springer, New York, Sesond edition, 2009.

[56] J. C. Gottschal. Continuous culture. In J. Lederberg, editor, *Encyclopedia of Microbiology*, volume 1, pages 559–572. Academic Press, San Diego, CA, 1992.

[57] J.-L. Gouze and T. Sari. A class of piecewise linear differential equations arising in biological models. *Dyn. Syst.*, 17:299–316, 2002.

[58] H. C. Gram. Über die isolierte Färbung der Schizomyceten in Schnitt- und Trockenpräparaten. *Fortschr. Med.*, 2:185–189, 1884.

[59] T. J. Grevengoed, E. L. Klett, and R. A. Coleman. Acyl-CoA metabolism and partitioning. *Annu. Rev. Nutr.*, 34:1–30, 2014.

[60] E. A. Groisman. Feedback control of two-component regulatory systems. *Annu. Rev. Microbiol.*, 70:103–124, 2016.

[61] J. P. Grover. Resource competition in a variable environment: Phytoplankton growing according to the Variable-Internal-Stores model. *Amer. Nat.*, 138:811–835, 1991.

[62] J. P. Grover, S.-B. Hsu, and F.-B. Wang. Competition between microorganisms for a single limiting resource with cell quota structure and spatial variation. *J. Math. Biol.*, 64:713–743, 2012.

[63] A.-K. Gustavsson, D. D. van Niekerk, C. B. Adiels, B. Kooi, M. Goksör, and J. L. Snoep. Allosteric regulation of phosphofructokinase controls the emergence of glycolytic oscillations in isolated yeast cells. *FEBS J.*, 281:2784–2793, 2014.

[64] P. Hariharan, D. Balasubramaniam, A. Peterkofsky, H. R. Kaback, and L. Guan. Thermodynamic mechanism for inhibition of lactose permease by the phosphotransferase protein IIAGlc. *Proc. Natl. Acad. Sci. U.S.A.*, 112:2407–2412, 2015.

[65] P. J. Harrison, H. L. Conway, and R. C. Dugdale. Marine diatoms grown in chemostats under silicate or ammonium limitation. I. Cellular chemical composition and steady-state growth kinetics of *Skeletonema costatum*. *Mar. Biol.*, 35:19–31, 1976.

[66] N. G. Henry. Effect of decreasing growth temperature on cell yield of *Escherichia coli*. *J. Bacteriol.*, 98:232–237, 1969.

[67] D. Herbert. Some principles of continuous culture. In G. Tunevall, editor, *Recent Progress in Microbiology*, pages 381–396, Stockholm, 1958. Almquist & Wiksell.

[68] D. Herbert. The chemical composition of micro-organisms as a function of their environment. *Symp. Soc. Gen. Microbiol.*, 11:391–416, 1961.

[69] C. F. Higgins. ABC transporters: From microorganisms to man. *Annu. Rev. Cell Bioi.*, 8:67–113, 1992.

[70] A. V. Hill. The possible effects of the aggregation of the molecules of haemoglobin on its dissociation curves. *J. Physiol.*, 40:4–7, 1910.

[71] W. S. Hlavacek, J. R. Faeder, M. L. Blinov, R. G. Posner, M. Hucka, and W. Fontana. Rules for modeling signal-transduction systems. *Sci. STKE*, 2006:re6, 2006.

[72] T. Holme and H. Palmstierna. Changes in glycogen and nitrogen-containing compounds in *Escherichia coli* B during growth in deficient media. I. Nitrogen and carbon starvation. *Acta. Chem. Scand.*, 10:578–586, 1956.

[73] N. T. Ingolia, S. Ghaemmaghami, J. R. Newman, and J. S. Weissman. Genome-wide analysis *in vivo* of translation with nucleotide resolution using ribosome profiling. *Science*, 324:218–223, 2009.

[74] O. L. R. Jacobs. *Introduction to Control Theory*. Oxford University Press, Oxford, 1993.

[75] M. R. Jeffrey and S. J. Hogan. The geometry of generic sliding bifurcations. *SIAM Rev.*, 53:505–525, 2011.

[76] K. H. Johansson, A. E. Barabanov, and K. J. Astrom. Limit cycles with chattering in relay feedback systems. *IEEE Trans. Autom. Control*, 247:1414–1423, 2002.

[77] K. H. Johansson, A. Rantzer, and K. J. Astrom. Fast switches in relay feedback systems. *Automatica J. IFAC*, 35:539–552, 1999.

[78] H. R. Kaback. Active transport in *Escherichia coli*: Passage to permease. *Annu. Rev. Biophys. Biophys. Chem.*, 15:279–319, 1986.

[79] G. Karlebach and R. Shamir. Modelling and analysis of gene regulatory networks. *Nat. Rev. Mol. Cell Biol.*, 9:770–780, 2008.

[80] A. F. Khadem, M. C. F. van Teeseling, L. van Niftrik, M. S. M. Jetten, H. J. M. Op den Camp, and A. Pol. Genomic and physiological analysis of carbon storage in the verrucomicrobial methanotroph "*Ca.* Methylacidiphilum fumariolicum" SolV. *Front Microbiol.*, 3:345, 2012.

[81] B. Kholodenko, M. B. Yaffe, and W. Kolch. Computational approaches for analyzing information flow in biological networks. *Sci. Signaling*, 5:re1, 2012.

[82] S. Klamt, H. Grammel, R. Straube, R. Ghosh, and E. D. Gilles. Modeling the electron transport chain of purple non-sulfur bacteria. *Mol. Syst. Biol.*, 4:156–174, 2008.

[83] S. Klamt, U.-U. Haus, and F. Theis. Hypergraphs and cellular networks. *PLoSComput. Biol.*, 5:e1000385, 2009.

[84] S. Klamt, J. Saez-Rodriguez, J. A. Lindquist, L. Simeoni, and E. D. Gilles. A methodology for the structural and functional analysis of signaling and regulatory networks. *BMC Bioinf.*, 7:56–81, 2006.

[85] A. Koch. Bacterial wall as target for attack: Past, present, and future research. *Clin. Microbiol. Rev.*, 16(4):673–687, 2003.

[86] R. Kolter, D. A. Siegele, and A. Tormo. The stationary phase of the bacterial life cycle. *Annu. Rev. Microbiol.*, 47:855–874, 1993.

[87] D. S. Kompala, D. Ramkrishna, and G. T. Tsao. Cybernetic modelling of microbial growth on multiple substrates. *Biotechnol. Bioeng.*, 26:1272–1281, 1984.

[88] S. A. L. M. Kooijman. *Dynamic Energy Budget Theory for Metabolic Organisation*. Cambridge University Press, 2009.

[89] P. Kowalczyk and P. T. Piiroinen. Two-parameter sliding bifurcations of periodic solutions in a dry-friction oscillator. *Physica D*, 237:1053–1073, 2008.

[90] G. Kramer, R. R. Sprenger, M. A. Nessen, W. Roseboom, D. Speijer, L. de Jong, M. J. Texeira de Mattos, J. Back, and C. G. de Koster. Proteome-wide alterations in *Escherichia coli* translation rates upon anaerobiosis. *Mol. Cell. Proteomics*, 9.11:2508–2516, 2010.

[91] E. A. Laws, S. Pei, P. Bienfang, S. Grant, and W. G. Sunda. Phosphate-limited growth of *Pavlova lutheri* (prymnesiophyceae) in continuous culture: determination of growth-rate-limiting substrate concentrations with a sensitive bioassay procedure. *J. Phycol.*, 47:1089–1097, 2011.

[92] D. J. Lee, S. D. Minchin, and S. J. W. Busby. Activating transcription in bacteria. *Annu. Rev. Microbiol.*, 66:125–152, 2012.

[93] Y.-J. Lee, A. Prange, H. Lichtenberg, M. Rohde, M. Dashti, and J. Wiegel. In situ analysis of sulfur species in sulfur globules produced from thiosulfate by *Thermoanaerobacter sulfurigignens* and *Thermoanaerobacterium thermosulfurigenes*. *J. Bacteriol.*, 189:7525–7529, 2007.

[94] R. E. Lenski, M. R. Rose, S. C. Simpson, and S. C. Tadler. Long-term experimental evolution in *Escherichia coli*. I. Adaptation and divergence during 2,000 generations. *Amer. Nat.*, 138:1315–1341, 1991.

[95] G.-W. Li, D. Burkhardt, C. Gross, and J. S. Weissman. Quantifying absolute protein synthesis rates reveals principles underlying allocation of cellular resources. *Cell*, 157:624–635, 2014.

[96] J. Lin, S.-M. Lee, H.-J. Lee, and Y.-M. Koo. Modeling of typical microbial cell growth in batch culture. *Biotechnol. Bioprocess Eng.*, 5:382–385, 2000.

[97] H. Lodish, A. Berk, S. L. Zipursky, P. Matsudaira, D. Baltimore, and J. Darnell. *Molecular Cell Biology*. New York: W. H. Freeman, New York, Fourth edition, 2000.

[98] M. T. Madigan, J. M. Martinko, P. V. Dunlap, and D. P. Clark. *Brock Biology of Microorganisms*. Pearson Benjamin Cummings, San Francisco, CA, Twelfth edition, 2009.

[99] J. Malmborg and B. Bernhardsson. Control and simulation of hybrid systems. *Commun. Nonlinear Sci.*, 30:337–347, 1997.

[100] A. G. Marr, E. H. Nilson, and D. J. Clark. The maintenance requirement of *Escherichia coli*. *Ann. N. Y. Acad. Sci*, 102:536–548, 1962.

[101] J. A. J. Metz, S. A. H. Meszena, F. J. A. Jacobs, and J.S. van Heerwaarden. Adaptive dynamics: A geometrical study of the consequences of nearly faithful reproduction. Technical Report WP-95-099, IIASA, Laxenburg, Austria, 1995.

[102] J. A. J. Metz, R. M. Nisbet, and S. A. H. Geritz. How should we define 'fitness' for general ecological scenarios? *TRENDS in Ecology & Evolution*, 7:198–202, 1992.

[103] H.-P. Meyer, O. Käppeli, and A. Fiechter. Growth control in microbial cultures. *Ann. Rev. Microbiol.*, 39:299–319, 1985.

[104] L. Michaelis and M. L. Menten. Die Kinetik der Invertinwirkung. *Biochem. Z.*, 49:333–369, 1913.

[105] C. De Michele and G. Salvadori. A generalized Pareto intensity-duration model of storm rainfall exploiting 2-copulas. *J. Geophys. Res.*, 108(D2):2156–2202, 2003.

[106] A. P. Mishina and I. V. Proskuryakov. *Higher Algebra: Linear Algebra, Polynomials, General Algebra (in Russian)*. State Publishing House of Physical and Mathematical Literature, Moscow, 1962.

[107] J. Monod. The growth of bacterial cultures. *Annu. Rev. Microbiol.*, 3:371–394, 1949.

[108] M. K. Morris, J. Saez-Rodriguez, P. K. Sorger, and D. A. Lauffenburger. Logic-based models for the analysis of cell signaling networks. *Biochemistry*, 49:3216–3224, 2010.

[109] F. C. Neidhardt, J. L. Ingraham, and M. Schaechter. *Physiology of the Bacterial Cell: A Molecular Approach*. Sinauer Associates, Sunderland, Massachusetts, 1990.

[110] M. A. Nesmeyanova. Polyphosphates and enzymes of polyphosphate metabolism in *Escherichia coli*. *Biochemistry (Moscow)*, 65:309–314, 2000.

[111] O. A. Nev and H. A. van den Berg. Microbial metabolism and growth under conditions of starvation modelled as the sliding mode of a differential inclusion. *Dyn. Systems*, DOI: 10.1080/14689367.2017.1298726, 2017.

[112] O. A. Nev and H. A. van den Berg. Variable-Internal-Stores models of microbial growth and metabolism with dynamic allocation of cellular resources. *J. Math. Biol.*, 74:409–445, 2017.

[113] D. G. Nicholls and S. J. Ferguson. *Bioenergetics 2*. Academic Press, 1992.

[114] Y. Noguchi, Y. Nakai, N. Shimba, H. Toyosaki, Y. Kawahara, S. Sugimoto, and E. Suzuki. The energetic conversion competence of *Escherichia coli* during aerobic respiration studied by ^{31}P NMR using a circulating fermentation system. *J. Biochem.*, 136:509–515, 2004.

[115] M.O.J. Olson, M. Dundr, and A. Szebeni. The nucleolus: An old factory with unexpected capabilities. *Trends Cell Biol.*, 10:189–196, 2000.

[116] S. Pan, Z. Shen, W. Liu, X. Han, H. Miao, and H. Ma. Nutrient compositions of cultured *Skeletonema costatum*, *Chaetoceros curvisetus*, and *Thalassiosira nordenskiöldii*. *Chinese J. Oceanol. Limnol.*, 28:1131–1138, 2010.

[117] H. Parnas and D. Cohen. The optimal strategy for the metabolism of reserve materials in micro-organisms. *J. Theor. Biol.*, 56:19–55, 1976.

[118] S. J. Pirt. The maintenance energy of bacteria in growing cultures. *Proc. Roy. Soc. Lond.*, 133:300–302, 1965.

[119] E. Plahte and S. Kjoglum. Analysis and genetic properties of gene regulatory networks with graded response functions. *Physica D*, 201:150–176, 2005.

[120] J. Preiss. Biochemistry and metabolism of intracellular reserves. In J. S. Poindexter and E. R. Leadbetter, editors, *Bacteria in Nature III: Structure, Physiology, and Genetic Adaptability*, pages 189–258. Plenum, 1989.

[121] N. Price, J. Reed, J. Papin, S. Wiback, and B. O. Palsson. Network-based analysis of metabolic regulation in the human red blood cell. *J. Theor. Biol.*, 225:185–194, 2003.

[122] L. Reitzer. Nitrogen assimilation and global regulation in *Escherichia coli*. *Annu. Rev. Microbiol.*, 57:155–176, 2003.

[123] G-Y. Rhee. A continuous culture study of phosphate uptake, growth rate and polyphosphate in *Scenedesmus sp. J. Phycol.*, 9:495–506, 1973.

[124] P. R. Rich. The molecular machinery of Keilin's respiratory chain. *Biochem. Soc. Trans.*, 31:1095–1105, 2003.

[125] M. Riley, T. Abe, M. B. Arnaud, M. K. Berlyn, F. R. Blattner, R. R. Chaudhuri, J. D. Glasner, T. Horiuchi, I. M. Keseler, T. Kosuge, H. Mori, N. T. Perna, G. Plunkett, K. E. Rudd, M. H. Serres, G. H. Thomas, N. R. Thomson, D. Wishart, and B. L. Wanner. *Escherichia coli* K-12: A cooperatively developed annotation snapshot–2005. *Nucleic Acids Res.*, 34:1–9, 2006.

[126] S. J. Russell and P. Norvig. *Artificial Intelligence: A Modern Approach*. Upper Saddle River: Prentice Hall, 3rd edition; Pearson new international edition edition, 2014.

[127] B. E. M Schaub and H. van Gemerden. Simultaneous phototrophic and chemotrophic growth in the purple sulfur bacterium *Thiocapsa roseopersicina*. *FEMS Microbiol. Ecol.*, 13:185–196, 1994.

[128] H. Schiller and M. Arnold. Convergence of continuous approximation for discontinuous ODEs. *Appl. Numer. Math.*, 62(10):1503–1514, 2012.

[129] C. H. Schilling, D. Letscher, and B. Ø. Palsson. Theory for the systemic definition of metabolic pathways and their use in interpreting metabolic function from a pathway-oriented perspective. *J. Theor. Biol.*, 203:229–248, 2000.

[130] H. G. Schlegel and C. Zaborosch. *General Microbiology*. Cambridge University Press, Cambridge, Seventh edition, 1993.

[131] K. L. Schulze and R. S. Lipe. Relationship between substrate concentration, growth rate, and respiration rate of *Escherichia coli* in continuous culture. *Arch. Microbiol.*, 48:1–20, 1964.

[132] J. M. Schumacher, S. Weiland, and W. P. M. H. Heemels. Linear complementarity systems. *SIAM J. Appl. Math.*, 60:1234–1269, 2000.

[133] J. Schüring, H. D. Schulz, W. R. Fischer, J. Böttcher, and W. H. Duijnisveld, editors. *Redox: Fundamentals, Processes and Applications*. Springer-Verlag, Heidelberg, 1999.

[134] M. Scott, C. W. Gunderson, E. M. Mateescu, Z. Zhang, and T. Hwa. Interdependence of cell growth and gene expression: Origins and consequences. *Science*, 330:1099–1102, 2010.

[135] M. Scott and T. Hwa. Bacterial growth laws and their applications. *Curr. Opinion Biotechnol.*, 22:599–565, 2011.

[136] M. Scott, S. Klumpp, E. M. Mateescu, and T. Hwa. Emergence of robust growth laws from optimal regulation of ribosome synthesis. *Mol. Syst. Biol.*, 10:747, 2014.

[137] R. Séroul. *Programming for Mathematicians*. Springer, Berlin, 2000.

[138] J. Sotomayor and A. L. F. Machado. Structurally stable discontinuous vector fields in the plane. *Qual. Theory Dyn. Syst.*, 3:227–250, 2002.

[139] J. Sotomayor and M. A. Teixeira. Regularization of discontinuous vector fields. In *International Conference on Differential Equations*, pages 207–223, 1995.

[140] S. H. Strelitz. On the Routh-Hurwitz problem. *Am. Math. Mon.*, 84:542–544, 1977.

[141] N. Sutin. Electron exchange reactions. *Annu. Rev. Nucl. Sci.*, 12:285–328, 1962.

[142] A. J. Sweetman and D. E. Griffiths. Studies on energy-linked reactions. Energy-linked transhydrogenase reaction in *Escherichia coli*. *Biochem. J.*, 121:125–130, 1971.

[143] M. Thanbichler and L. Shapiro. Chromosome organization and segregation in bacteria. *J. Struct. Biol.*, 156:292–303, 2006.

[144] M. Thanbichler, S. C. Wang, and L. Shapiro. The bacterial nucleoid: A highly organized and dynamic structure. *J. Cell. Biochem.*, 96:506–521, 2005.

[145] R. Thomas, D. Thieffry, and M. Kaufman. Dynamical behaviour of biological regulatory networks: I. Biological role of feedback loops and practical use of the concept of the loop-characteristic state. *Bull. Math. Biol.*, 57:247–276, 1995.

[146] A. Typas, M. Banzhaf, C. A. Gross, and W. Vollmer. From the regulation of peptidoglycan synthesis to bacterial growth and morphology. *Nat. Rev. Microbiol.*, 10:123–136, 2011.

[147] V. I. Utkin. Variable structure systems with sliding modes. *IEEE Trans. Autom. Control*, 22:212–222, 1977.

[148] V. I. Utkin. *Sliding Modes in Control and Optimization*. Springer-Verlag, 1992.

[149] K. Valgepea, K. Adamberg, A. Seiman, and R. Vilu. *Escherichia coli* achieves faster growth by increasing catalytic and translation rates of proteins. *Mol. Biosyst.*, 9:2344–2358, 2013.

[150] H. A. van den Berg. A generic view of classic microbial growth models. *Acta Biotheor.*, 46:117–130, 1998.

[151] H. A. van den Berg. Modelling the metabolic versatility of a microbial trichome. *Bull. Math. Biol.*, 60:131–150, 1998.

[152] H. A. van den Berg. How microbes can achieve balanced growth in a fluctuating environment. *Acta Biotheor.*, 49:1–21, 2001.

[153] H. A. van den Berg. *Mathematical Models of Biological Systems*. Oxford University Press, New York, 2011.

[154] H. A. van den Berg. *Evolutionary Dynamics: The Mathematics of Genes and Traits*. Institute of Physics, 2015.

[155] H. A. van den Berg, Y. N. Kiselev, and Orlov. Optimal allocation of building blocks between nutrient uptake systems in a microbe. *J. Math. Biol.*, 44:276–296, 2002.

[156] H. A. van den Berg, Y. N. Kiselev, M. Orlov, and S. A. L. M. Kooijman. Optimal allocation between nutrient uptake and growth in a microbial trichome. *J. Math. Biol.*, 37:28–48, 1998.

[157] H. A. van den Berg, Yu. N. Kiselev, and M. V. Orlov. Homeostatic regulation in physiological systems: A versatile Ansatz. *Math. Biosci.*, 268:92–101, 2015.

[158] H. A. van den Berg, M. Orlov, and Y. N. Kiselev. The Malthusian parameter in microbial ecology and evolution: An optimal control treatment. *Comp. Math. Model.*, 19:406–428, 2008.

[159] H. van Gemerden. Microbial mats: A joint venture. *Mar. Geol.*, 113:3–25, 1993.

[160] A. Varma, B. W. Boesch, and B. O. Palsson. Stoichiometric interpretation of *Escherichia coli* glucose catabolism under various oxygenation rates. *Appl. Environ. Microbiol.*, 59:2465–2473, 1993.

[161] T. Vos, X. D. V. Hakkaart, E. A. F. de Hulster, A. J. A. van Maris, J. T. Pronk, and P. Daran-Lapujade. Maintenance-energy requirements and robustness of *Saccharomyces cerevisiae* at aerobic near-zero specific growth rates. *Microb. Cell Fact.*, 15:111–130, 2016.

[162] R.-S. Wang, A. Saadatpour, and R. Albert. Boolean modeling in systems biology: An overview of methodology and applications. *Phys. Biol.*, 9:055001, 2011.

[163] G. S. West. *Algae. Volume 1, Myxophyceae, Peridinieae, Bacillarieae, Chlorophyceae*. Cambridge University Press, Cambridge, 1916.

[164] D. E. Whitworth and P. J. A. Cock. Two-component signal transduction systems of the Myxobacteria. In D. E. Whitworth, editor, *Myxobacteria: Multicellularity and Differentiation*. ASM Press, 2008.

[165] F. M. Williams. A model of cell growth dynamics. *J. Theor. Biol.*, 15:190–207, 1967.

[166] J. Yuan, W. U. Fowler, E. Kimball, W. Lu, and J. D. Rabinowitz. Kinetic flux profiling of nitrogen assimilation in *Escherichia coli*. *Nat. Chem. Biol.*, 2:529–530, 2006.

[167] T. Yura, H. Nagai, and H. Mori. Regulation of the heat-shock response in bacteria. *Annu. Rev. Microbiol.*, 47:321–350, 1993.

[168] K. Ziegler, D. P. Stephan, E. K. Pistorius, H. G. Ruppel, and W. Lockau. A mutant of the cyanobacterium *Anabaena variabilis* ATCC 29413 lacking cyanophycin synthetase: Growth properties and ultrastructural aspects. *FEMS Microbiol. Lett.*, 196:13–18, 2001.

[169] M. H. Zwietering, I. Jongenburger, F. M. Rombouts, and K. van 't Riet. Modeling of the bacterial growth curve. *Appl. Environ. Microbiol.*, 56:1875–1881, 1990.